Collaborative Investigation of Coal Dust, Air Pollution, and Health Concerns in Curtis Bay, South Baltimore, Maryland, USA, 2022-2023

Photo credit: Ryan Gattis, panorama drone photograph from CSX Coal Field Flight on October 26, 2023.

Collaborative Partners

Community of Curtis Bay Association (CCBA)

South Baltimore Community Land Trust (SBCLT)

Mt. Winans Community Association

SB7 Coalition

Air and Radiation Administration, Maryland Department of the Environment

Department of Environmental Health & Engineering, Johns Hopkins Bloomberg School of Public Health (BSPH)

Department of Atmospheric and Oceanic Science, University of Maryland (UMD)

December 14, 2023

Acknowledgements

We thank community hosts of air monitors and environmental sampling, the residents of Curtis Bay, and individuals who reviewed the report. The collaboration benefited from additional input and guidance from: equipment manufacturers QuantAQ and Distributed Sensing Technologies (DSTech); researchers at the University of California-Davis and the University of Maryland Center for Community Engagement, Environmental Justice, and Health; and the Mt Winans Community Association. CCBA and SBCLT coordinated community direction, mobilized field measurement and sampling by summer youth environmental justice scholars, and compiled resident input. BSPH (Heaney research group) procured stationary monitoring equipment and supplies, deployed and maintained monitors, coordinated dust collection and analysis, and completed data analysis. UMD provided mobile monitoring equipment and analysis, as well as performed dust analysis. MDE provided scientific support and analysis, as well as co-location and calibration of monitoring equipment against the state regulatory network. This work and its contributors were supported in part by the Community Science and Innovation for Environmental Justice (CSI EJ) Initiative of the Johns Hopkins Center for a Livable Future, the National Institute of Environmental Health Sciences (NIEHS) P30 Center for Community Health: Addressing Regional Maryland Environmental Determinants of Disease (CHARMED) (grant no. P30ES032756), and NIEHS Training Program in Environmental Health Sciences (grant no. T32ES007141).

Report Contents

1. Executive Summary

"My kids have asthma. I don't open up my windows because of the dust and it's usually black dust so naturally I think it's coal dust. So, I don't open up my windows because it comes in the house and then everything is black." - Angela Shaneyfelt

Baltimore City alone was responsible for over a quarter of total US coal exports in the first quarter (first three months) of 2023. Coal combustion is a major source of particulate matter (PM) (including $PM_{2.5}$) and greenhouse gases which contribute significantly to global disease and adverse health and mortality and climate change. Unrefined coal is likewise detrimental to human health and the environment, and can escape from coal handling operations in the form of windblown dust. For decades, the residents of South Baltimore communities have raised concerns about the accumulation of dark dust on their homes and property that they attribute to the transport of coal via rail throughout South Baltimore and operation of the open-air coal export terminal in Curtis Bay.

To begin to investigate these community concerns and act on a commitment to environmental justice, a collaboration was formed in February 2022 between the Maryland Department of the Environment (MDE) Air and Radiation Administration (ARA), the Community of Curtis Bay Association (CCBA), the South Baltimore Community Land Trust (SBCLT), the CHARMED Center in the Department of Environmental Health and Engineering (EHE) at the Johns Hopkins Bloomberg School of Public Health (BSPH), and the Department of Atmospheric and Oceanic Sciences at the University of Maryland (UMD). This report summarizes the preliminary findings of this collaborative work which responds to South Baltimore residents' longstanding questions about the dark dust found on their homes and the open-air transport and storage of coal in their communities.

Measurement Methods

The collaboration measured pollution throughout the community using several methods:

- Collection and characterization of dust from surfaces and the air throughout the community;
- Continuous monitoring of particulate matter of various size fractions: PM_1, $PM_{2.5}$, PM_{10}, total suspended particles (~PM_{40}); along with gases: carbon dioxide (CO_2), carbon monoxide (CO), nitric oxide (NO), nitrogen dioxide (NO_2), ozone (O_3); and black carbon (BC); using a network of multi-pollutant air sensors deployed at 10 locations throughout the community;
- Episodic sampling of numerous additional pollutants using a mobile monitoring laboratory developed by UMD and the National Oceanic and Atmospheric Administration (NOAA); and
- Photos, videos, experiences, and testimonials from residents.

Key Findings

Analyses of the field measurements indicate 3 key findings:

1. Coal dust is present throughout the community.
    a. Coal particles were identified at all 8 community sampling locations and in 100% of samples during 3 different rounds of sampling (Aug, Sept, & Oct 2023), including at residences, and near businesses, a church, a park, and a school.
    b. Sampling locations ranged from the edge of the coal terminal to around ¾ of a mile away from the facility.

    c. More visible dark dust was found closer to the coal terminal than at locations farther away.
    d. Smaller coal dust particles that are of particular health concern were found along with larger particles throughout the community.
2. Coal dust finds its way into the community on a day-to-day basis and is correlated with both activity at the coal terminal and wind direction.
    a. We detected the signature of coal dust leaving the terminal's fenceline on average nearly once every hour and a half.
    b. High intensity coal dust signature events were longer in duration closest to the coal terminal—the average duration closest to terminal was >6 consecutive minutes and the longest event was 137 consecutive minutes.
3. The Curtis Bay community is overburdened by air pollution, with the community sensor network measuring average particle pollution levels that are higher than at nearby MDE regulatory monitors.
    a. This pollution burden comes from many different pollution sources in the area, including significant coal dust and diesel truck traffic.

Research Questions & Results

- **Is there evidence that coal dust blows away from the coal terminal and into the Curtis Bay community?** Using scanning electron microscopy and energy dispersive X-ray spectroscopy to obtain images of and characterize elemental composition of settled particles, coal dust was confirmed at all community sampling locations, including at residences, and near businesses, a church, a park, and a school. Sampling locations in the community ranged from the fenceline of the coal terminal to around ¾ of a mile away from the facility. Observed coal particle sizes (by length of longest visible dimension) ranged from large particles (PM_{10} and larger) to fine particles ($PM_{2.5}$). We also used ImageJ software to score the darkness of visible settled dust samples. Visible dark dust accumulation was significantly higher at locations nearer versus farther from the coal terminal (β = -0.0238, 95% CI [-0.0297, -0.0178], p<0.001).

- **How quickly is coal dust accumulating off-site of the coal terminal in the Curtis Bay community?** We observed the accumulation of coal dust after 3 days of exposure to ambient air at distances of up to ¾ mile from the coal terminal. Coal dust was also observed on field blank adhesive tape samples at multiple locations after 40 seconds of exposure to the ambient air, maintaining strict protocols to minimize cross-contamination.

- **What is the frequency, intensity and duration of coal dust events in the community, and are they associated with wind, facility operations, or both?** Using a statistical method to estimate contributions to air pollution from specific sources called non-negative matrix factorization (NNMF), we observed a clear signature of coal dust pollution—referred to as "putative coal dust (PCD) factor"—at sensor locations closest to the coal terminal. We estimated the frequency of high intensity PCD events defined as times exceeding the mean + 3 standard deviations (SD) of the PCD factor. Exceedance of the high intensity PCD threshold occurred on average 1 minute out of every hour and a half and lasted for >6 consecutive minutes. NMF successfully identified dust events at all sites, though not all events at all sites were coal dust. At locations closer to the terminal, the PCD factor was associated with both activities at the coal terminal (trains, bulldozers, and ships) and wind direction.

- **From cumulative and source-specific perspectives, what is the air pollution burden in the Curtis Bay community and what are the implications for public health and environmental justice?** The World Health Organization and US Environmental Protection Agency support that there is no safe level of $PM_{2.5}$. The open-air coal terminal is one of dozens of sources of air pollution regulated by MDE in the Curtis Bay area, including the Curtis Bay Energy medical waste incinerator, the BRESCO municipal solid waste incinerator, the Quarantine Road Landfill, the Patapsco Wastewater Treatment Plant, concrete crushing plants, asphalt manufacturing, chemical plants, and oil and gas terminals. Heavy diesel truck traffic is a significant mobile source of pollution in Curtis Bay with levels of black carbon along Pennington and Curtis Ave. similar to levels on major Baltimore highways.

Conclusions and Next Steps

Collectively, the results of this collaborative research confirm the off-site migration of coal dust in the Curtis Bay community. Considering health as a state of complete physical, mental, and social well-being and not simply the absence of disease or infirmity, it appears that the accumulation of dark dust, which our findings confirm includes coal dust, may have adverse impacts on the health and well-being of residents of Curtis Bay. Reducing coal dust particulates and cumulative pollution burden in Curtis Bay could decrease overall morbidity and mortality risk and also provide larger relative benefits to those with the highest risk, thereby decreasing health disparities while promoting health for all. Key next steps include the dissemination of the findings of this collaborative work to community and other stakeholders in order to inform decision-making – e.g., forthcoming MDE permit action. The collaborative research partners will also continue to gather data from an expanding network of sensors and field measurements to refine conclusions, deploy additional monitoring equipment using a grant provided to MDE by the U.S. Environmental Protection Agency, and relate these exposure measurements to health outcomes using a pilot grant provided to BSPH by the JHU CHARMED Center. Community-driven studies on specific pollution sources in the context of cumulative burdens, such as this one, open pathways to reducing harms from fence line pollution sources while increasing benefits directed to host communities. We therefore recommend increasing investment in this type of community, academic and government collaborations for targeted assessments to support health, equity, and environmental justice.

2. Background, Context, and Purpose of Collaborative Partnership

Community context and history

Curtis Bay and its South Baltimore neighbors, including the former residential communities of Fairfield, Wagner's Point and Hawkins Point which were displaced by the early 2000's, continue to bear the cumulative impacts of pollution from various sources including: the CSX coal export terminal, the Curtis Bay Energy medical waste incinerator, the BRESCO municipal solid waste incinerator, the Quarantine Road Landfill, the Patapsco Wastewater Treatment Plant, concrete crushing plants, asphalt manufacturing, chemical plants, and oil and gas terminals. Hundreds of diesel trucks per day move materials along two diesel truck routes, Pennington and Curtis Avenues, through the heart of the residential community with homes, small businesses and a recreation center in between.

Figure 1: Drone photograph showing Benjamin Franklin High School in the foreground and the CSX coal terminal 3,800 feet away. Image credit to Ryan Gattis, panorama drone photograph from CSX Coal Field Flight on October 26, 2023.

Resident Testimonials

Curtis Bay community residents have provided testimony, photographs, and videos about their experiences and observations with diverse sources of air pollution in their community and what implications it has for their environment and health.

Resident Testimonial
"Nobody wanted to move. But it came to it that you had to move. And it was difficult because it broke families up, and so everybody had to relocate. They said that some of the soil was contaminated for

years. I remember, behind our property, a place we used to call the pond. It was a lake of water back there that they said they were dumping chemicals into the water. And the water was polluted, it turned a real dark green in there. And my father told us "Don't go back and play in there no more" but we used to." - **Gilton Pitts, former Hawkins Point resident**

Resident Testimonial
"I moved into Curtis Bay as Fairfield was moving out because of the pollution and everything. They had to move out because no one did anything for 30 years to protect the health of residents and communities. I love my neighborhood. I am a gardener and every morning when I step outside, I don't know what I'm going to smell. On any given day, I don't know what may come about or what I will see. When I take my walk I have to get back inside so I won't be breathing all this stuff, including the coal dust. And the day of the coal explosion, I was in my house and it woke me up terrified." **- Edith Gerald, Curtis Bay resident**

Residents have reported dark dust linked to the nearby CSX coal terminal on the outside and inside of their homes for decades. Photographs, video and written descriptions of daily experience with the dust and assocated negative health and quality of life concerns are presented in this report alongside new scientific evidence responding to longstanding resident concerns.

Figure 2. View of the CSX coal terminal from the Curtis Bay Recreation Center ~1,000 feet away.

"We have to spray the house off because the dust is terrible and to be breathing this stuff in all these years can't be good." - Holly Loyd, 30 year Curtis Bay resident

Figure 3. Photos of dark dust on residents' homes in Curtis Bay, taken between April and Dec 2023.

Resident Testimonial

"We had a pool for my grandson and we go out, you know, we filled it up the night before so it would be kind of warm the next morning for him but there was this black soot all on top of the water. All on top of the rim of the pool there you have to wipe the black coal dust off every day or empty it every day. And then in the house if you open the windows, it's black all over every day. This has been since I've been here before the explosion. You know pollen? You know it's that green film you know like it covers everything? That's how the coal dust is, it covers everything. Even on the car windshield. You come out and some people have to maybe a couple times a day, wipe it clean. Since i've moved up here my breathing has gotten worse. My grandson now, he can't run from there to there without struggling." **- Janet Clarke, Curtis Bay resident**

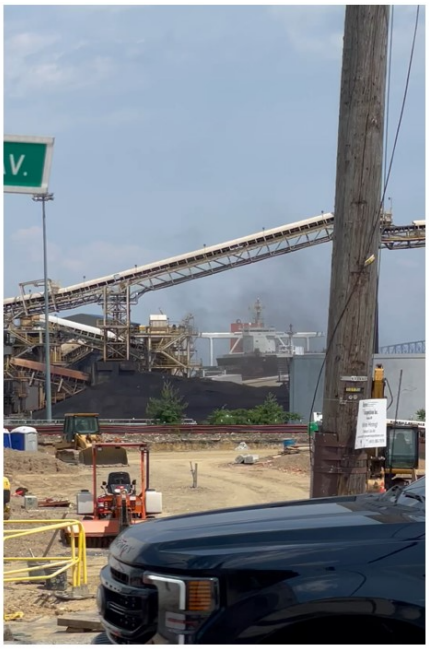

Figure 4. Plume of visible dust at the coal terminal, June 1, 2021.

Resident Testimonial "I've been a concerned mother and resident of Curtis Bay for 30 years. In the summertime the kids sweat off black stuff from the coal terminal. We have to spray the house off because the dust is terrible and to be breathing this stuff in all these years can't be good. And that's before the explosion. Way before the explosion started we had this problem but it just got brought to the attention after the explosion." **- Holly Loyd, Curtis Bay resident**
Resident Testimonial "You can't even open your windows because of the coal dust. In the summertime, if you open your windows and you open them up early in the morning then like six o'clock, seven o'clock or whatever, by the time you get ready to go to bed you got coal dust all on the outside window and even on the inside of your window where it comes through the screen full of coal dust." **- Curtis Bay resident**
Resident Testimonial "I live and breathe the air in Curtis Bay. Coal covers everything you own. It destroys the earth and your health and home." - **Daphne Heppding, Curtis Bay resident**
Resident Testimonial "This is what I've been going through since I moved here about a year ago now. Everyday on the outside of my home here I came out here and I would wipe the dust that's coming off of it. I would get some water and I would wash it down and then by the time I come back out here later on tonight this is back looking like this with more dust. As you know this is a concern of mine because I have oxygen in my home for my respiratory condition. Also, there's kids in this neighborhood and we have a rec center here and I'm really concerned about it and I think that something needs to be done. It needs to get taken care of and really get taken care of and fast." - **Curtis Bay resident**

Resident Testimonial

"The issue of coal dust in communities matters because it is affecting our respiratory health. It causes lung problems and we have kids growing up in these communities. For me it's great and means a lot that people and youth doing something about this. It's time for toxic polluting industries to see the harm they have on the community instead of building money. I'm very proud of my son as well of the other youth who are working together and standing up for their communities. Our health matters more than money." - **Humberto Sanchez, Lakeland resident**

Resident Testimonial

"Look at the people in West Virginia that died from black lung, from coal dust. So you bring it here in the city, in Curtis Bay and you spread it all around? We've got coal dust all along the outside window sills and even on the inside of our window, where it comes through the screens. It's nasty. My wife is tired of washing window sills and windows." **Mr. Schultz, Curtis Bay resident**

Resident Testimonial

"I live in Mt. Winans directly across the CSX train tracks where uncovered coal is transported. I have heard concerns from fellow residents in my community and across South Baltimore about both noise and air pollution and am committed to continue to work together until we achieve needed changes." - **Melissa Robinson, Mt. Winans resident**

99th

percentile nationwide for proximity to hazardous facilities requiring "Risk Management Plans"

(Source: US EPA EJScreen)

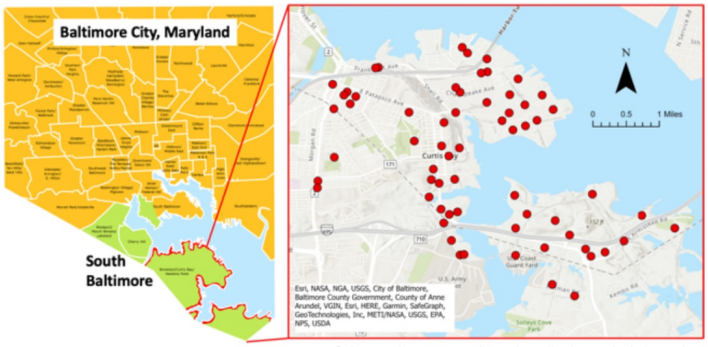

Source: MD Dept. of the Environment Air and Radiation Administration

Figure 5. Cumulative pollution burden in Curtis Bay, South Baltimore.

The CSX coal terminal and dozens of other facilities, some less than half a mile from residential housing, produce a variety of hazardous air pollutants regulated under the Clean Air Act[1], with potential health impacts ranging from asthma, cancer, and premature death. The concentration of industry

handling hazardous materials places Curtis Bay in the 99th percentile nationwide for proximity to facilities required to have a "Risk Management Plan" due to enhanced risk of explosions, leaks or spills. The past century has been punctuated by a series of such incidents - including the coal terminal explosion on December 30th, 2021.

Resident Testimony "I am a longtime member of the Curtis Bay community. My name is Halyna Murdryj and I have lived in Curtis Bay since 1958. I have experienced quite a few of these explosions be it Fairfield, Wagner's Point or Curtis Bay. I have had my dalliance with cancer before in my life. I no doubt will have another soon. I saw black and gray smoke rising. I went outside because I heard everyone coming outside and I said there's something going on at the coal pier. I did smell, like everyone did, coal burning but I didn't realize how huge the explosion was until the next morning when I found everything on my front porch covered not with black dust, which I have experienced before, but with black granules." **- Halyna Murdryj, Curtis Bay resident**
Resident Testimonial "When the explosion happened we thought somebody set off a bomb or something you know it's like, like a bomb went off. It rocked, it actually rocked this whole block. People were running out here to find out what's going on they thought the whole place blew up down there. That was one nasty explosion. It was almost like a hydrogen bomb or something went off. It actually shook the houses here on Church Street. People don't want to live here because of the coal pier. That could be the best thing they've ever done. The best thing they could do is get rid of the coal pier." **-Curtis Bay resident**
Resident Testimonial "My sister is a part of this effort to stand up for the health of our entire community and our neighbors across South Baltimore. It matters because in the long run it is going to affect our health and it is amazing what the people in our community are doing to prevent this problem. If it wasn't for them trying to fix the problem, our communities would still be ignored. It is impeccable what they are doing for us." **- Brooklyn resident**
Resident Testimonial "I love my community of Cherry Hill and my South Baltimore neighbors. As a resident with serious health issues connected to the pollution and toxins in our environment, this community and youth led effort is so important to me. I am proud of the next generation of community leaders who are working tirelessly to advance our South Baltimore communities away from a history of environmental injustice to a brighter and healthy future." **- Cleo Walker, Cherry Hill resident**

In response to the daily exposure to pollution and acute industrial incidents, residents and local organizations have formulated a systemic approach for a just transition (https://ilovecurtisbay.com/environmentaljustice/) to address long standing EJ concerns while advancing a positive vision for healthy, safe and stable communities. A sustained community and worker-led collaborative effort involving academia and government is imperative to begin to initiate measures that reduce harms and share benefits from the concentration of industrial development on the fenceline of Curtis Bay and its South Baltimore neighbors.

Resident Testimonial

"As a lifelong Mt. Winans resident, It is disheartening to witness the perpetuation of profit over people, with little consideration for the resulting consequences. We see this everytime the trains filled with coal, completely uncovered, pass through our community just 60 feet from our homes, on their way to our neighbors in Curtis Bay. We also see it when the trucks carry trash into - and toxic ash out of - the incinerator through our community on the way to the dump in Curtis Bay. A long history of environmental injustice connects our communities but we are done trying to deal with it alone. I am so proud to be in this together alongside young people who put community-led improvements for our health and quality of life at the center." - **Angela Smothers, Mt. Winans resident**

Resident Testimonial

"As a former teacher at Curtis Bay Elementary, quite frankly I said I would never live in this community because of the hazards of the fumes and the conditions it caused my students. I had a lot of students who at a young age, 3 or 4, developed asthma and I thought it was largely based on the factories in this area. Three days out of the week you will come across unpleasant smells and odors. Decades of intense environmental justice has already cost South Baltimore the displacement of at least 3 entire communities. While I couldn't be more proud of my daughter and fellow community members across South Baltimore neighborhoods for joining together in this effort for our health and quality of life, we need to see all this research turn into concrete action that makes our lives better. It hasn't happened yet and we will keep going until we see it." -**Tiffany Thompson, Curtis Bay resident**

Collaborative Partnership

To begin to investigate these community concerns and act on a commitment to environmental justice, a collaboration was formed in February 2022 between the Maryland Department of the Environment (MDE) Air and Radiation Administration (ARA), the Community of Curtis Bay Association (CCBA), the South Baltimore Community Land Trust (SBCLT), the CHARMED Center in the Department of Environmental Health and Engineering (EHE) at the Johns Hopkins Bloomberg School of Public Health (BSPH), and the Department of Atmospheric and Oceanic Sciences at the University of Maryland (UMD). This report summarizes the preliminary findings of this collaborative work which responds to South Baltimore residents' longstanding questions about the dark dust found on their homes and the open-air transport and storage of coal in their communities. The partnership coordinated deployment of pollution measurement efforts across the community, including samples of dust from surfaces and the air, deployment of multipollutant air sensors, measurements from mobile monitoring equipment, and collection of photos, videos, experiences, and testimonials from residents.

Air Pollution and Health

Air pollution is the presence of substances in the air–both outdoors and indoors–that are harmful to living organisms and the environment. Air pollution is one of the most significant contributors to mortality and adverse health outcomes around the world and in the United States (US).

The World Health Organization estimates that air pollution is the cause of nearly seven million premature deaths annually around the world.[2] The most recent State of the Air report from the American Lung Association found that 119.6 million people in the US live in areas with unhealthy levels of air pollution.[3]

Anthropogenic or human-caused activity is the greatest contributor to air pollution worldwide. Industrial activities such as waste incineration, energy generation, oil/fuel processing and refinement, bulk material storage and transport, industrial animal agriculture, and a plethora of other industries are major sources of local and regional air pollution.[4] Other sources include mobile sources like automobile and rail transportation, indoor sources like tobacco products and cooking stoves, and natural sources like wildfires. These sources emit pollutants including particulate matter, various types of gases (e.g., carbon dioxide, methane, and volatile organic compounds [VOCs]), and air toxics which can impact human health and the environment with both short- and long-term exposures.

As a part of the Clean Air Act, established in 1970, the US Environmental Protection Agency (EPA) sets standards for and regulates emissions of hazardous air pollutants (i.e., the six criteria air pollutants[5]). State regulatory agencies including the Maryland Department of the Environment Air and Radiation Administration support the EPA's mission to protect environmental health in the US through state-level regulation and enforcement and permitting of facilities that contribute to air pollution.

Particulate Matter Air Pollution and Health

The health impacts of particulate matter (PM)–namely fine particulate matter (particles of 2.5 microns in diameter or less or $PM_{2.5}$) and coarse particulate matter (particles of 10 microns in diameter or less or PM_{10})–have been comprehensively studied and consistently linked with numerous adverse health outcomes. The severity of health effects varies by the size of the particulate matter. Smaller particles can travel deeper into the body, and therefore, can have more detrimental health consequences. Both short- and long-term exposures to PM have been linked to adverse health effects.

Particles in the $PM_{2.5}$ size range are small enough to penetrate deep into the lungs and even enter the blood stream. According to the Global Burden of Disease Study 2019 from the Institute for Health Metrics and Evaluation, $PM_{2.5}$ pollution–both outdoor and indoor–is the fourth highest risk factor for death globally, after high blood pressure, tobacco use, and dietary risk factors.[6] The World Health Organization and the EPA support that there is no safe level of $PM_{2.5}$ exposure.[7-9] Several studies have linked $PM_{2.5}$ to premature mortality[10-13], respiratory disease[14-16], cardiovascular disease[16-18], nervous system effects[19,20], low birthweight[21,22], and mental health impacts[23-25]. Short-term (or acute)[26] and long-term (or chronic) exposures[27] to $PM_{2.5}$ pollution, and exposures below regulatory guidelines[28,29] have been linked to adverse health outcomes.

Particles in the PM_{10} size range can penetrate the respiratory tract and reach the upper parts of the lungs. These larger particles are known to have significant health impacts, even though they do not penetrate as deeply into the body as $PM_{2.5}$ particles. However, several studies suggest possible associations between PM10 or coarse-mode pollution and all-cause mortality[30]; cardiovascular, cerebrovascular, and respiratory mortality[30]; incident lung cancer[31,32]; and cardiovascular disease[33] and respiratory[34] hospital admissions.

Coal Handling and Air Pollution in Curtis Bay, South Baltimore, Maryland

Baltimore City alone was responsible for 28.6% of total US coal exports in the first quarter of 2023. CSX's coal terminal at Curtis Bay exports coal via barge and ship. The terminal can process millions of tons of coal in a year; it handled 7.1 million tons of coal in 2022 and 8.6 million in 2021. Incoming coal arrives by open-topped train cars. An average train will have about 115 cars, and it takes approximately six hours to empty a train.

Despite the growing popular movement away from reliance upon fossil fuels and other non-renewable energy sources, coal remains a significant resource for global energy production and industry.[35] Coal is extracted from the earth via mining such as open-pit, surface, and mountaintop removal mining which has devastating and destructive impacts upon surrounding ecosystems. Bulk coal material can be transported from coal mines over long distances via trucks, trains, barges, and bulk carrier ships to coal handling and storage facilities. At coal handling and preparation plants, for example, coal is pulverized and processed for transport to other facilities or fed directly into coal-fired power plants for energy generation. Another example of coal storage facilities is a coal terminal. Covered or uncovered coal terminals are designed for the storage, loading, and unloading of coal and are located near navigable waterways for international shipping or long-haul domestic distribution.

Coal dust is an inevitable byproduct of the handling and processing of bulk coal material, whether inside of a coal mine or at an open-air coal terminal.[36] Being decomposed plant matter subjected to high temperature and pressure in the earth's crust, coal is primarily composed of carbonaceous material; this is the component that burns and releases energy. Coal and, by extension, coal dust also are comprised of other organic compounds (e.g., aromatic hydrocarbons), minerals (e.g., silica or quartz, pyrite, clay minerals, and calcite), and trace elements toxic to human health (e.g., arsenic, mercury, and lead).[36]

Fugitive coal dust emissions from the mining, handling, storage, and transport of coal are a major occupational, environmental, and community health concern. Coal dust particle size distributions can vary significantly depending on the source and method of generation (e.g., storage, grinding and pulverization, or mining), ranging from fine particulate matter (PM) such as PM of aerodynamic diameter ≤ 1 µm (PM_1) and PM of aerodynamic diameter ≤ 2.5 µm ($PM_{2.5}$) to larger particulates like PM of aerodynamic diameter ≤ 10 µm (PM_{10}) and greater.

Regulatory particulate matter standard for unconfined sources

Background - How coal is handled at CSX

CSX's coal terminal at Curtis Bay exports coal via barge and ship. The terminal can process millions of tons of coal in a year; it handled 7.1 million tons of coal in 2022 and 8.6 million in 2021. Incoming coal arrives by open-topped train cars. An average train will have about 115 cars, and it takes approximately six hours to empty a train. A surfactant is applied to the coal at the mine of origin to minimize loss of coal to the wind while in transit. At the terminal, each car is unloaded by tilting it over a pit housed within three partially enclosed dumping sheds. A water jet is applied within the shed whenever coal is dumped into the pit.

Dumped coal is then transported via conveyors to a transfer tower where it is lifted vertically and distributed to one of two horizontal, covered conveyors approximately 150 feet above ground. Water is applied to the coal as it travels to and along the horizontal aerial conveyors. The aerial conveyors' single purpose is to convey coal to either the north side or the south side of the terminal. These conveyors connect to a series of stacker tubes with open windows. Coal drops from the horizontal conveyers into the stacker tubes and flows out the openings to form conical piles of coal around the stacker tubes and directly below the aerial conveyors. There are eight tubes: five serving the north terminal and three serving the south terminal. The conical piles are widened using bulldozers throughout the process. Once piles are formed, they are wetted periodically using spray nozzles located above the piles and at ground level around the perimeter of the piles.

A third, smaller coal storage area located closer to the piers is used for smaller quantities of specified coal products. This area employs a stacker conveyor to form the coal storage pile. Wet suppression is also used in this area for dust control.

When coal is to be loaded on a ship or barge for transport the process is similar to the delivery process. Coal from the formed piles is fed by gravity into ground-level openings above an underground conveyor system where it is then transported to the transfer tower and then to covered conveyors to awaiting ships or barges. There are two loading piers with three loading mechanisms: two for ships and one for barges. Bulldozers push the coal into position above the openings to the underground conveyors as needed to ensure a steady flow of coal. A mist is applied to the coal as it travels through the underground conveyors. At the ship loading area a telescoping chute is used to minimize drop height from the conveyors to a ship's hold.

Under certain circumstances, ships can also be loaded directly from the rail car dumpers using covered conveyors. In such instances, coal is not piled for storage.

Regulatory standards

For particulate matter, there are regulatory standards that pertain to two distinct types of air pollution sources – confined sources and unconfined sources. A confined source is an installation that discharges into the atmosphere through a stack, duct, hood, flue, or other conduit. An unconfined source is an installation that causes emissions that are not enclosed in a stack, duct, hood, flue, or other conduit but which escape into the atmosphere through openings such as windows, vents or doors, ill-fitting closures, or poorly maintained equipment. The coal handling operation at the CSX terminal is considered an unconfined source from a regulatory perspective.

The regulations govern particulate matter from unconfined sources in the following manner:

> "A person may not cause or permit emissions from an unconfined source without taking reasonable precautions to prevent particulate matter from becoming airborne. These reasonable precautions shall include, when appropriate as determined by the Department, the installation and use of hoods, fans, and dust collectors to enclose, capture, and vent emissions. In making this determination, the Department shall consider technological feasibility, practicality, economic impact, and the environmental consequences of the decision."

There is also a general regulatory requirement regarding the creation of a nuisance or air pollution that applies universally to all permitted and unpermitted sources. The applicable regulatory

language is that “An installation or premises may not be operated or maintained in such a manner that a nuisance or air pollution is created.”

In this regard, air pollution is defined as “…the presence in the outdoor atmosphere of substances in quantities, having characteristics, and being of a duration which, from any single source or in combination with other sources, are, or may be predicted with reasonable certainty to be, injurious to human, plant, or animal life or to property, or which unreasonably interfere with the proper enjoyment of the property of others by reason of the emission of odors, solids, vapors, liquids, or gases…”

Controlling dust

The CSX terminal controls dust primarily through enclosing or partially enclosing the railcar dumpers and conveyors, as well as the application of water at various points and at various times as the coal is transported throughout the terminal. Water is applied to incoming coal initially at the point where it is dumped, and additional water is applied to the coal as it is conveyed through the terminal’s conveyance system. Water is also applied to the static storage piles as the coal piles are being created and until the stored coal is loaded onto a ship or barge for exporting elsewhere. Spray nozzles are activated when wind speeds reach 12 miles per hour, but the terminal operators can also manually turn on the water jets when conditions warrant. The ordering hierarchy for spraying is: timed watering, watering triggered by high winds and then manual activation of the water sprays. More detail on the operation of the water sprays follows:

- Standard automatic mode: regular spray cycle, the water sprays are operated once every four hours.
- Wind detection mode: system located on aerial conveyors, when the system detects wind speeds higher than 12 miles per hour (mph), the wind spray cycle mode will activate and will automatically increase the watering frequency to once every hour.
- Early warning system: that is a part of the weather service feature and can identify these higher speed windstorms up to 3 hours before the event occurs.
- High wind mode: When higher wind events are detected, the spray system has the capability of automatically adjusting both the ground and tower sprays toward the direction of the wind to maximize water coverage to the coal storage piles.
- Manual mode: the operator has the capability to target specific areas by turning on certain water sprays.
- Override capability: If the system is disabled manually and a high wind event is approaching or occurring, the wind spray cycle mode will override and automatically activate the system.

A water truck is used to keep dust down on paved and unpaved surfaces throughout the terminal grounds. Rail car dumping takes place in a partially enclosed shed. Water jets are activated within the shed whenever dumping occurs.

CSX installed a thirty-foot high DustTamer Wind Fence for 315 linear feet along the south side of the property to help effectively reduce the wind speeds and minimize potential fugitive dust. The DustTamer Wind Fence is designed to exert a drag force on oncoming wind velocity and reduce wind speeds. The fence allows air to pass through and helps equalize the differential pressure, thereby lowering the wind velocity.

Material conveyors are completely enclosed in the underground reclaim tunnels. The elevated conveyors are covered. Some small portions of the conveyor system are not covered or enclosed, and those conveyors are equipped with windscreens, where practical, to minimize the effect of the wind across the conveying belt. The underground North and South reclaim tunnels are equipped with water sprays to minimize dust.

The speed at which coal is loaded onto ships and barges is adjusted to help minimize dust. If the coal is chunky, CSX can load up to 6700 tph of coal, but if the coal is finer (powdery) the loading rate is reduced to 2800 tph.

CSX Fenceline Monitoring Requirements

The permit for the rebuild of the equipment that was damaged in the December 2021 coal dust explosion included the following provision (Condition D.5) relating to fenceline monitoring:

> *"CSX will be required to submit a Fence Line Monitoring Plan to ARA for review and approval within 60 days of the issue date of the permit. The Fence Line Monitoring Plan must include equipment types designated by the Department to measure particulate pollution leaving the site and shall include equipment to measure applicable meteorological conditions.*
>
> *Within 60 days following the issue date of this permit, the Permittee shall submit to the Department, for review and approval, a Fence Line Monitoring Plan. The plan shall include, at a minimum, the following information:*
>
> a. *A plan for the installation and operation of a fence line monitoring system designed to monitor for fugitive dust.*
> b. *One (1) continuous federal equivalent method (FEM) monitor for both PM-IO and PM-2.5 and at least one (1) collocated PM-2.5/PM10 sensor.*
> c. *Multiple PM-2.5/PM-10 sensors around the CSX property.*
> d. *A 10-meter meteorological monitoring system that meets all the requirements of the Quality Assurance Handbook for Air Pollution Measurement Systems - Volume IV: Meteorological Measurements should also be installed at an appropriate location on the CSX property."*

The permit for the rebuild of the damaged equipment was issued by MDE on September 7, 2022. CSX submitted the required fenceline monitoring plan on November 6, 2022 and was granted partial approval by the Department on March 7, 2023 and final approval on June 26, 2023.

CSX has procured and installed particulate matter (PM) Federal Equivalent Method (FEM) monitors, low-cost sensors, and a meteorological tower for the fenceline PM monitoring network. As of March 23, 2023, the FEM and meteorological tower were fully installed at the site. The low-cost sensors were installed at FEM monitor locations to begin collocation testing.

After installation, the instrumentation was calibrated and put into service for the start of the integration and normalization period.

Figure 6. CSX coal export terminal fenceline monitoring plan.

Low-cost sensor devices were collocated with the FEM monitors at locations AQ5 and AQ8 before deployment around the fenceline in September 2023. With the exception of AQ7, the balance of the monitoring locations has low-cost sensors deployed and collecting data. Monitoring station AQ5 has three low-cost sensors and AQ8 has one low-cost sensor for ongoing collocation. The LCS for location AQ7 is planned for installation by the end of October.

Routine flow checks on the FEMs occur monthly. The meteorological tower received a 6-month calibration on September 26, 2023.

CSX is currently finalizing the QAPP (quality assurance project plan) for submission to the Department. A dashboard for presenting date to the public is under development.

References

1. United States Environmental Protection Agency. Summary of the Clean Air Act. Internet. Accessed Dec 05, 2023. https://www.epa.gov/laws-regulations/summary-clean-air-act
2. World Health Organization. Air Pollution. Accessed Dec 05, 2023. https://www.who.int/health-topics/air-pollution#tab=tab_2
3. American Lung Association. *State of the Air 2023*. 2023. https://www.lung.org/research/sota
4. Johnston J, Cushing L. Chemical exposures, health, and environmental justice in communities living on the fenceline of industry. *Current environmental health reports*. 2020;7:48-57. doi:10.1007/s40572-020-00263-8
5. United States Environmental Protection Agency. Criteria Air Pollutants. Accessed Dec 05, 2023. https://www.epa.gov/criteria-air-pollutants
6. Fuller R, Landrigan PJ, Balakrishnan K, et al. Pollution and health: a progress update. *The Lancet Planetary Health*. 2022;6(6):e535-e547. doi:10.1016/S2542-5196(22)00090-0
7. United States Environmental Protection Agency. *Policy Assessment for the Reconsideration of the National Ambient Air Quality Standards for*

Particulate Matter. EPA-452/R-22-004. 2022. https://www.epa.gov/system/files/documents/2022-05/Final%20Policy%20Assessment%20for%20the%20Reconsideration%20of%20the%20PM%20NAAQS_May2022_0.pdf
8. United States Environmental Protection Agency. *Integrated Science Assessment (ISA) for Particulate Matter (Final Report, Dec 2019). EPA/600/R-19/188.* 2019. https://cfpub.epa.gov/ncea/isa/recordisplay.cfm?deid=347534
9. World Health Organization. *WHO global air quality guidelines: particulate matter (PM2.5 and PM10), ozone, nitrogen dioxide, sulfur dioxide and carbon monoxide (License: CC BY-NC-SA 3.0 IGO)*. 2021. https://iris.who.int/handle/10665/345329
10. Azimi P, Stephens B. A framework for estimating the US mortality burden of fine particulate matter exposure attributable to indoor and outdoor microenvironments. *Journal of Exposure Science & Environmental Epidemiology*. 2020;30(2):271-284. doi:10.1038/s41370-018-0103-4
11. Saini P, Sharma M. Cause and Age-specific premature mortality attributable to PM2.5 Exposure: An analysis for Million-Plus Indian cities. *Science of The Total Environment*. 2020;710:135230. doi:10.1016/j.scitotenv.2019.135230
12. Henneman L, Choirat C, Dedoussi I, Dominici F, Roberts J, Zigler C. Mortality risk from United States coal electricity generation. *Science*. 2023;382(6673):941-946. doi:10.1126/science.adf4915
13. Liu T, Meng H, Yu M, et al. Urban-rural disparity of the short-term association of PM_{2.5} with mortality and its attributable burden. *The Innovation*. 2021;2(4)doi:10.1016/j.xinn.2021.100171
14. Liu K, Hua S, Song L. PM2.5 Exposure and Asthma Development: The Key Role of Oxidative Stress. *Oxidative Medicine and Cellular Longevity*. 2022;2022:3618806. doi:10.1155/2022/3618806
15. Li X, Liu X. Effects of PM2.5 on Chronic Airway Diseases: A Review of Research Progress. *Atmosphere*. 2021;12(8). doi:10.3390/atmos12081068
16. Pun VC, Kazemiparkouhi F, Manjourides J, Suh HH. Long-Term PM2.5 Exposure and Respiratory, Cancer, and Cardiovascular Mortality in Older US Adults. *American Journal of Epidemiology*. 2017;186(8):961-969. doi:10.1093/aje/kwx166
17. Henning RJ. Particulate Matter Air Pollution is a Significant Risk Factor for Cardiovascular Disease. *Current Problems in Cardiology*. 2024;49(1, Part B):102094. doi:10.1016/j.cpcardiol.2023.102094

18. Krittanawong C, Qadeer YK, Hayes RB, et al. PM2.5 and Cardiovascular Health Risks. *Current Problems in Cardiology*. 2023;48(6):101670. doi:10.1016/j.cpcardiol.2023.101670
19. Shou Y, Huang Y, Zhu X, Liu C, Hu Y, Wang H. A review of the possible associations between ambient PM2.5 exposures and the development of Alzheimer's disease. *Ecotoxicology and Environmental Safety*. 2019;174:344-352. doi:10.1016/j.ecoenv.2019.02.086
20. Li J, Wang Y, Steenland K, et al. Long-term effects of PM2.5 components on incident dementia in the northeastern United States. *The Innovation*. 2022;3(2)doi:10.1016/j.xinn.2022.100208
21. Kirwa K, McConnell-Rios R, Manjourides J, Cordero J, Alshawabekeh A, Suh HH. Low birth weight and PM(2.5) in Puerto Rico. *Environ Epidemiol*. 2019;3(4)doi:10.1097/ee9.0000000000000058
22. Rodríguez-Fernández A, Ramos-Castillo N, Ruiz-De la Fuente M, Parra-Flores J, Maury-Sintjago E. Association of Prematurity and Low Birth Weight with Gestational Exposure to PM2.5 and PM10 Particulate Matter in Chileans Newborns. *International Journal of Environmental Research and Public Health*. 2022;19(10). doi:10.3390/ijerph19106133
23. Xue T, Guan T, Zheng Y, et al. Long-term PM2.5 exposure and depressive symptoms in China: A quasi-experimental study. *The Lancet Regional Health – Western Pacific*. 2021;6doi:10.1016/j.lanwpc.2020.100079
24. Surace T, Quitadamo C, Caldiroli A, et al. Air Pollution and Perinatal Mental Health: A Comprehensive Overview. *Journal of Clinical Medicine*. 2023;12(9). doi:10.3390/jcm12093146
25. Ai H, Wu J, Zhou Z. The long-run effects of fetal PM2.5 exposure on mental health: evidence from China. *Environmental Science and Pollution Research*. 2023;30(12):34158-34173. doi:10.1007/s11356-022-24661-7
26. Bhaskaran K, Hajat S, Armstrong B, et al. The effects of hourly differences in air pollution on the risk of myocardial infarction: case crossover analysis of the MINAP database. *BMJ*. 2011;343:d5531. doi:10.1136/bmj.d5531
27. Kloog I, Ridgway B, Koutrakis P, Coull BA, Schwartz JD. Long- and short-term exposure to PM2.5 and mortality: using novel exposure models. *Epidemiology*. 2013;24(4):555-61. doi:10.1097/EDE.0b013e318294beaa
28. Pappin A, Christidis T, Pinault Lauren L, et al. Examining the Shape of the Association between Low Levels of Fine Particulate Matter and Mortality across Three Cycles of the Canadian Census Health and Environment Cohort. *Environmental Health Perspectives*. 2019;127(10):107008. doi:10.1289/EHP5204
29. Di Q, Wang Y, Zanobetti A, et al. Air Pollution and Mortality in the Medicare Population. *New England Journal of Medicine*. 2017;376(26):2513-2522. doi:10.1056/NEJMoa1702747
30. Orellano P, Reynoso J, Quaranta N, Bardach A, Ciapponi A. Short-term exposure to particulate matter (PM10 and PM2.5), nitrogen dioxide (NO2), and ozone (O3) and all-cause and cause-specific mortality: Systematic review and meta-analysis. *Environment International*. 2020;142:105876. doi:10.1016/j.envint.2020.105876
31. Puett R, Hart J, Yanosky J, et al. Particulate Matter Air Pollution Exposure, Distance to Road, and Incident Lung Cancer in the Nurses' Health Study Cohort. *Environmental Health Perspectives*. 2014;122(9):926-932. doi:10.1289/ehp.1307490
32. Raaschou-Nielsen O, Andersen ZJ, Beelen R, et al. Air pollution and lung cancer incidence in 17 European cohorts: prospective analyses from the European Study of Cohorts for Air Pollution Effects (ESCAPE). *The Lancet Oncology*. 2013;14(9):813-822. doi:10.1016/S1470-2045(13)70279-1
33. Powell H, Krall J, R., Wang Y, Bell M, L., Peng R, D. Ambient Coarse Particulate Matter and Hospital Admissions in the Medicare Cohort Air Pollution Study, 1999–2010. *Environmental Health Perspectives*. 2015;123(11):1152-1158. doi:10.1289/ehp.1408720
34. Tecer LH, Alagha O, Karaca F, Tuncel G, Eldes N. Particulate matter (PM2. 5, PM10-2.5, and PM10) and children's hospital admissions for asthma and respiratory diseases: A bidirectional case-

crossover study. *Journal of Toxicology and Environmental Health, Part A*. 2008;71(8):512-520. doi:10.1080/15287390801907459
35. Yolcan OO. World energy outlook and state of renewable energy: 10-Year evaluation. *Innovation and Green Development*. 2023;2(4):100070. doi:10.1016/j.igd.2023.100070
36. Raju B, Rom WN. Silica, Some Silicates, Coal Dust and Para-Aramid Fibrils: IARC Monographs on the Evaluation of Carcinogenic Risks to Humans, Vol. 68. JSTOR; 1998.

3. Coal Terminal-specific Community Exposure and Impacts

3a. Characterizing Fugitive Coal Dust in Curtis Bay, South Baltimore, Maryland

Research questions addressed

- Is there evidence that coal dust blows away from the coal terminal and into the Curtis Bay community?
- How quickly is coal dust accumulating off-site of the coal terminal in the Curtis Bay community?

White tape settled dust collections

Introduction

Curtis Bay community members have reported dark, black dust accumulating on both outdoor and indoor surfaces of their homes for decades. To visually document outdoors settled dust accumulation, we developed and deployed "white tape collectors" around Curtis Bay at consenting residences and local businesses. The white tape collectors are a visual, low-cost method of observing variations in accumulation of settled dust over time and at varying distances away from the coal terminal and other industrial facilities. White tape collectors were first deployed on May 3, 2023, and all collectors were retrieved on May 31, 2023, for a 28-day sampling period. Curtis Bay residents, local businesses, and organizations at four locations participated in this sampling field campaign (Figure 1). Locations A and B are near the southern and northern, respectively, fencelines of the coal terminal and connected rail lines. Locations C and D are residential sampling sites, approximately 1300 feet and ¾ mi away, respectively, from the coal terminal. Location D is near a local school and in a residential area.

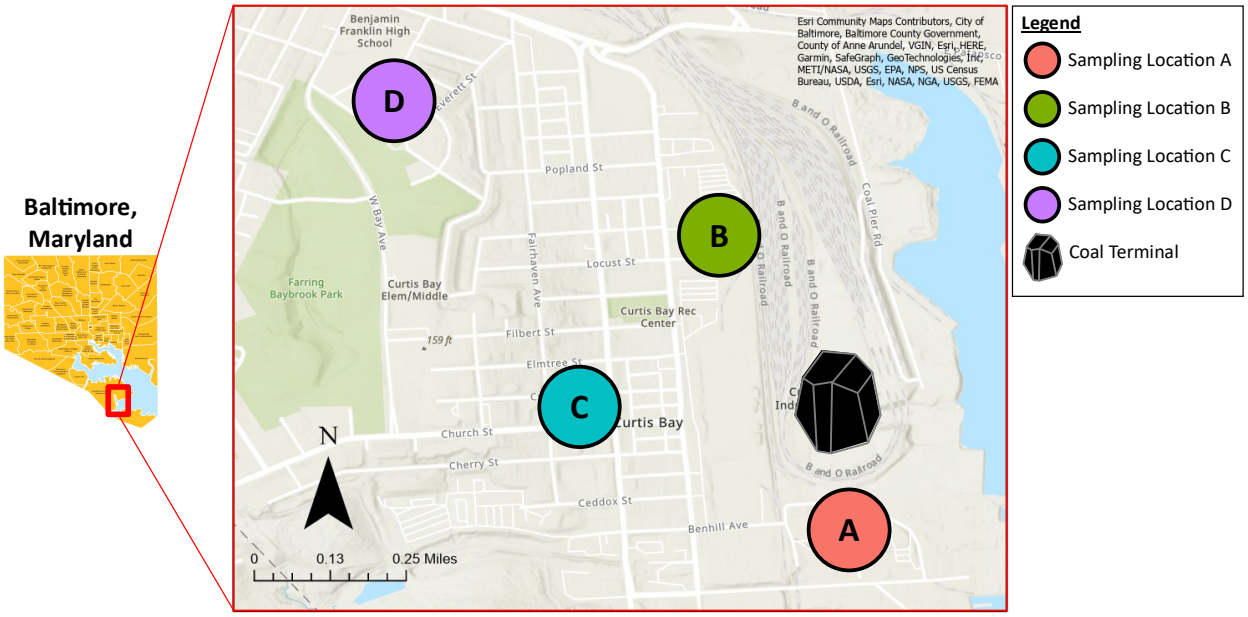

Figure 1. Approximate sampling locations of white tape collectors deployed to visibly accumulate settled dust over a 28-day period in the Curtis Bay community ranging from near the coal terminal fenceline to nearly ¾ of a mile from the coal terminal (May 3, 2023 to May 31, 2023).

Methods

Each white tape collector consists of a six-inch segment of white, double-sided adhesive poster tape (Hillman Group, Forest Park, OH, USA) adhered to a wooden shim (Nelson Wood Shims, Cohasset, MN, USA). These materials are readily available from a local hardware store.

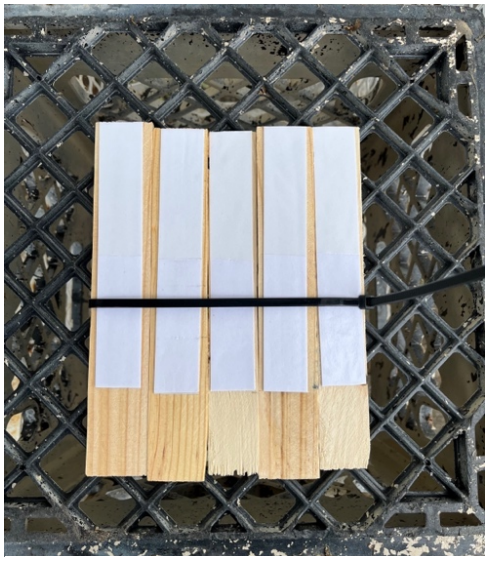

Figure 2. White tape collectors secured to a crate under a covered porch at residential Location C, approximately 1300 feet from the coal terminal in Curtis Bay, MD.

Five white tape collectors were placed at each location (Figure 2). The tape collectors were mounted side-by-side on a stable and covered (when possible) horizontal outdoor surface. Each of the five tape collectors were exposed to ambient air in Curtis Bay for varying durations: 3, 7, 13, 21, and 28 days. The first tape collector retrieval occurred at Day 2 due to logistical constraints at the site. To initiate dust collection, we removed the non-stick paper backing and recorded the time of exposure. After exposure, collectors were sealed in labeled bags (noting location, collection date, and time).

Employing an accessible, detailed method of analysis, we used light microscopy to capture close-up images of the particles accumulated on the white tape collectors. The coloration and morphology of collected material were compared to a laboratory-generated, positive control white tape collector with material from a bulk coal sample from the coal terminal in Curtis Bay. This positive control was developed and analyzed post-field collection and photography.

Two white tape collectors remained covered in the laboratory to serve as a baseline, zero days of dust accumulation in Curtis Bay. Due to color variations (i.e., slight yellowing) between the white tape used, a different baseline tape collector corresponded with each batch constructed. Following the final, 28th day retrieval, we photographed each tape collector under uniform laboratory lighting. Using ImageJ software (version 1.54g)[1] we measured the mean grey value of each tape collector image, effectively assigning a brightness score to the exposed tape. The inverse of the brightness score provided a darkness score–a correlate for the amount of settled dust. We then divided the darkness score for each sample by the darkness score of its corresponding baseline/Day 0 tape collector.

Using non-parametric Mann-Whitney U tests, we compared the distributions of darkness scores relative to baseline between locations. Via simple and multiple linear regression, the change in darkness score relative to baseline over time at each of the four locations and the rate of change in darkness between sampling locations were examined.

Results

Visually comparing the white tape collectors, we can see a decreasing trend in darkness of settled material with increasing distance from the coal terminal, as well as increasing darkness with increasing days exposed in the community (Figure 3).

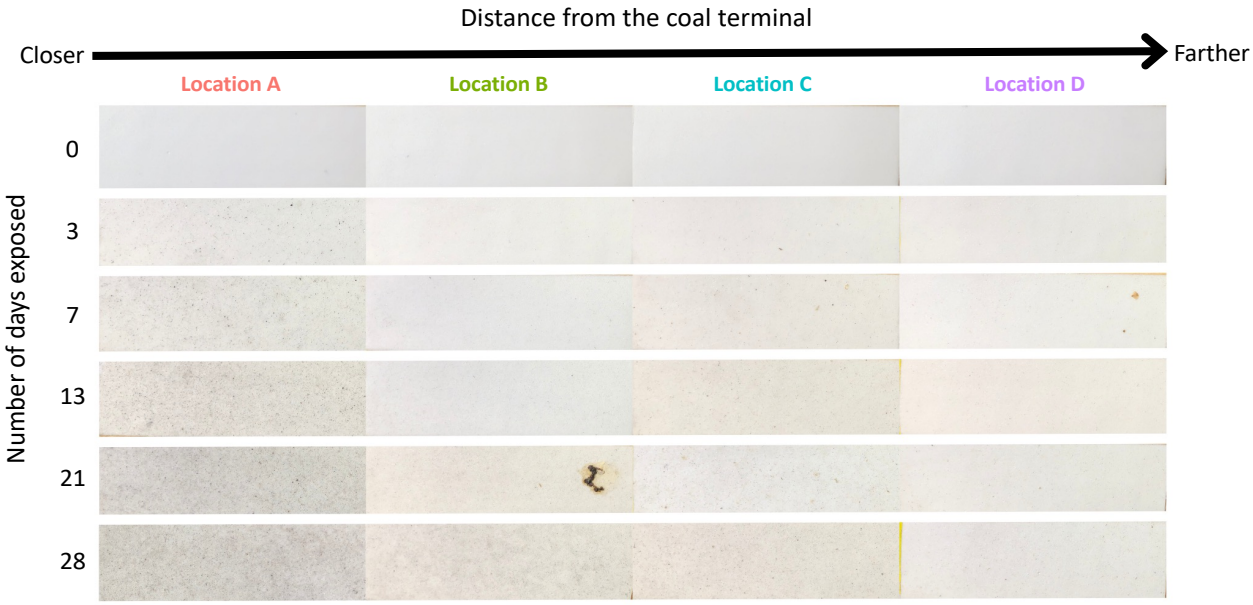

Figure 3. Grid of white tape collectors used to visibly capture settled dust in coal terminal fenceline and residential areas of Curtis Bay, MD. Note increasing distance from the coal terminal from left to right and increasing number of days exposed to accumulate settled dust from top to bottom.

We used light microscopy to examine the color and morphology of settled dust on the white tape and compare collected particles to the bulk coal positive control material from the coal terminal (Figure 3). Note the black coloration and angular morphology of the bulk coal positive control material. Several particles collected at Locations A, C, and D exhibited matching black coloration, sheen in light, and angular morphology. Locations C and D are residential sampling sites approximately 1300 feet and 3800 feet, respectively, away from the coal terminal. Qualitatively, more black particles were collected on white tape collectors nearer to the facility, compared to further away in residential sampling locations (Figure 4).

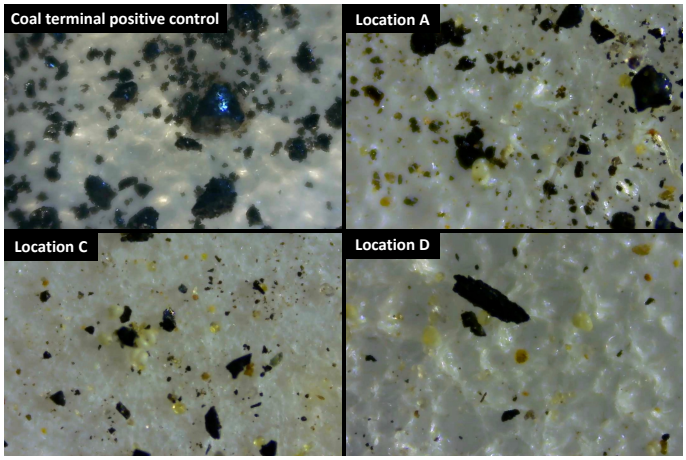

Figure 4. Light microscopy images of the positive control sample from the coal terminal (top left) and putative coal settled dust collections from Curtis Bay, MD. Note coal terminal fenceline Location A (top right), proximal residential Location C (bottom left), and distal residential Location D (bottom right).

We used light microscopy to examine the color and morphology of settled dust on the white tape and compare collected particles to the bulk coal positive control material from the coal terminal (Figure 3). Note the black coloration and angular morphology of the bulk coal positive control material. Several particles collected at Locations A, C, and D exhibited matching black coloration, sheen in light, and angular morphology. Locations C and D are residential sampling sites approximately 1300 feet and 3800 feet, respectively, away from the coal terminal. Qualitatively, more black particles were collected on white tape collectors nearer to the facility, compared to further away in residential sampling locations (Figure 4).

We also used ImageJ software (version 1.54g) to assign a darkness value to each of the white tape strips as a correlate of dust accumulation to compare between sampling sites and amount of time exposed to gather settled dust. Note Locations A and B are near the fenceline of the coal terminal, Location C is a Curtis Bay community resident's home, and Location D is near Benjamin Franklin High School.

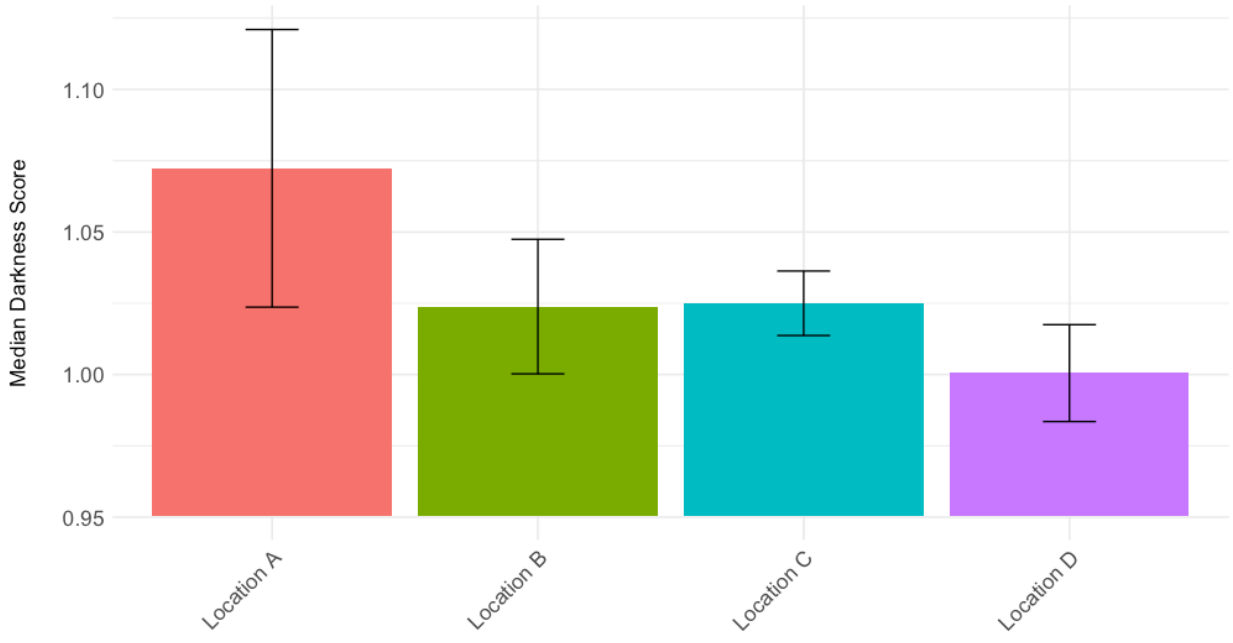

Figure 5. Median darkness value of white tape strip collectors at each sampling location over the 28-day sampling period in Curtis Bay, MD. Note y-axis minimum at 0.95.

Median darkness scores for Locations A, B, C, and D, respectively, were 1.072, 1.024, 1.025, and 1.001 (Figure 5). The distribution of darkness scores at Location A was significantly greater than that of Locations B (Mann-Whitney U = 204, $n_A = n_B = 15$, $p < 0.001$), C (Mann-Whitney U = 206, $n_A = n_C = 15$, $p < 0.001$), and D (Mann-Whitney U = 225, $n_A = n_D = 15$, $p < 0.001$). The distribution of darkness scores at Location D were also significantly lower than the other three locations (Location B: Mann-Whitney U = 162, $n_D = n_B = 15$, $p < 0.05$; Location C: Mann-Whitney U = 198, $n_D = n_C = 15$, $p < 0.001$). Locations B and C did not significantly differ. However, the median darkness relative to baseline is higher at Location C compared to Location B.

Univariate and multivariate linear regression were used to determine if days exposed to accumulate settled dust and sampling location significantly predict darkness score relative to baseline/Day 0 (Figure 6). The multiple linear regression model was:

$$\hat{Y} = 1.061 + 0.00218\ (Days\ Exposed) - 0.0238\ (Location)$$

The overall model was statistically significant (adjusted $R^2 = 0.7614$; $F(2, 57) = 48.07$; $p < 0.001$). As the number of days exposed increased, the darkness score significantly increased ($\beta = 0.00218$, 95% CI [0.00145, 0.00290], $p < 0.001$; Table 1; Figure 6). We also observed a statistically significant decrease in average darkness score with increasing distance from the coal terminal over 28-day time period ($\beta = -0.0238$, 95% CI [-0.0297, -0.0178], $p < 0.001$; Table 1; Figure 5).

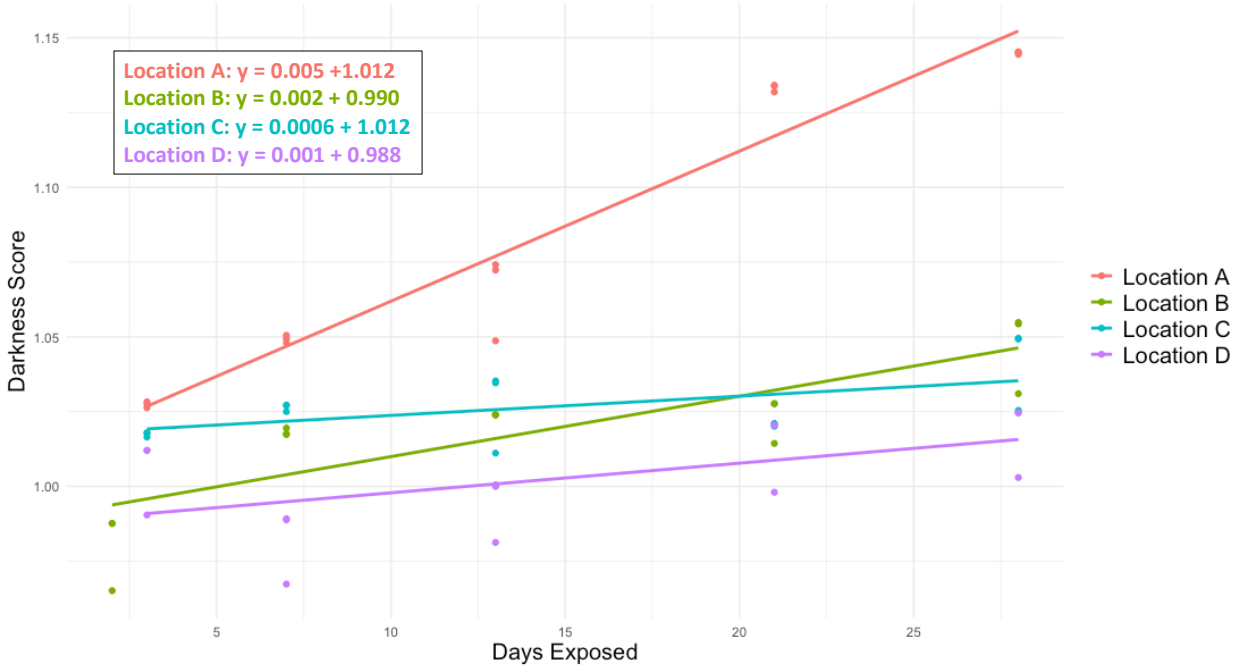

Figure 6. Multiple linear regression plot depicting the change in darkness scores assigned to white tape collectors by sampling location and days exposed to accumulate settled dust in Curtis Bay, MD.

Table 1. Summary of multiple linear regression model predicting darkness score relative to baseline.

Variables	β	Std. Error	t Value	Pr(>|t|)
Days exposed	0.0021811	0.0003611	6.04	< 0.001
Location	-0.023762	0.0029643	-8.016	< 0.001
Intercept	1.060898	0.0096214	110.265	< 0.001
Residual SE	0.02567	F (2, 57)	50.25	
Multiple R	0.6381	p-value	< 0.001	
Adjusted R2	0.6254			

Discussion and Conclusions

Known rules of atmospheric physics dictate how far atmospheric particles travel. The process of removal of particles from the atmosphere, dry deposition, results from a combination of gravitational settling and turbulent diffusion transporting particles to the Earth's surface where they stick (rain causes wet deposition, not relevant here).[2] The diameter of a particle in the atmosphere is usually defined as the equivalent aerodynamic diameter – assuming unit density and spherical shape, and these determine the relevant physics. The bulk of coal dust usually lies between 10 and 100 (or a few 100) μm in diameter. The larger the particle, the greater the role of gravitational settling. Small particles (0.1 to 1 μm diameter) are removed via turbulent diffusion, not gravitational settling, and generally persist in the lower atmosphere for hours or days. For coal dust, 10 μm particles fall at a rate of about 1 cm s^{-1}, while 100 μm particles fall at a rate of about 100 cm s^{-1}.

Video evidence shows that coal dust is lofted to 100 to 300 m above the surface. The 10 μm particles will fall to the surface in ~1–3 x 10^4 s (about 15 min to an hour) while 100 μm particles will fall in 100 to 300 s. For a typical wind speed of 5 m s^{-1} (~11 MPH) the transport distance of 100 μm particles will be 500 to 1500 m (~0.3 to 1.0 miles); smaller particles will travel farther, and larger particles will fall out closer to the coal terminal. It is possible that the plume of coal dust will sometimes pass over the samplers closest to the fence line, but for large sample sizes, we do not expect many small (~ 1 μm or less) particles to fall out near the coal terminal or to be collected by white tape collectors. The largest particles will, on average, be collected close to the coal pile. Most of Curtis Bay, Brooklyn, and Hawkins Point lies within ~2 miles (~3 km) of the coal terminal. We expect to collect many coal dust particles in the size range of 10 to 100 μm diameter at all of these sites. Beyond ~2 miles, a combination of dispersion and dry deposition will greatly limit the collection of coal dust. The darkness score decreasing with distance from the coal pile is consistent with known gravitational settling velocities – most of the particles are big and fall from the air within a few hundred yards of the source leaving less coal dust to fall farther away.

We employed white tape collectors to capture settled dust in the Curtis Bay community at varying distances away from the coal terminal and durations over a 28-day period. This is an accessible, low-cost, and demonstrative method which supports longstanding community observations and nuisance from dark dust settling on their homes, property, vehicles, and outdoor public spaces.

An important limitation of the ImageJ darkness scoring is the impact of variable lighting between images of the white tape strips, despite attempts to maintain a consistent lighting environment. Visually, the darkening of white tape strips by sampling location and time exposed is clearly evident, but not consistently reflected in the ImageJ darkness scoring. For example, the Day 28 darkness score relative to the Day 0 baseline at Location C is lower than Location D, while the white tape collector at Location C is visibly darker (Figure 7). Even in somewhat variable lighting conditions, we obtained statistically significant findings. In a controlled studio lighting environment, this method can be even more reliable and powerful.

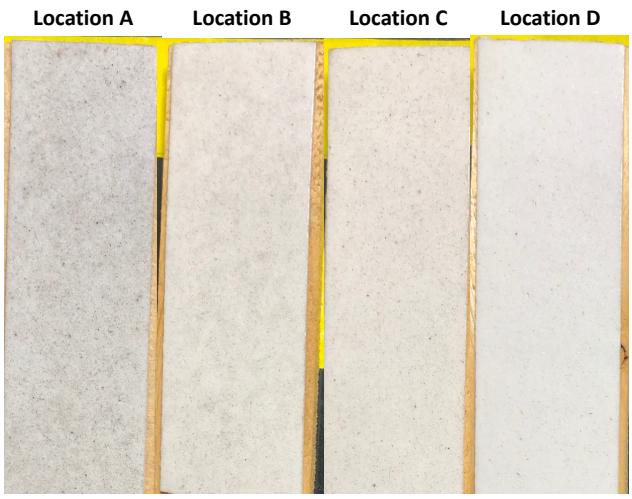

Figure 7. Images of settled dust collection white tape after 28 days of exposure to accumulate dust in Curtis Bay, MD, USA. Location A is at the fenceline of the coal terminal, Location B is in a peri-residential area near the coal terminal fenceline, and Locations C and D are in residential areas of Curtis Bay.

Both visually and statistically, accumulation of dark dust, which matches the appearance of confirmed coal particles in color and morphology, decreases moving further from the coal terminal and increases with the number of days exposed. Location A, nearest to the coal terminal, also had the highest rate of accumulation compared to other three sampling locations.

Moving beyond observation of dark dust, the coming section will describe efforts to definitively identify and characterize particulates on surfaces and in ambient air in the Curtis Bay community.

Surface particulate tape lift and passive ambient particle accumulation (PAPA) sampling

Introduction

Building upon the white tape collections to accumulate dark dust, we employed further sampling methods to determine more definitively: (1) the types of particles in settled dust, (2) if the presence of coal is confirmed offsite of the coal terminal, (3) how quickly coal dust may accumulate, and (4) at what distances from the coal terminal does coal dust accumulate. Samples collected in both residential and industrial areas in Curtis Bay were then imaged via scanning electron microscopy (SEM) and characterized via energy dispersive X-ray spectroscopy (EDX).

Methods

Sampling settled dust

Two settled dust sampling methods were used: surface particulate tape lifts (hereafter tape lifts) and passive ambient particle accumulation (PAPA) sampling. Tape lifts are the direct lifting of settled dust particles from surfaces, whereas PAPA samples were left on a surface to accumulate settled dust from ambient air over a three-day period. We conducted multiple tape lift field campaigns for both methods, as follows:

- Surface particulate tape lift campaigns (Figure 8)
    - August 22, 2023 – sampled by M. Aubourg; Locations 1 and 2

- September 25, 2023 – sampled by South Baltimore youth climate activist, G. Sawtell, M. Aubourg; Locations 1, 2, 3

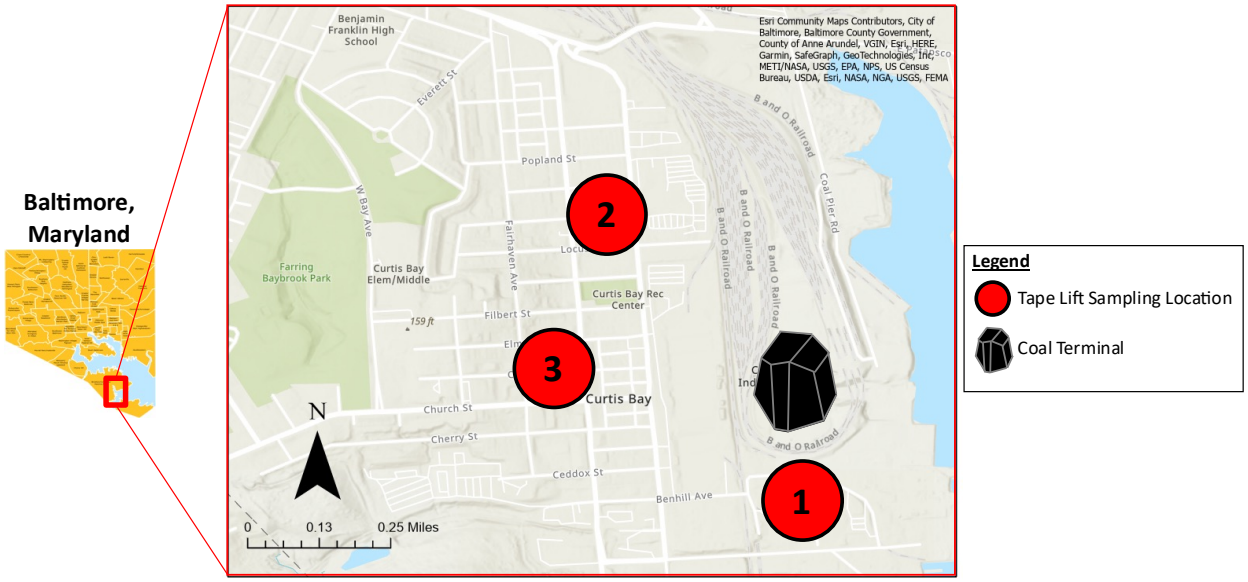

Figure 8. Approximate surface particle tape lift sampling locations in Curtis Bay, MD. Locations 1 and 2 were sampled during the August 22, 2023 field sampling campaign. All three locations were sampled during the September 25, 2023 field sampling campaign.

- Passive ambient particle accumulation (PAPA) sampling campaign (Figure 9)
  - October 26, 2023 to October 29, 2023 – G. Sawtell and M. Aubourg; Locations A through E

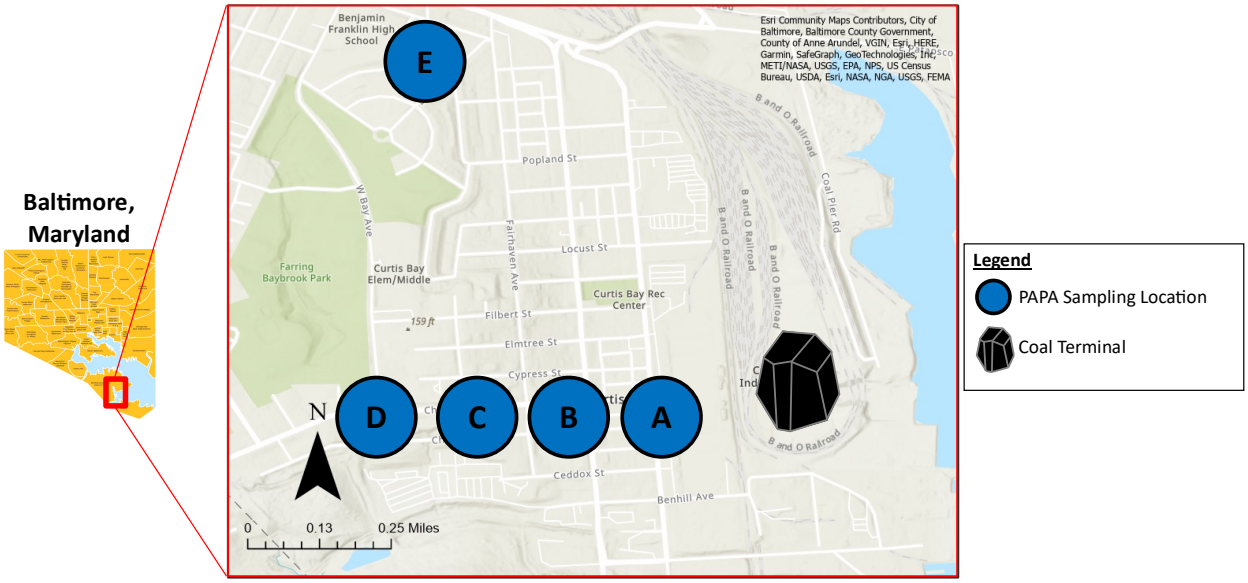

Figure 9. Approximate passive ambient particle accumulation (PAPA) sampling locations in Curtis Bay, MD. All locations accumulated settled dust over a 3-day period (October 26, 2023 to October 29, 2023).

To facilitate consistent field sampling materials and protocol between sampling campaigns, we constructed field sampling kits for both tape lifts and PAPA samples. Small (1 to 1.5 inch) segments of double-sided conductive carbon tape (Ted Pella, Inc., Redding, CA, US) were sealed in labeled (noting sample identifier, date/time of collection) PetriSlides (Millipore, Merck KGaA, Darmstadt, DE). Sampling

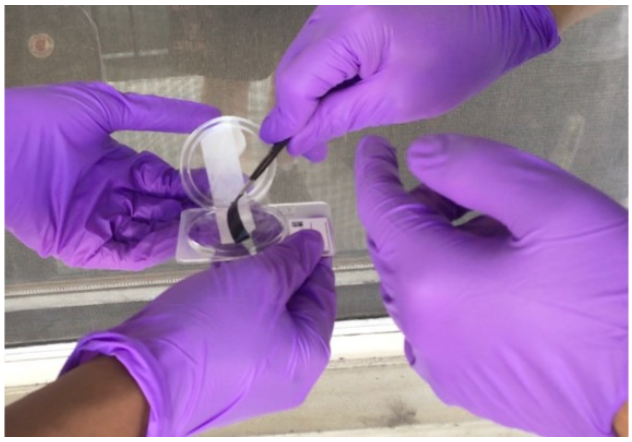

Figure 10. South Baltimore youth climate activists led the initial implementation and protocol refinement of the surface particle tape lift method used in subsequent tape lift sampling campaigns. Note the use of gloves during collection as the segment of carbon tape is being carefully removed from the sampling kit for field collections on the window sill below.

kits were developed in a sterilized and cleaned biosafety cabinet in a room where no positive control material had entered. Two lab blanks were developed at the start and completion of creation of sampling kits for collection methods. Two lab blanks were created during sample processing following field collection for tape lift field campaigns.

The tape lift protocol used was adapted from the American Society for Testing and Materials Standard Practice for Sampling for Particulate Contamination by Tape Lift (ASTM E1216-21).[3] South Baltimore youth climate activists were the first to employ the tape lift method in the community and led the refinement of this protocol for subsequent sampling campaigns. At each field sampling site (Figure 8), we obtained one field blank by exposing carbon tape to ambient air for approximately 30 seconds. Two tape lifts were collected from the same sampling surface. Only non-porous and dry surfaces were sampled for accumulated dust (Figure 10).

With PAPA sampling, two segments of double-sided conductive carbon tape were left exposed to accumulate settled dust for three days (October 26, 2023 to October 29, 2023). One field blank was collected at each site by exposing the tape to ambient air for approximately 30 seconds. A white tape collector was co-located at each sampling site to examine visible accumulation of settled dust, which is not possible against the black carbon tape (Figure 11).

For all field sampling campaigns, PetriSlides containing field samples were stored in sealed containers and individual packaging to minimize the possibility for cross-contamination. Between interactions with sampling media, samplers' hands and materials were cleaned with wipes and 70% ethanol, respectively. New gloves were donned between deployment of all field blanks and tape lifts or PAPA deployments. Sampling campaigns are documented by chain of custody developed by the BSPH team.

Following field collections, positive controls were developed using (1) National Institute of Standards and Technology (NIST) subbituminous coal standard reference material (SKU 2682c; NIST certified bulk analysis 66% carbon, 6% ash, and 0.49% sulfur) and (2) a bulk coal sample from the coal terminal in Curtis Bay.

Figure 11. Passive ambient particle accumulation (PAPA) sampling at Location C, a residential sampling site in Curtis Bay, MD (October 26, 2023 to October 29, 2023). Note the two conductive carbon tape segments with co-located white tape collector to visualize settled dust.

Settled dust imaging and particle characterization

Blanks, controls, field collections, and their particles were imaged via scanning electron microscopy (SEM). Particles were characterized via energy X-ray dispersive spectroscopy (EDX) at the University of Maryland Advanced Imaging and Microscopy Laboratory (UMD AIM Lab) at the Johns Hopkins University Materials Characterization and Processing Facility operated by a trained analyst from BSPH.

A small segment (approximately 8 x 8 mm) of each tape lift or PAPA sample was mounted and imaged with secondary electrons (UMD AIM Lab and BSPH) and backscattered electrons (UMD AIM Lab).

Operators from the UMD AIM Lab and BSPH performed a randomized, systematic analysis of tape lifts and PAPA samples to obtain semi-quantitative information about the proportion of coal dust particles loading each sample. A 10x10 grid was superimposed upon a low magnification (30-45x) image at the center of each mounted sample. AIM Lab operators randomly selected 10 grid cells, then imaged and analyzed five to 10 particles (5-100 µm diameter) at random from each cell (Hitachi SU-70 FEG SEM; Bruker XFlash 6-60 EDS). The BSPH operator randomly selected three grid cells (350 to 500x) on each sample, then randomly selected higher magnification sections (2500x) to image and analyze three to five particles (500 nm to 50 µm diameter) from the field of view, magnifying when needed (JEOL JSM-IT700HR InTouchScope™ Field Emission SEM; EDAX Octane Elect EDS/EDX System).

Operators from BSPH conducted an initial exploratory analysis of PAPA samples to investigate the particle types deposited on the samples. Particles analyzed in exploratory analysis do not overlap with particles analyzed in systematic, randomized analysis.

Particles from field collections were compared to the NIST sub-bituminous coal standard reference material (SRM) and the bulk coal sample from the coal terminal in Curtis Bay. Note the heterogeneous composition of bulk coal with various types of ranks of coal (i.e., lignite, sub-bituminous, bituminous, anthracite, from least to greatest carbon content).

Particles on the NIST sub-bituminous SRM had the characteristic worn crystalline structure and size distribution of coal and coal dust (Figure 12A). The elemental composition is typical of bulk, sub-

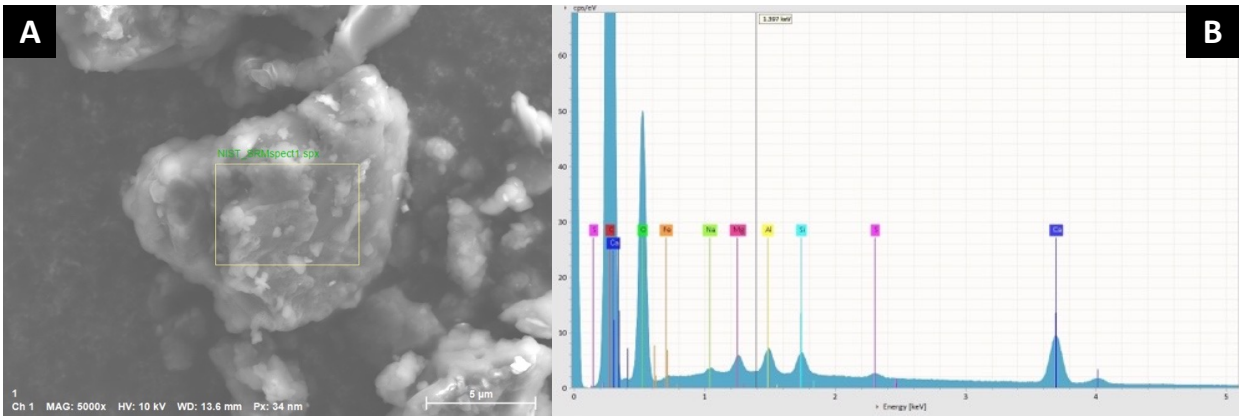

Figure 12. A. Example of sub-bituminous coal particle from NIST Standard Reference Material (SRM) at 5000x magnification. Note worn crystalline shape. **B.** Elemental analysis via energy dispersive X-ray spectroscopy (EDX) of the NIST SRM coal particle. The composition of this particle is, to the nearest percent, 68% carbon (C), 24% oxygen (O), 6% calcium (Ca), and 1% each aluminum (Al), silicon (Si), sulfur (S), and iron (Fe). Compositions are expressed by mass, so 1 lb. of coal would contain 0.68 lb. carbon etc.

bituminous coal, similar to the NIST certified content: 68% carbon (C), 24% oxygen (O), 6% calcium (Ca), and 1% each aluminum (Al), silicon (Si), sulfur (S), and iron (Fe) (Figure 12B).

Next, we analyzed the bulk coal sample from the coal terminal in Curtis Bay. First, we examined large sections of the 8x8 mm sample of carbon tape under low (30-43x) magnification to verify that usable numbers of particles had adhered to the tape, and that at least some of them had the size and shape of coal or coal dust as verified with the NIST SRM (Figure 13).

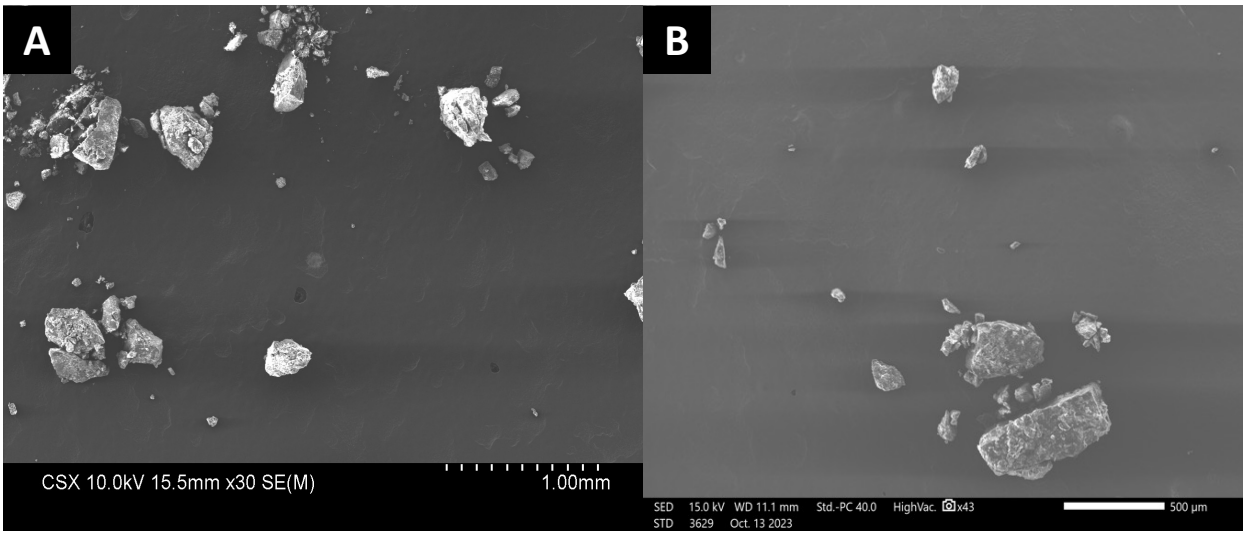

Figure 13. Low magnification (30x and 43x, respectively) scanning electron microscopy (SEM) images of positive control bulk coal material from the coal terminal in Curtis Bay, MD. SEM images taken at the UMD AIM Lab **(A)** and by the BSPH operator **(B)**. Note worn crystalline shape and approximately 5 µm < L < 500 µm size (L refers to the length of the longest visible dimension).

Several particles were then selected at random to image under high magnification and to determine elemental content. Their composition was consistent with bituminous coal, having a slightly higher carbon content than sub-bituminous coal: 79% C, 14% O, 3% N, 1% Fe, 1% S (Appendix Figure 1). One speck with a different morphology was analyzed and found to be nearly pure carbon (Appendix Figure 2). This is consistent with anthracite: 88% C, 8% O, 3% N, 0.5% S.

Several polluting sources surround the Curtis Bay community including residential diesel truck traffic, heavy machinery operation, and multiple coal-fired or waste-to-energy power plants. To demonstrate that the method would not misclassify other carbon-rich particles as coal dust, we show an example of soot on a gypsum particle[4] and fly ash[5,6] (Appendix Figure 3).

The elemental composition of soot is predominantly carbon, however, the size and shape are dramatically different. Fly ash is comprised predominantly of oxygen with much less carbon content than a coal particle. Similarly to soot, the spherical morphology differ drastically to coal and crustal particles.

The conductive carbon tape used for settled dust sampling also contains high carbon content with some oxygen and trace amounts of aluminum (Al) and silicon (Si), per the manufacturer and EDX of carbon tape (BSPH). The appearance and elemental composition of the carbon tape differs from the coal particles, making differentiation clear.

To identify a coal particle from settled dust tape lifts and PAPA samples, we employed the following criteria derived from positive control material and relevant literature, generally, classifying coal particles as sub-bituminous, bituminous, and anthracite, when possible:

- Morphology
    - Angular, transitional, or rounded[7,8]
- Particle size
    - Length of longest visible dimension of particle (L)
    - Large coarse particles (L > 10 µm)
    - Coarse particles (2.5 µm < L ≤ 10 µm)
    - Fine particles (L ≤ 2.5 µm)
- Elemental composition by weight percentage
    - Sub-bituminous coal -> 45-65% carbon (C), 30-40% oxygen (O)
    - Bituminous coal -> 65-85% C, 5-20% O
    - Anthracite -> 85% ≤ C, 15% ≥ O
    - Minor or trace elements: S, Fe, Al, Si, Cl, P, K, N

For fine particles, we must consider possible interference of the carbon tape substrate in the elemental composition obtained from EDX analysis. Elemental spectra of fine particles may be influenced by electron beam penetration into the carbon tape substrate and electron scattering, causing increased carbon peaks and decreased peaks of minor and trace elements.[7] Sellaro, Sarver, and Baxter 2015 observed higher carbon peaks in EDX spectra for smaller particles with L < 1.5 µm. Therefore, identification as a coal particle, another carbonaceous particle, or crustal material is more uncertain. In the BSPH analysis of PAPA samples, fine particles with morphology expected of coal particles, carbon content ≥ 90%, oxygen content ≤ 10%, and only three other elements identified are considered "putative coal dust," due to the identified presence of coal and assumed lognormal particle size distribution by radius. Fine particles with morphology expected of coal particles, lower carbon content and more information about particle elemental composition, aligning with coal dust, are considered to be coal dust particles. Coarse-mode particles exhibiting a similar profile (coal-like morphology, very high carbon content, few other elements identified) are also considered putative coal dust in the coarse-mode size fraction.

Results

Surface particle tape lifts

Using the tape lift method, **multiple coal particles were observed at the coal terminal fenceline (Location 1) and residential (Locations 2 and 3) sampling sites.**

Examination of lab blanks under low and medium magnification revealed no discernable crustal, mineral, or coal dust particles (Appendix Figure 4).

The tape lift segment from Location 1 near the fenceline of the coal terminal (Figure 8) revealed, under low and medium magnification, numerous particles with the morphology and size typical of coal and crustal material (Appendix Figure 4).

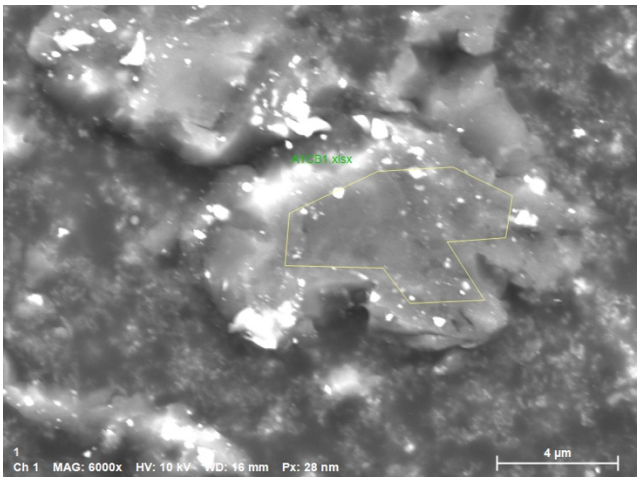

Figure 14. High magnification (6000x) scanning electron microscopy image of a coal dust particle collected on the Location 1 tape lift (August 22, 2023), near the fenceline of the coal terminal in Curtis Bay, MD. The elemental composition was 79% C, and 13% O, with Cl, N, Fe, S, and Ca comprising another 8%. Note similarity of size, shape, and composition to known coal samples.

To positively identify coal dust and to determine the relative contribution of coal dust to the total population of particles, we performed elemental analysis on randomly selected particles. As an example of a particle matching bituminous coal dust see Figure 14 that has the morphological and elemental characteristics of bituminous coal: 79% C, 13% O, 8% Cl, N, Fe, S, and Ca combined (Figure 19).

Another particle chosen at random was a conglomerate (Figure 15). Elemental analysis of various components of this particle or set of particles revealed the largest section was bituminous coal but iron and subbituminous coal were also present.

Particles that were not predominately coal were also identified on this sample. We found a small steel particle (Appendix Figure 5A) and a pair of clay particles with small (approximately 3 µm L) grains of salt (Appendix Figure 5B).

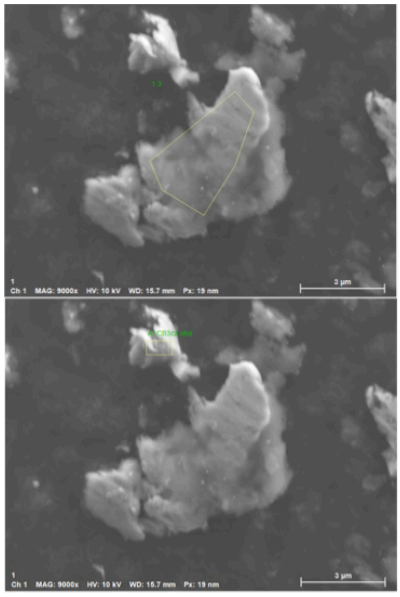

Bituminous Coal
Mass Fraction
68% C
6% O
24% Fe
~2% Ni, Si…

Sub-bituminous Coal
Mass Fraction
62% C
24% O
~10% Si, Ca, F, Fe, Na, Cl…

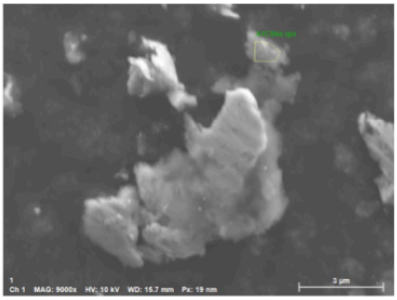

Mixed
Mass Fraction
45% Fe
32% C
12% O
~10% Ni, Si, Ca…

Figure 15. Scanning electron microscopy images (9000x) and elemental composition by Energy dispersive X-ray spectroscopy analysis of a conglomerate particle collected at Location 1 (August 22, 2023), near the fenceline of the coal terminal in Curtis Bay, MD. The yellow shapes indicate sections selected for elemental analysis.

In total, 15 particles were analyzed from the Location 1 tape lift sample collected near the fenceline of the coal terminal. Nine were predominantly coal dust, two were steel, three mineral dust (including clay) and one aluminum.

The final tape lift collection from the August 22, 2023 field sampling campaign was at Location 2, a residential sampling site near the coal terminal and directly adjacent to a heavy diesel truck route (Figure 8). Examination under low magnification reveals hundreds of particles per square mm (Figure 16). Fourteen particles were selected at random for elemental analysis; Figure 17 shows a typical bituminous coal particle and its elemental composition: 81% C, 16% O, 1% S, and trace amounts of Si, Al,

Na, Ca, Cl. A particle more consistent with the bulk composition of anthracite (Figure 18) was also found and analyzed: 88% C, 11% O, 0.6% S, and other trace elements. Of the 14 particles analyzed from residential Location 2, seven were crustal material, six were coal dust, one particle was organic matter

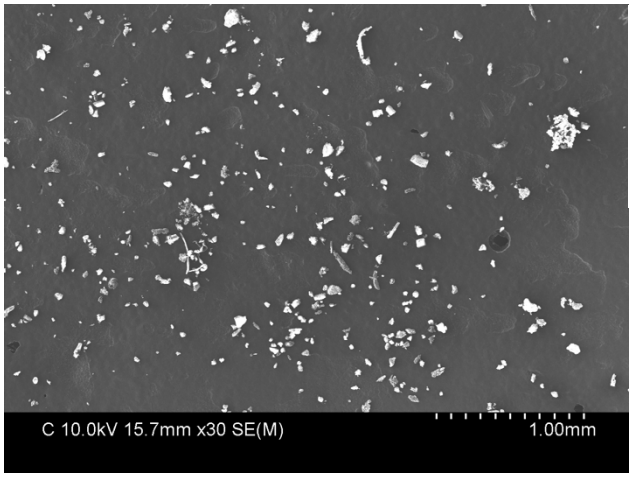

Figure 16. Low magnification (30x) scanning electron microscopy image of the tape lift from Location 2 (August 22, 2023), a residential sampling site in Curtis Bay, MD near the coal terminal and a heavy diesel truck traffic route. Hundreds of particles with the size and shape of coal and mineral are captured.

(Appendix Figure 6).

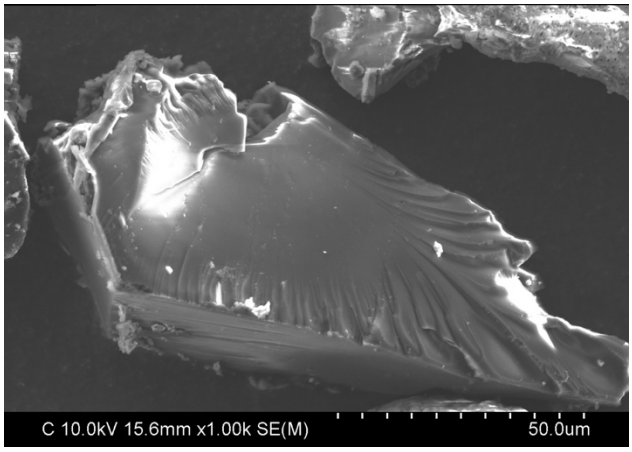

Figure 18. High magnification (1000x) scanning electron microscopy image of a particle from a tape lift at Location 2 (August 22, 2023), a residential sampling site in Curtis Bay, MD. The particle possesses the appearance and bulk elemental composition of anthracite coal: 88% C, 11% O, 0.6% S, and other trace elements.

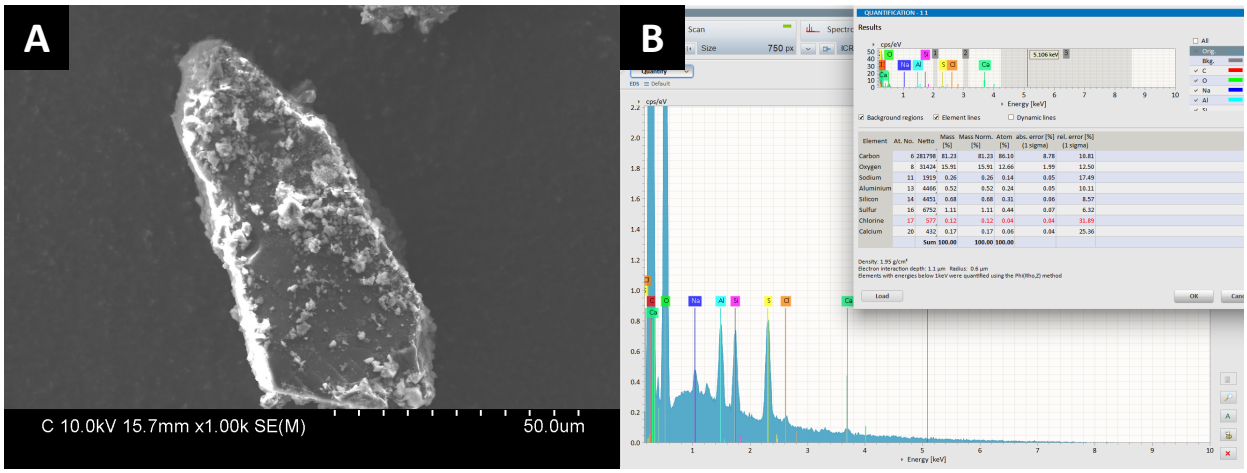

Figure 17. A. Scanning electron microscopy image of a particle from a tape lift at Location 2 (August 22, 2023), a residential sampling site in Curtis Bay, MD. The size and shape are consistent with coal dust. **B.** Energy dispersive X-ray spectroscopy elemental analysis of particle. The composition, 81% C, 16% O, 1% S, plus trace minerals confirms the identity as coal dust.

Tape lift samples at Location 3 were analyzed without the systematic protocol, utilizing an exploratory analysis. Coal dust particles were also found at this residential location which is around 1300 feet from the coal terminal.

Passive ambient particle accumulation (PAPA) sampling

Coal particles were observed at all five residential PAPA sampling locations in the Curtis Bay community in the exploratory analysis, and in the majority of samples in the systematic analysis. In both exploratory and systematic analyses, particles were randomly selected, imaged via SEM (secondary electrons), and elementally characterized via EDX for identification. Coal particles were differentiated from other observed particle types (e.g., crustal material and pollen) by morphology, size, and chemical composition.

Exploratory Analysis of PAPA Samples

Two lab blanks were developed during the creation of field sampling kits housing the conductive carbon tape. Both lab blanks were largely clear of particles except for a few fibrous or dust particles but no mineral or coal particles (Appendix Figure 7).

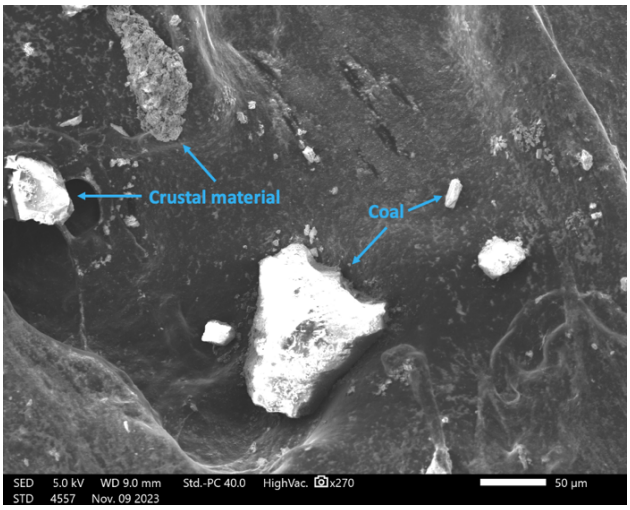

Figure 19. Moderate magnification (250x) scanning electron microscopy image of coal and crustal particles sampled at Location A, nearest site to the coal terminal and nearby industry in Curtis Bay, MD. Collected during the 3-day passive ambient particulate accumulation sampling campaign (October 26, 2023 to October 29, 2023).

We analyzed field blanks from Location A (approximately 700 feet from the coal terminal), Location C (approximately 2000 feet from the coal terminal), and Location E (approximately 3800 feet from the coal terminal). Even after approximately 30 seconds of exposure to ambient air, coal dust was found on all three field blanks, in contrast to the clean lab blanks (Appendix Figure 8). The most particles were deposited on the Location A (nearest to the coal terminal) field blank, a moderate amount were found on the Location C field blank, and the fewest particles were deposited on the Location E (furthest from the coal terminal) field blank.

Exploratory analysis of the residential Location A PAPA sample yielded primarily large size coal and crustal particles. This is expected due to the close proximity to the coal terminal (approx. 700 feet from the coal terminal fenceline) and heavy commuter and diesel traffic routes (Location A in Figure 9). Coal particles identified in the exploratory analysis at Location A included large coarse-mode, coarse-, and, putatively, fine particles (Figure 19).

The greatest diversity of particle types was observed at Locations B (approx. 1100 feet from the coal terminal fenceline) and C (approx. 2000 feet from the coal terminal fenceline), both in residential areas and near frequented community spaces. Identified dust included coal particles, crustal material, and steel (Figure 20). Multiple fine coal particles were found at sampling Location B (Figure 21). Large coarse and coarse-mode coal and crustal particles comprised the majority observed at both sites.

Similarly, to the residential locations more proximal to the coal terminal, fine, coarse, and large coarse-mode coal particles were found at Locations D (approx. 2400 feet from the coal terminal fenceline) and

E (approx. 3800 feet from the coal terminal fenceline) sampling sites. Other confirmed particle types observed include crustal material and pollen (Appendix Figure 9). The pollen particle presented a similar elemental composition to a coal particle, however, the morphology vastly differed from a coal particle, highlighting the importance of considering morphology with particle identification criteria.

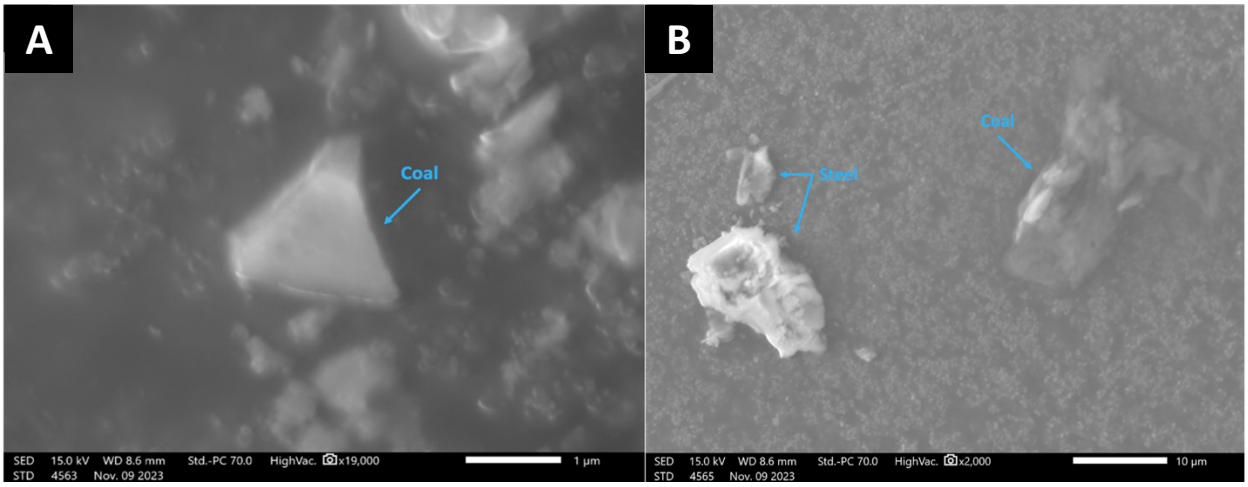

Figure 20. High (19000x and 2000x, respectively) magnification scanning electron microscopy images of a **(A)** fine (L ≤ 2.5 µm) coal particle and **(B)** large coarse steel and coal particles sampled from Location B, a residential sampling site in Curtis Bay, MD. Sample collected during the 3-day passive ambient particulate accumulation sampling campaign (October 26, 2023 to October 29, 2023).

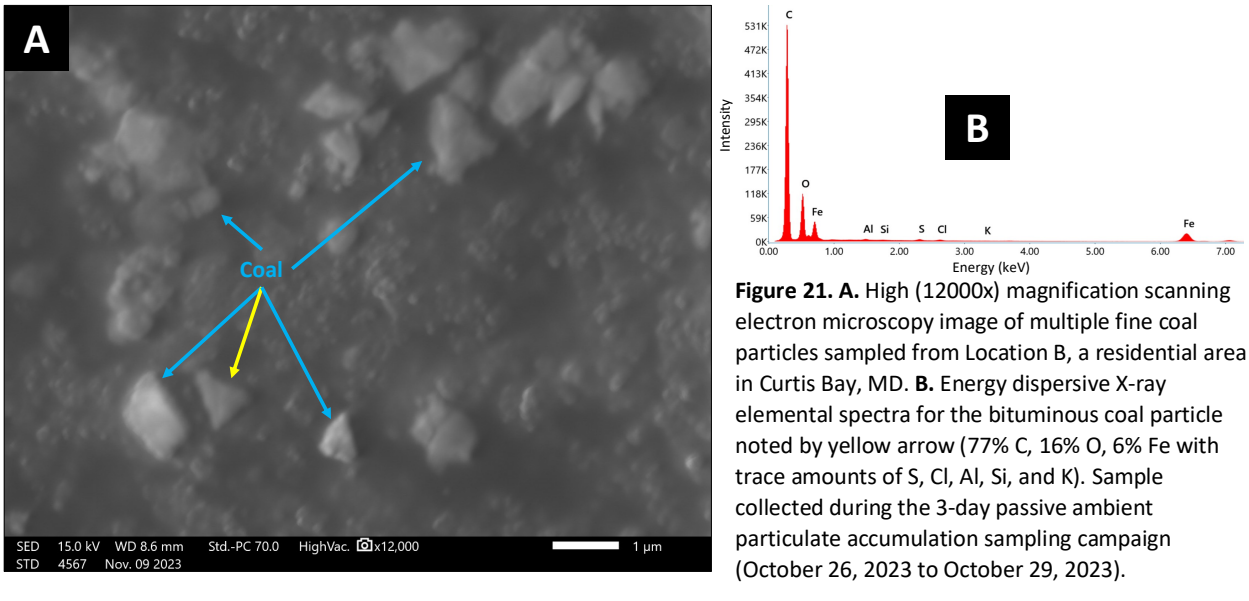

Figure 21. A. High (12000x) magnification scanning electron microscopy image of multiple fine coal particles sampled from Location B, a residential area in Curtis Bay, MD. **B.** Energy dispersive X-ray elemental spectra for the bituminous coal particle noted by yellow arrow (77% C, 16% O, 6% Fe with trace amounts of S, Cl, Al, Si, and K). Sample collected during the 3-day passive ambient particulate accumulation sampling campaign (October 26, 2023 to October 29, 2023).

In summary, our exploratory analysis of PAPA samples identified coal and crustal particles at all five sampling locations, along with steel and pollen particles (Figure 22). Large coarse, coarse, and fine coal particles were observed at all five locations, in addition to crustal material, pollen, and steel.

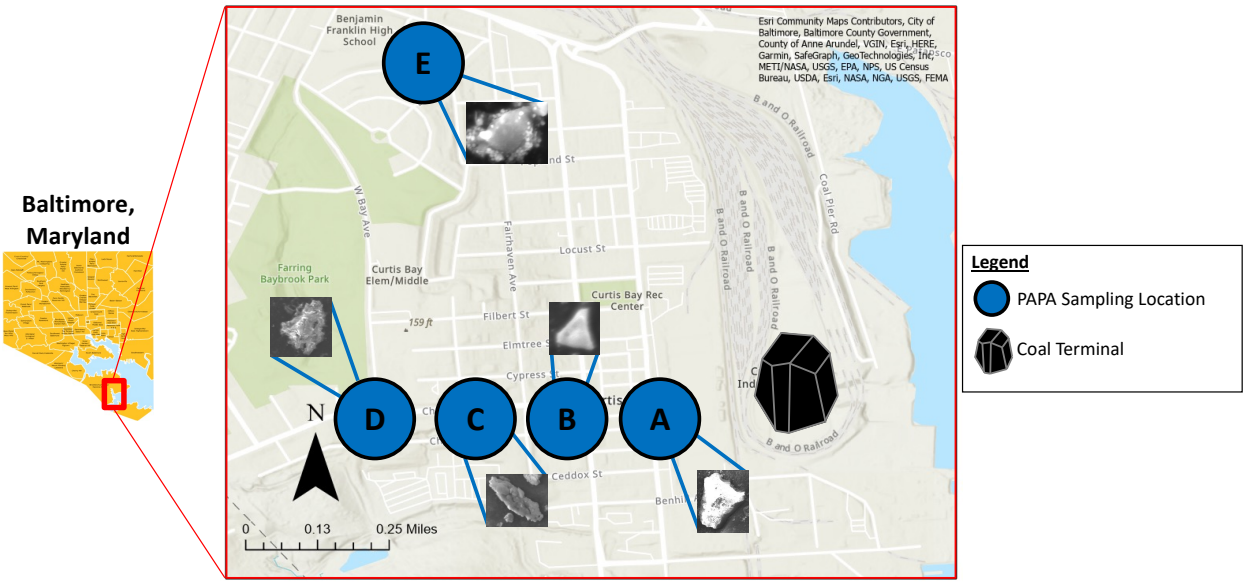

Figure 22. Map of approximate passive ambient particulate accumulation (PAPA) sampling locations with scanning electron microscopy images of coal particles (from exploratory analysis) observed at each sampling site. Samples collected during the 3-day PAPA sampling campaign (October 26, 2023 to October 29, 2023).

Systematic Analysis of PAPA Samples

We then conducted systematic analysis of 12 randomly selected particles accumulated on PAPA samples to compare identities, size fractions, and abundance of ambient settled dust accumulation at multiple locations throughout Curtis Bay. **Mirroring the exploratory analysis, coal particles of varying sizes were identified at all sampling locations** (Table 2).

Table 2. Summary of particles analyzed at each location (N=12); characterized as coal, crustal material, other particle types, and putative fine coal dust. Putative fine coal dust is characterized by particles with expected morphology of coal particles, high carbon content by mass percent from energy dispersive X-ray, and few other elemental components identified.

	Location A	Location B	Location C	Location D	Location E
Coal, n (%)	5 (42)	4 (33)	4 (33)	7 (58)	4 (33)
Crustal Material, n (%)	7 (58)	3 (25)	4 (33)	4 (33)	3 (25)
Other, n (%)	0 (0)	1 (8)	4 (33)	1 (8)	4 (33)
Putative coal dust, n (%)	0 (0)	4 (33)	0 (0)	0 (0)	1 (8)

Location A (approx. 700 feet away from the coal terminal fenceline) is a residential sampling location nearest to the coal terminal and on a neighborhood block with heavy commuter and diesel truck traffic routes directly to the east and west. At Location A, 42% (n = 5 particles) of particles analyzed were identified as coal (Table 2), primarily fine particulate matter coal (Table 3). The majority of particles at this location were identified as crustal material (n = 7, 58%; Table 2).

Location B (approx. 1100 feet away from the coal terminal fenceline) is also a residential sampling site, near public community space and several other homes. Most particles identified at this location were coal (n = 4, 33%) and putative coal dust (n = 4, 33%) (Table 2; Appendix Figure 10).

Table 3. Size distributions of coal particles identified at each passive ambient particle accumulation (PAPA) sampling location.

	Location A (N = 12)	Location B (N = 12)	Location C (N = 12)	Location D (N = 12)	Location E (N = 12)
	($N_{large\ coarse}$ = 3)	($N_{large\ coarse}$ = 3)	($N_{large\ coarse}$ = 1)	($N_{large\ coarse}$ = 3)	($N_{large\ coarse}$ = 2)
Large Coarse Coal n (%$_{total\ large\ coarse\ at\ location}$)	1 (33)	1 (33)	0 (0)	2 (67)	1 (50)
	(N_{coarse} = 6)	(N_{coarse} = 4)	(N_{coarse} = 3)	(N_{coarse} = 5)	(N_{coarse} = 3)
Coarse Coal n (%$_{total\ coarse\ at\ location}$)	1 (17)	0 (0)	0 (0)	2 (40)	1 (33)
	(N_{fine} = 3)	(N_{fine} = 5)	(N_{fine} = 8)	(N_{fine} = 4)	(N_{fine} = 7)
Fine Coal n (%$_{total\ fine\ at\ location}$)	3 (100)	3 (60)	4 (50)	3 (75)	2 (29)

Most coal particles identified were fine coal particles (n = 3; Figure 23) with one large coarse-mode coal particle (Table 3). Crustal material comprised 25% of particles analyzed with 3 particles identified. The most putative coal dust particles were identified at this location in both coarse and fine size fractions.

At Location C (approx. 2000 feet away from the coal terminal fenceline), a residential sampling site near a community church, there was an even distribution of coal, crustal, and other particles (n = 4, 33%; Table 2). All coal particles identified were of fine particulate size fraction (Figure 24; Table 3).

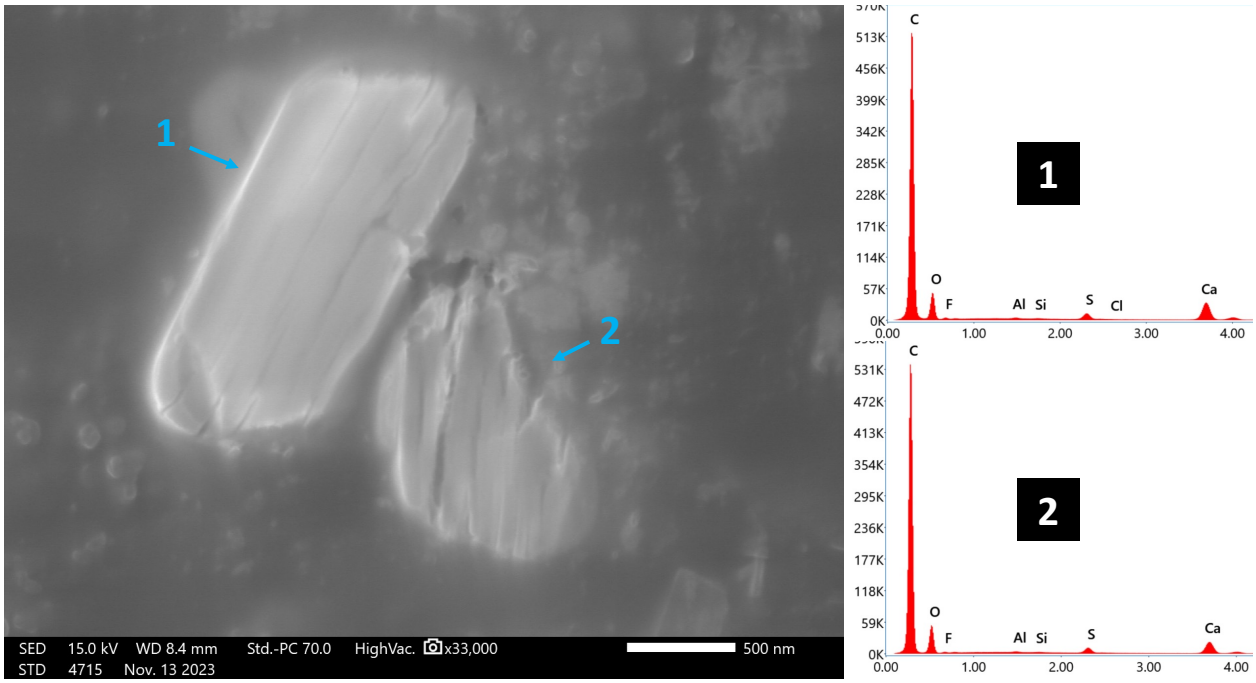

Figure 23. High (33,000x) magnification scanning electron microscopy images of fine (L ≤ 2.5 µm) coal particles observed at Location B, a residential site in Curtis Bay, MD. Note angular and crystalline morphologies. Corresponding energy dispersive X-ray spectra on the right for each particle, confirming the elemental composition of coal. Sample collected during the 3-day passive ambient particulate accumulation sampling campaign (October 26, 2023 to October 29, 2023).

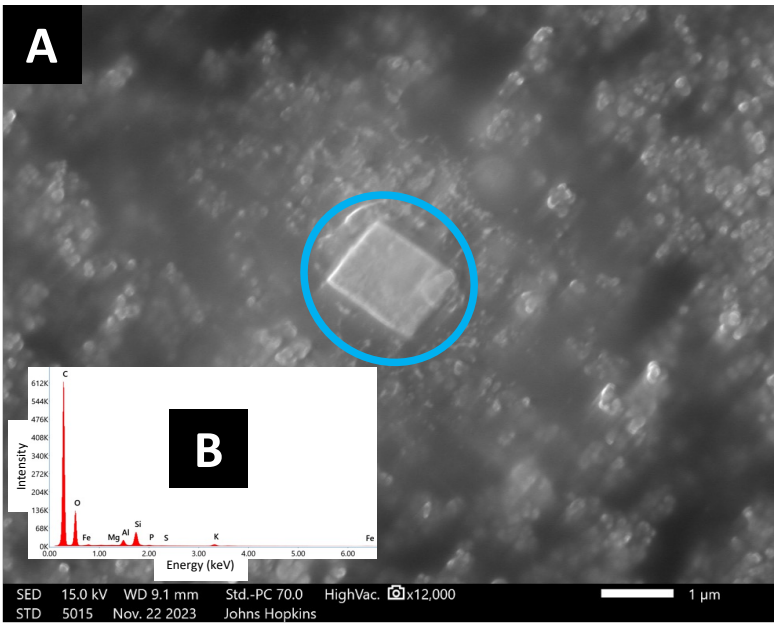

Figure 24. A. Example of fine (L = 1.678 µm) bituminous coal dust particle (blue circle) collected from passive ambient particulate accumulation (PAPA) sampling at Location C, a residential site in Curtis Bay, MD (October 26, 2023 to October 29, 2023). **B.** Energy dispersive X-ray spectra for the particle. Elemental composition: 80% C, 17% O, 1% Si, and ≤ 0.61% each Al, K, Mg, Fe, P, S. ***Note***: Blue circle indicates particle analyzed, not location of beam for EDX analysis.

Coal dust comprised the majority of particles (n = 7, 58%) identified at Location D, another residential sampling site near to a major community park (approx. 2400 feet away from the coal terminal fenceline). Large coarse (n = 2), coarse (n = 2), and fine (n = 3) coal particles were quite evenly distributed across the size distribution at this location (Table 3).

Location E (approx. 3800 feet away from the coal terminal fenceline) is the farthest PAPA sampling site from the coal terminal, near the local high school and surrounded by residential streets. Four coal particles, mostly fine particles (n = 2) and including both large coarse (n = 1) and coarse-mode (n = 1) particles, were identified at this location (Figure 25; Tables 2 and 3). Other particles identified include pollen and crustal material. Coal PM2.5 sources of accumulation at this site include the coal terminal and nearby trains frequently carrying coal to the coal terminal and leaving the facility. Location E is the nearest to coal-carrying train lines which are proven significant sources of $PM_{2.5}$ air pollution.[9,10]

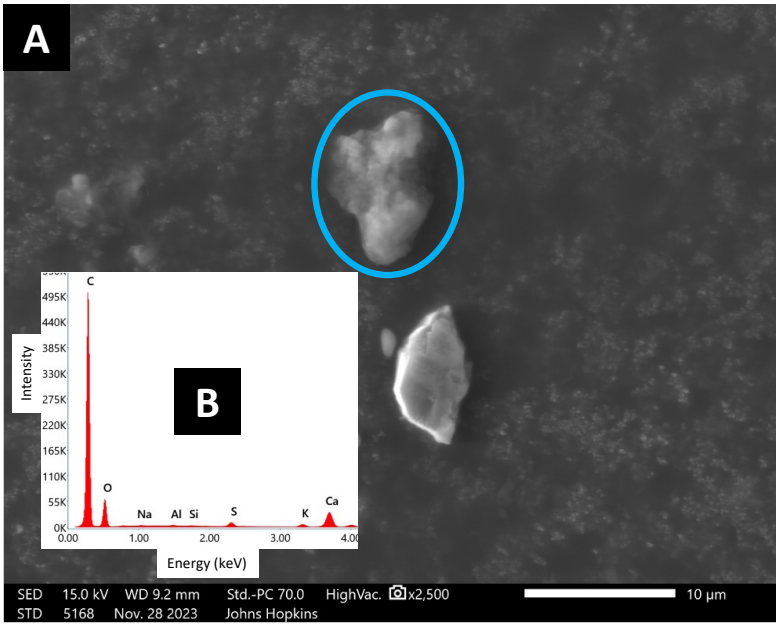

Figure 25. A. Example of large coarse-mode (L = 10.24 µm) bituminous coal dust particle (blue circle) collected from passive ambient particulate accumulation (PAPA) sampling at Location E, a residential site in Curtis Bay, MD, furthest from the coal terminal (October 26, 2023 to October 29, 2023). **B.** Energy dispersive X-ray spectra for the particle. Elemental composition: 83% C, 12% O, 4% Ca, and ≤ 0.57% each K, S, Na, Al, Si. ***Note***: Blue circle indicates particle analyzed, not location of beam for EDX analysis.

Conclusions

We employed two sampling methods to collect samples of settled dust in the Curtis Bay community: surface particulate tape lifts and passive ambient particle accumulation (PAPA) sampling. Multiple field sampling campaigns of tape lifts occurred in 2023 with one field campaign of PAPA sampling. With both methods, coal dust was observed via morphology with SEM imaging, and via elemental composition with EDX on 8 out of 8 (100%) samples and all sampling locations.

Through this analysis, we confirmed that coal dust is substantial contributor to settled dust from ambient air in the community in size fractions ranging from large coarse, coarse, and fine particulate matter. Other particle types identified were crustal or soil material, pollen, and particulates related to nearby industrial activity including as aluminum and steel.

The presence of coal was identified near the coal terminal fenceline, and approximately 600, 11oo, 2000, 2400, and 3800 feet away from the coal terminal. Due to the PAPA sampling method, we confirmed that coal dust accumulates upon settled surfaces from ambient air after just a three-day period. Finding coal dust particles on field blanks exposed to ambient air for approximately 30 seconds suggests constant contributions of coal dust to air pollution in the community, possibly outside of transient fugitive dust emission events.

Sampling locations included coal terminal fenceline sites, but primarily residential and community spaces. Again, coal particulate matter was identified at all sampling sites–a finding to support community-identified concerns with possible health effects of coal dust.

The strength of the systematic analysis is limited by the small sample size of 12 particles per PAPA sample, as well as the findings of putative coal dust, causing some uncertainty to the identity of deposited particles. However, certain confirmations of coal particles at all sampling sites still fully validates community concerns with the presence and impact of coal dust in the community and offsite of the coal terminal.

References

1. Schneider CA, Rasband WS, Eliceiri KW. NIH Image to ImageJ: 25 years of image analysis. *Nature Methods*. 2012/07/01 2012;9(7):671-675. doi:10.1038/nmeth.2089
2. Seinfeld JH, Pandis SN. *Atmospheric chemistry and physics: from air pollution to climate change*. John Wiley & Sons; 2016.
3. ASTM International. ASTM E1216-21: Standard Practice For Sampling For Particulate Contamination By Tape Lift. 2021.
4. Guo Z, Li Z, Farquhar J, et al. Identification of sources and formation processes of atmospheric sulfate by sulfur isotope and scanning electron microscope measurements. *Journal of Geophysical Research: Atmospheres*. 2010;115(D7)doi:10.1029/2009JD012893
5. Rawat K, Yadav AK. Characterization of coal and fly ash (generated) at coal based thermal power plant. *Materials Today: Proceedings*. 2020;26:1406-1411. doi:10.1016/j.matpr.2020.02.292
6. Kutchko BG, Kim AG. Fly ash characterization by SEM–EDS. *Fuel*. 2006;85(17):2537-2544. doi:10.1016/j.fuel.2006.05.016
7. Sellaro R, Sarver E, Baxter D. A Standard Characterization Methodology for Respirable Coal Mine Dust Using SEM-EDX. *Resources*. 2015;4(4):939-957. doi:10.3390/resources4040939
8. Powers MC. A new roundness scale for sedimentary particles. *Journal of Sedimentary Research*. 1953;23(2):117-119.
9. Ostro B, Spada N, Kuiper H. The impact of coal trains on PM2.5 in the San Francisco Bay area. *Air Quality, Atmosphere & Health*. 2023;16(6):1173-1183. doi:10.1007/s11869-023-01333-0
10. Ostro B, Spada N, Kuiper H. *Assessment of Coal and Petroleum Coke Pollution: Air Quality, Health, and Environmental Justice*. 2023:81 p. https://ucdavis.app.box.com/s/sh55sgeix0r39k07zfsai1tcamux8qpw

Appendix

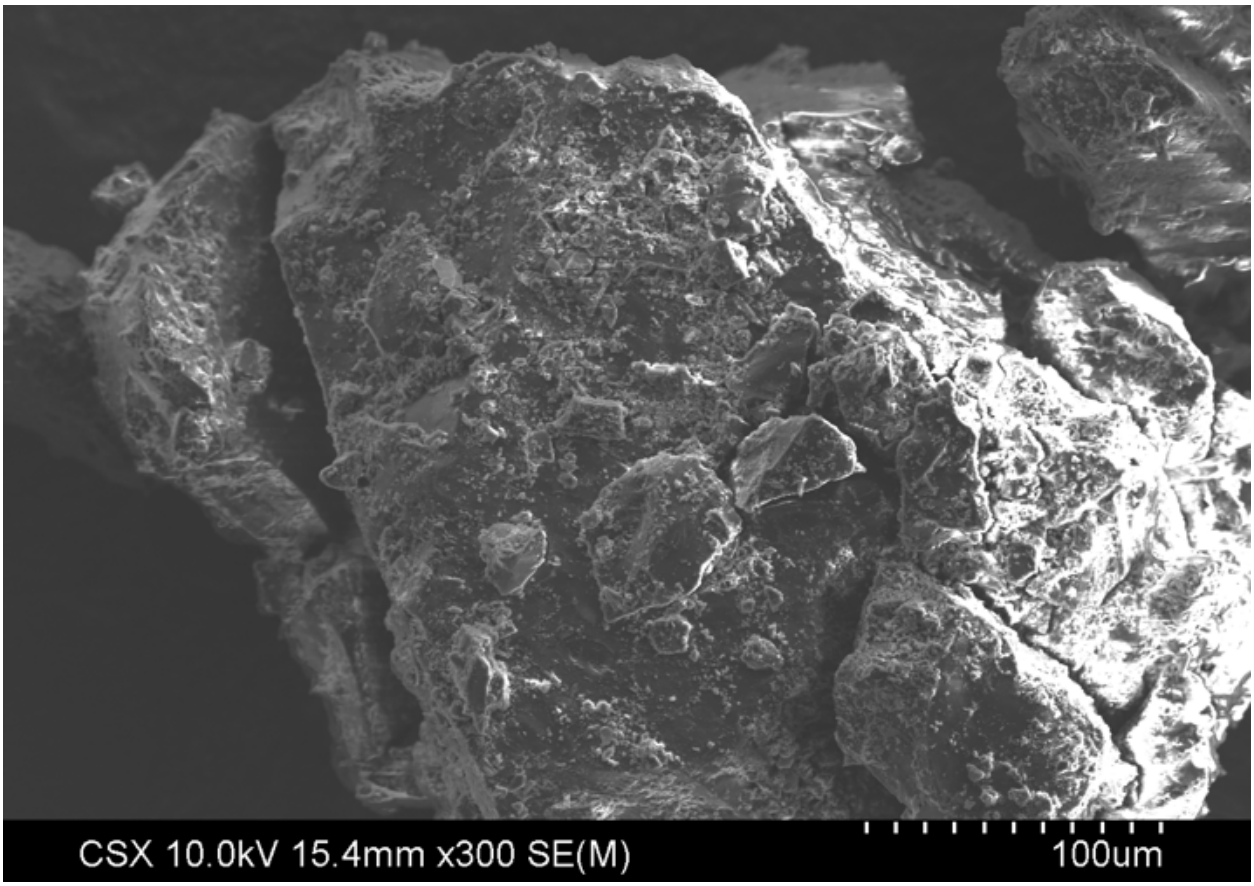

Appendix Figure 1. Medium (300x) magnification scanning electron microscopy image of coal particle in positive control material from the coal terminal in Curtis Bay, MD. This is a typical example of bituminous coal composed of 79% carbon (C), 14% oxygen (O), 3% nitrogen (N), 1% iron (Fe), 1% sulfur (S) (percent by mass as determined Energy dispersive X-ray

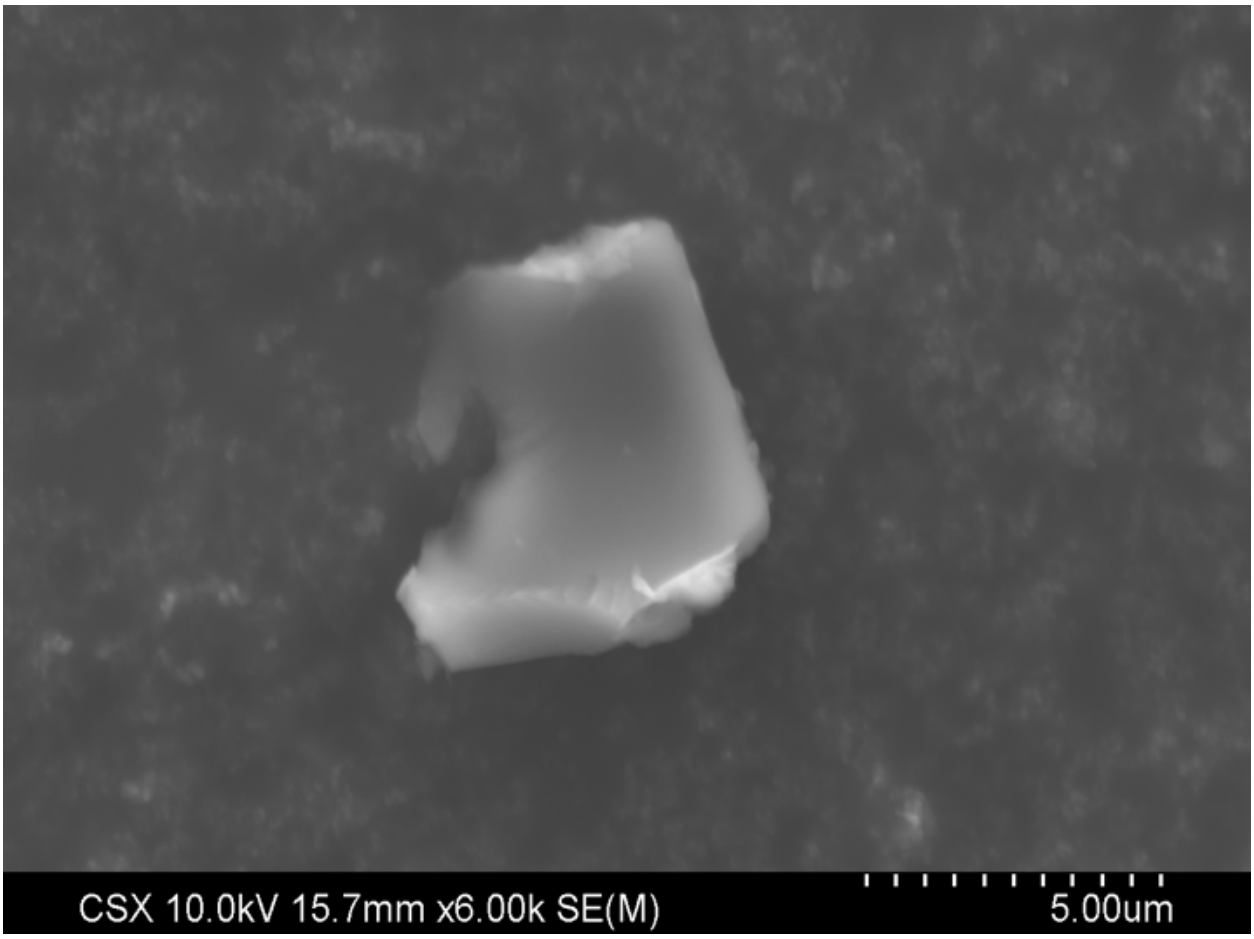

Appendix Figure 2. High (6000x) magnification scanning electron microscopy image of coal particle in positive control material from the coal terminal in Curtis Bay, MD. This particle has a glass-like appearance and is 88% carbon (C), 8% oxygen (O), 3% nitrogen (N), and 0.5% sulfur (S) (percent by mass as determined Energy dispersive X-ray spectroscopy analysis), typical of anthracite.

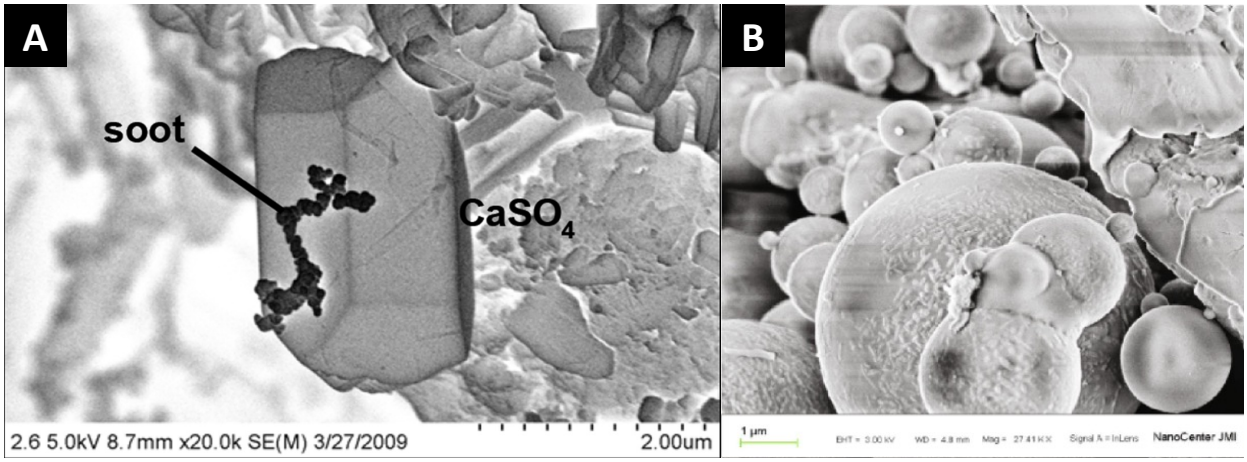

Appendix Figure 3. A. Image of a gypsum ($CaSO_4$) particle with soot attached to it. Note the small size (<2 µm diameter) and "string of pearls" morphology of soot is dramatically different from coal dust. Particle sampled from air near Beijing [Guo *et al.*, 2010]. **B.** Image of coal fly ash from coal-based Gandhinagar Thermal Power Station, Gandhinagar, Gujarat, IN. Note the small size (approximately <1-6 µm diameter) and spherical morphology of fly ash particles, differing from coal particles [Rawat and Yadav 2020].

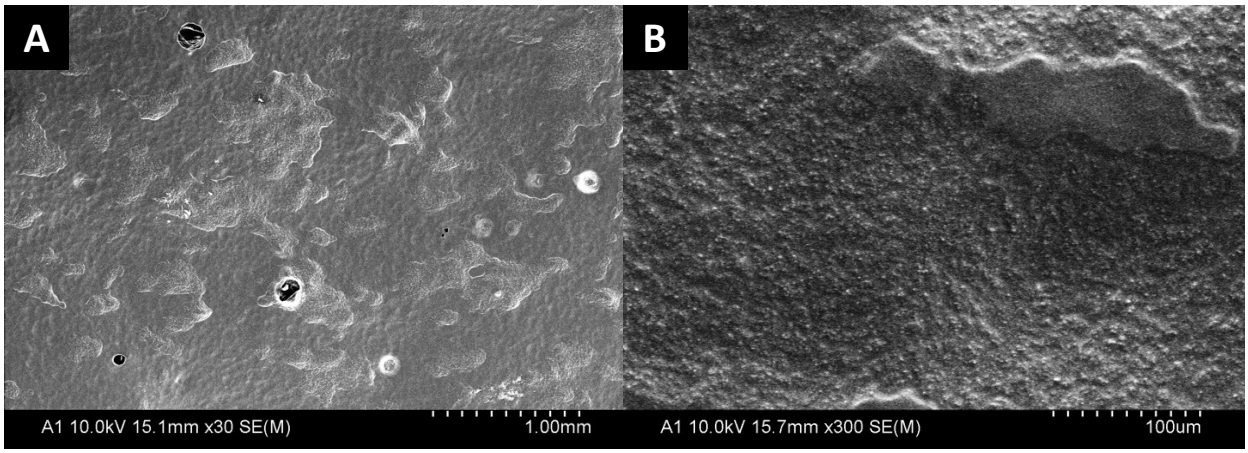

Appendix Figure 4. Low (30x) **(A)** and medium (300x) **(B)** magnification scanning electron microscopy images of the laboratory blank developed during the August 22, 2023 tape lift field sampling campaign. No coal dust particles are apparent. Black and white circles are topographic features of the carbon tape.

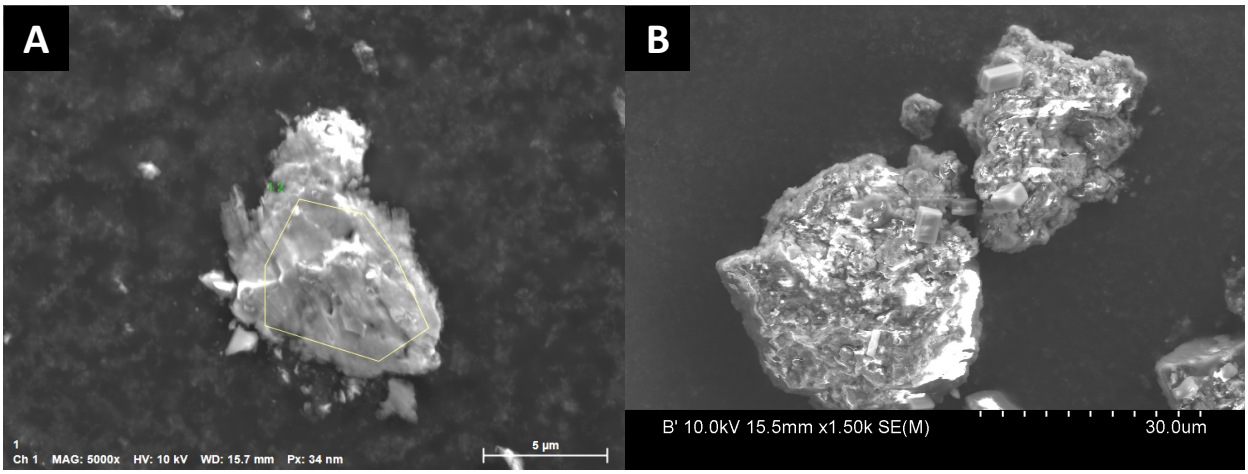

Appendix Figure 5. Particles sampled at Location 1 during the August 22, 2023 tape lift sampling field campaign, near the fenceline of the coal terminal in Curtis Bay, MD. **A.** Particle sampled at Location 1 with elemental composition of steel (66% Fe, 7% Ni, 4% O, and 1% Si). **B.** Clay mineral dust particles with bulk composition 60% O, 21% Si, 12% C, 4% Al, and minor amounts of Mg, Na, Al, Fe, K, and Cl; small, regular crystals are composed of sea salt (41% Na, 41% Cl, 31% C, and 1%

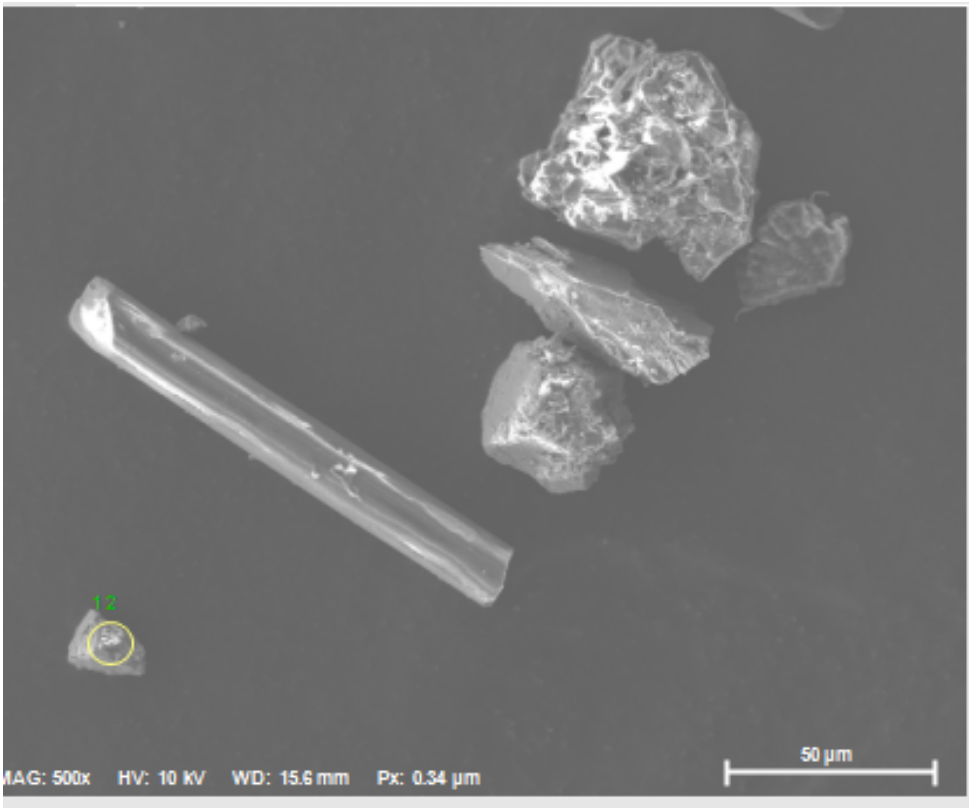

Appendix Figure 6. Moderate magnification (500x) scanning electron microscopy image of a particle from a tape lift at Location 2 (August 22, 2023), a residential sampling site in Curtis Bay, MD. Particles possess the appearance crustal material and coal dust. Elemental composition indicates sand (SiO_2), clay and feldspar, (alumino-silicates), limestone ($CaCO_3$) as well as coal dust.

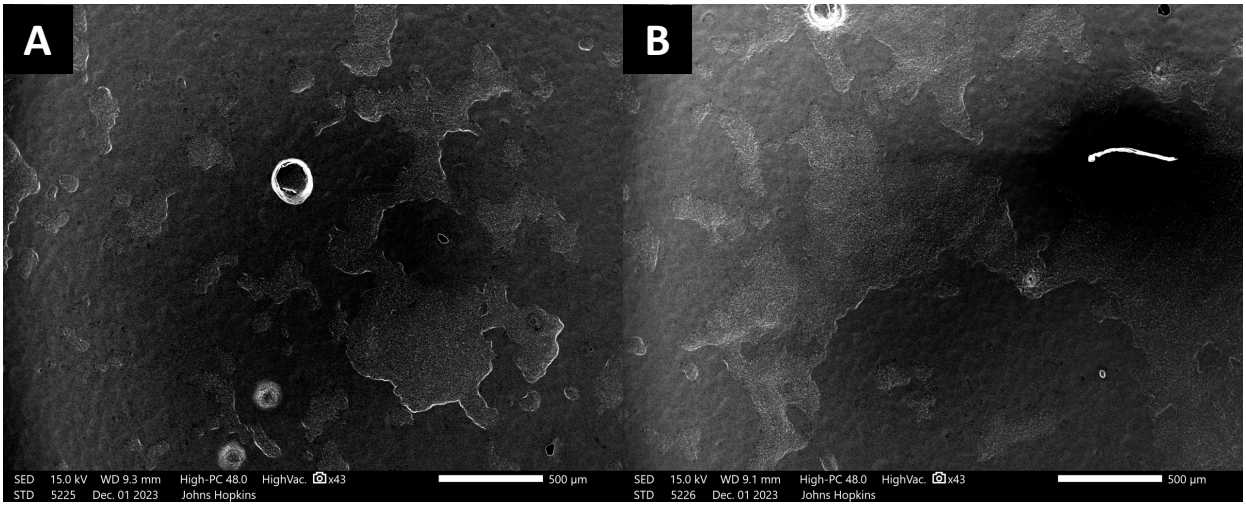

Appendix Figure 7. Low magnification (43x) images of lab blanks developed directly before **(A)** and after **(B)** construction of field sampling kits for the passive ambient particulate accumulation (PAPA) field sampling campaign. Lab blanks are clear of coal or crustal material particles except for a few fiber and dust particles.

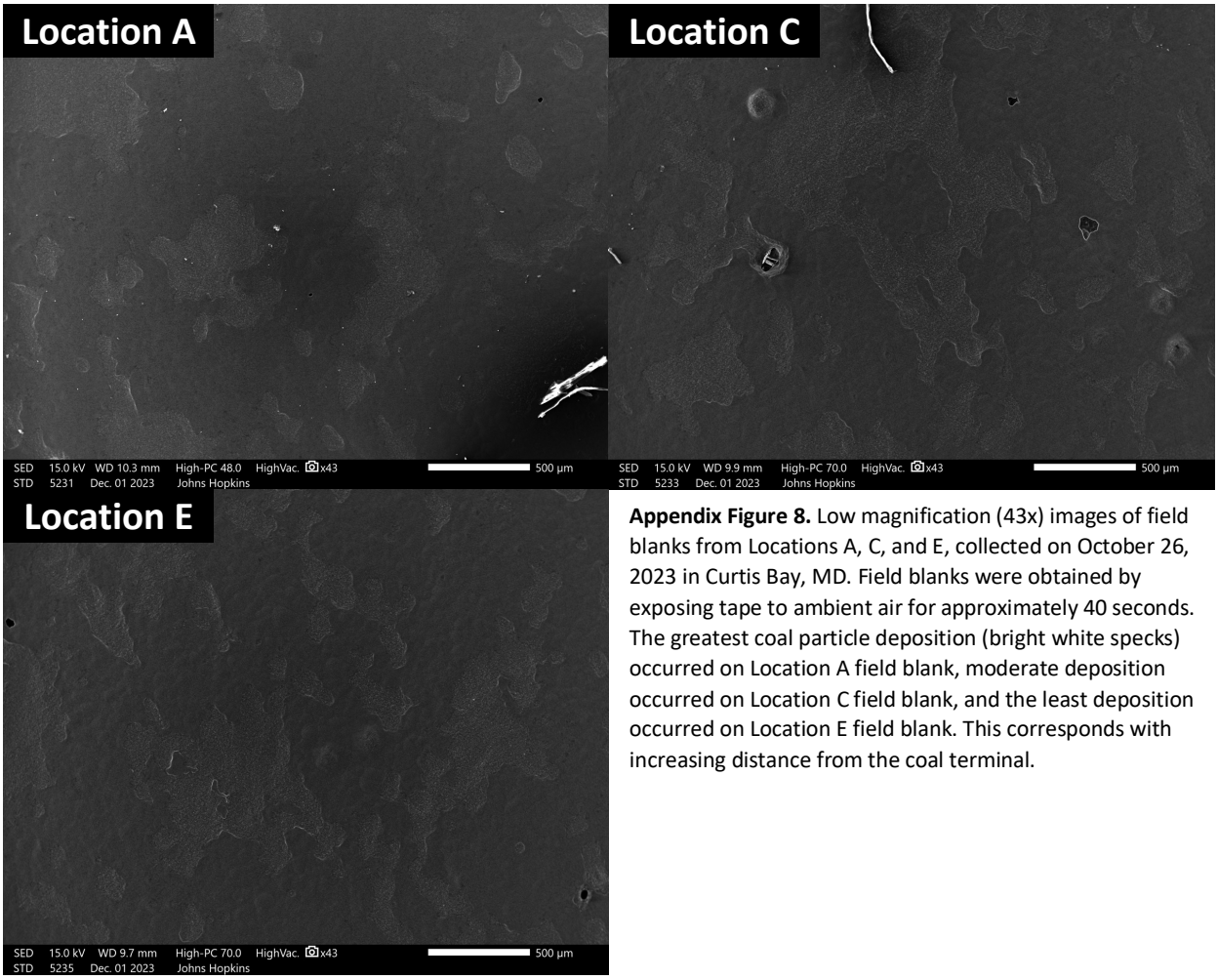

Appendix Figure 8. Low magnification (43x) images of field blanks from Locations A, C, and E, collected on October 26, 2023 in Curtis Bay, MD. Field blanks were obtained by exposing tape to ambient air for approximately 40 seconds. The greatest coal particle deposition (bright white specks) occurred on Location A field blank, moderate deposition occurred on Location C field blank, and the least deposition occurred on Location E field blank. This corresponds with increasing distance from the coal terminal.

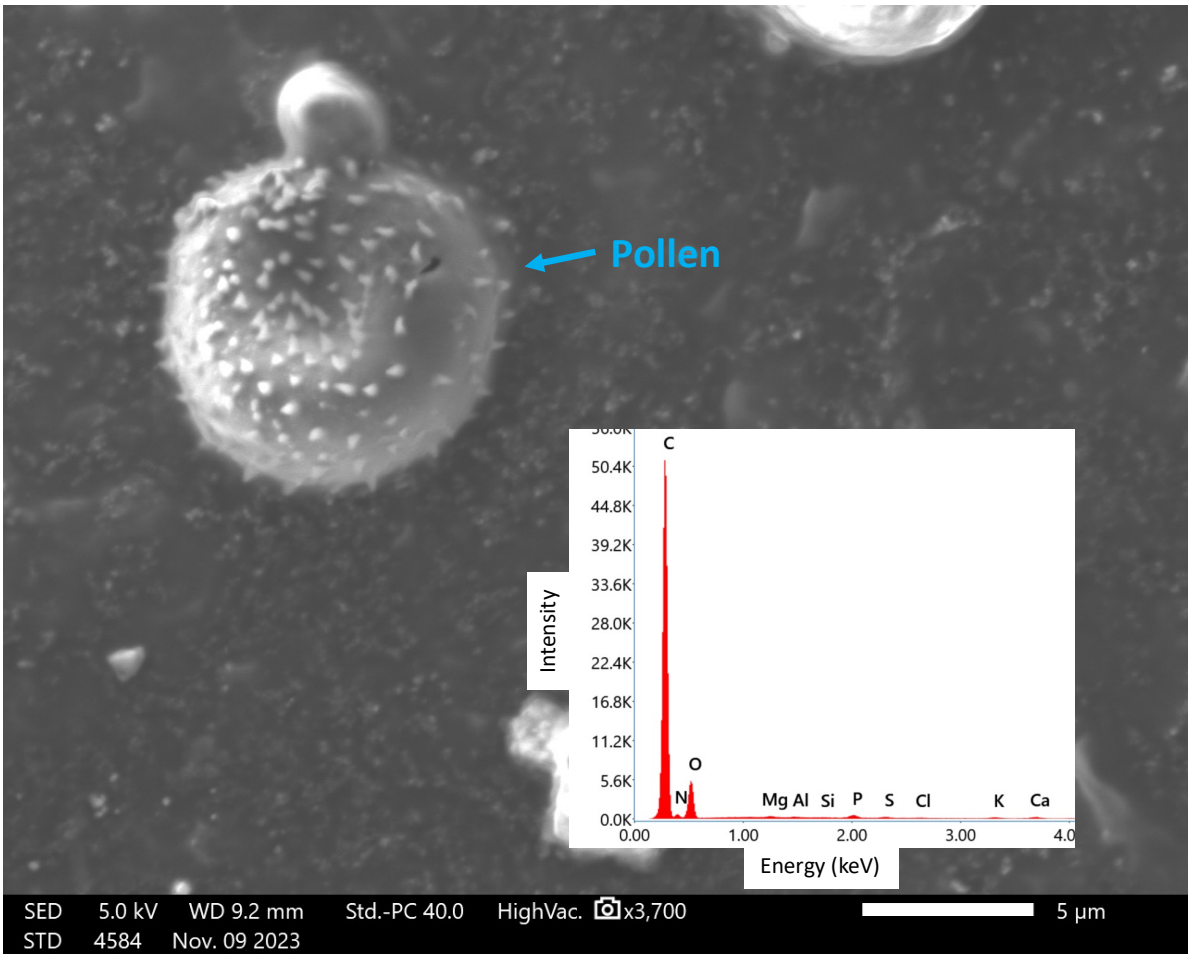

Appendix Figure 9. Scanning electron microscopy image of pollen particle with resulting energy dispersive X-ray spectrum conveying a similar elemental composition to a coal particle. Emphasizes the importance of including morphology in particle identification criteria with passive ambient particle accumulation (PAPA) sample analysis.

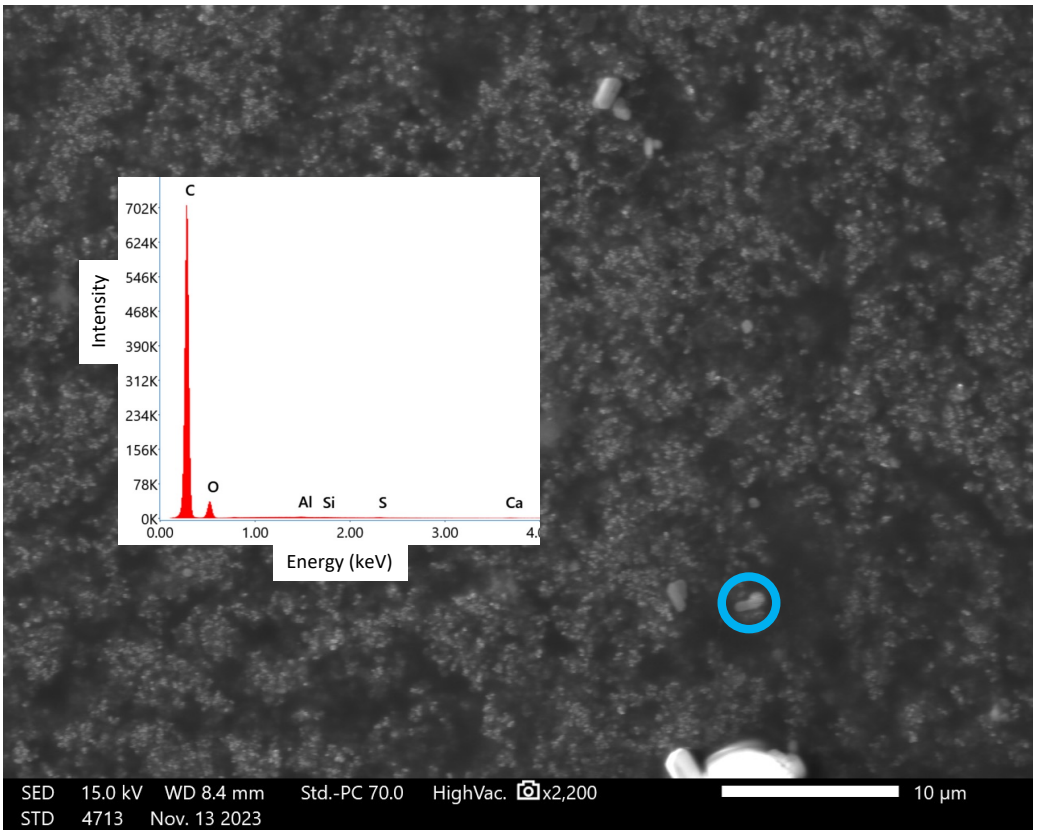

Appendix Figure 10. Example of fine (L = 1.792 µm) putative coal dust particle (blue circle) collected from passive ambient particulate accumulation (PAPA) sampling at Location B, a residential site in Curtis Bay, MD (October 26, 2023 to October 29, 2023). Energy dispersive X-ray shown. Note the high intensity carbon peak (93% mass) and diminished contribution of oxygen (7%), and approximately 0.08% aluminum, silicon, sulfur, and calcium–elements observed in coal particles. ***Note***: Blue circle indicates particle analyzed, not location of beam for EDX analysis.

3. Coal Terminal-specific Community Exposure and Impacts

3b. Use of Multi-pollutant Air Sensor Network to Identify Coal Dust and Other Sources of Air Pollution in Curtis Bay, South Baltimore, Maryland

Research questions addressed

What is the frequency, intensity, and duration of coal dust events in the community, and are they associated with wind, facility operations, or both?

Background

To address the driving research questions for the Curtis Bay Collaborative Effort, including evidence of and frequency of impacts of coal dust through the community, an unsupervised classification technique was used to source apportion pollutant signals within the Curtis Bay dataset. This method was called non-negative matrix factorization or NMF. The NMF method is an objective, mathematical approach to apportion 'sources' or signals within a dataset. In Curtis Bay, NMF provides an objective way to assess if a 'coal dust' signature exists in the community, and a systematic approach to understanding the frequency if such a source were found in the data. Thereupon, as any such signatures can be identified and further assessment of the nature and/or cause of such events can be explored. Results from the NMF procedure are discussed below.

Description of South Baltimore Air Monitoring Network, Curtis Bay, Baltimore, Maryland

In spring 2022, the South Baltimore Community Air Monitoring Network was established, which consists of 10 locations (Figure 1). Curtis Bay community organizations, community members, and local businesses suggested and approved monitor deployment locations based on proximity to the terminal, access to solar/AC power, and a vested interest in quantifying pollution in their community. Locations are numbered from 1 to 10, based on their proximity to the terminal, with Location 1 being the closest. The Curtis Bay Recreation Center, a longstanding community gathering space, was next to Location 4. Location 8 was operated by a local community organization and serves as a within Curtis Bay community background site, relative to the terminal and other industrial facilities.

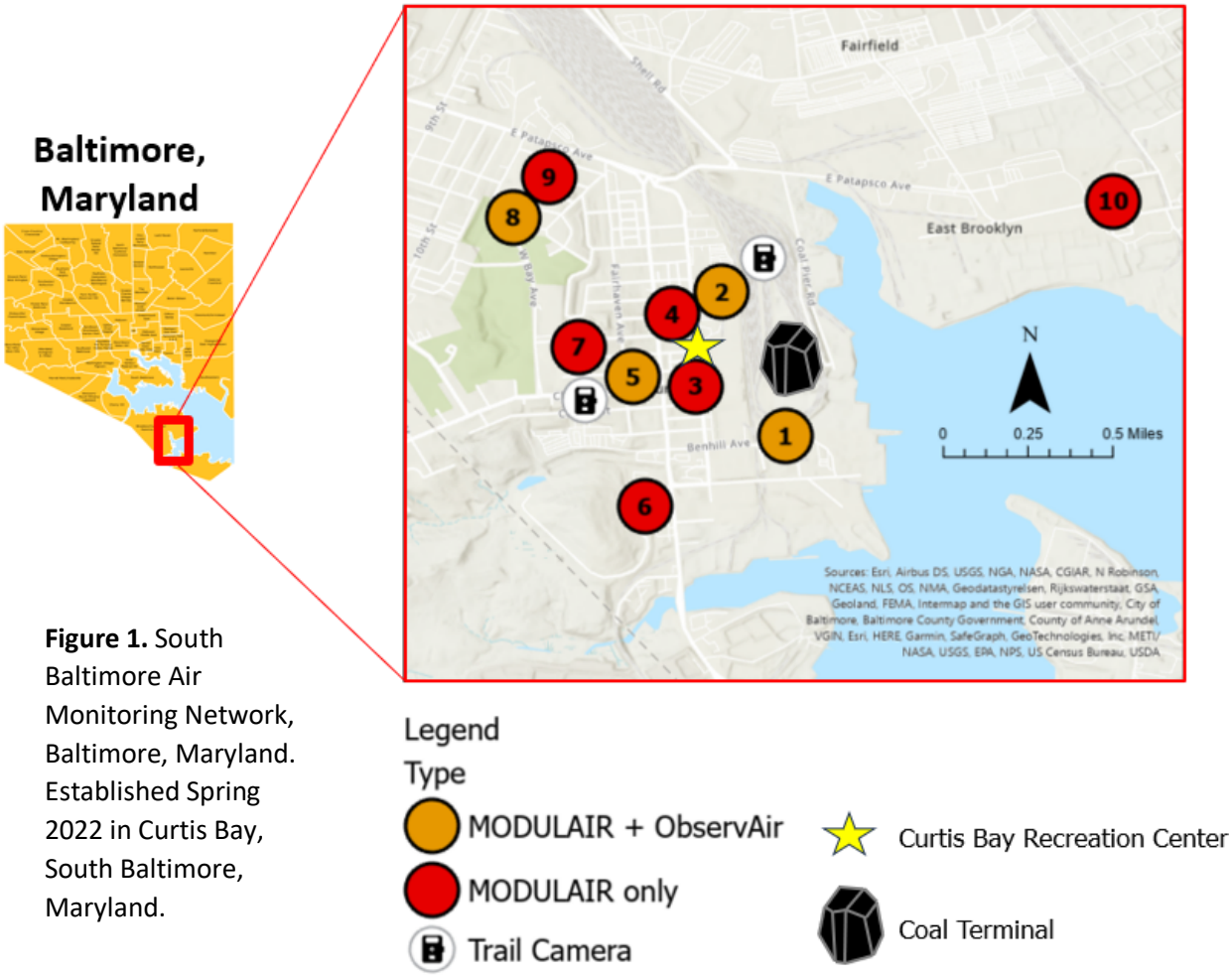

Figure 1. South Baltimore Air Monitoring Network, Baltimore, Maryland. Established Spring 2022 in Curtis Bay, South Baltimore, Maryland.

Information about air sensors and other equipment employed in this network have been described previously.[1] QuantAQ MODULAIR air sensors (pictured at a deployment site in Figure 2) were deployed at all 10 sites to measure particulate matter of various size fractions: PM_1, $PM_{2.5}$, PM_{10}, total suspended particles (~PM_{40}); gases: carbon dioxide (CO_2), carbon monoxide (CO), nitric oxide (NO), nitrogen dioxide (NO_2), ozone (O_3); and meteorological variables: temperature, relative humidity, wind speed, and wind direction. At four of the ten sites (Locations 1, 2, 5, and 8), we also deployed Distributed Sensing Technologies (DSTech) ObservAir air sensors (Figure 3), which measure black carbon (BC); particulate matter: PM_1, $PM_{2.5}$, PM_4, PM_{10}; gases: CO, NO_2; and meteorological variables: temperature and relative humidity. Additionally, CamPark trail cameras (Figure 4) were deployed at 2 locations in the network with the goal of recording coal terminal activity patterns and comparing these observations to air quality data from the Curtis Bay Community Air Network.[1]

Because of rolling deployments to build the network, date ranges for available air quality data vary between locations. These date ranges are listed in the Appendix.

Figure 2. QuantAQ MODULAIR air sensor.

Figure 3. Distributed Sensing Technologies (DSTech) ObservAir air sensor.

Figure 4. CamPark trail camera.

Quality Assurance/Quality Control (QA/QC) of Air Monitoring Data

Environmental observations are intrinsically subject to randomized and systematic error due to the conditions in which measurements are taken and fundamental properties of instrumentation. As such, observed data must be quality controlled. As an anecdotal example, consider an electrical impulse unassociated with the ambient environmental which could be interpreted as a 'real' signal by the instrument and introduce a false artifact in the data. To screen for such a phenomenon, a series of steps examined each of the parameters measured. First, collaborative input developed and applied

corrections to final 1-min resolution MODULAIR PM_{10}, total suspended particles (TSP), and wind direction data. Any PM_{10} or TSP values with relative humidity (RH) greater than or equal to 80% while, PM_{10} concentrations were greater than or equal to 200 $\mu g/m^3$, and TSP concentrations were greater than or equal to 500 $\mu g/m^3$ were omitted from the final dataset.

Secondly, we also developed corrections to the 2-second resolution ObservAir black carbon (BC) data. First, we disregarded black carbon concentrations when there was a rapid internal relative humidity change (>1%/min). Further, we instituted time-based flags, where data analysts observed erratic values during short- and long-term shutoffs (After > 15-min gap b/w observations, flag the following 60 minutes (including the first 60 min of data); After > 2.5-min gap b/w observations, flag the 5 previous observations and following 15 minutes). Finally, we also disregarded BC concentrations during time of low battery voltage (< 7.5 V) and when the BC concentrations were equal to exactly -5 $\mu g/m^3$ (usually associated with start-up times). Independent operators applied the flags to verify the same numbers of records removed.

Within the meteorological data it was noted that wind direction was pinned to zero degrees when wind speed dropped to zero. In these instances, wind direction was set to a non-numeric value. Wind speed of zero was retained. This removed potential incorrect biasing of data since 'zero degrees' is a northerly direction, which does not exist if the wind is not blowing.

Previous quality control steps were applied prior to co-location of monitors with regulatory monitors in Maryland. To explore the agreement between the deployed monitors and regulatory monitors, we analyzed data from time periods of co-location. The co-location period took place from February to March 2023. We co-located one (1) QuantAQ MODULAIR and one (1) DSTech ObservAir at the Howard County Near Road (HCNR) and one (1) QuantAQ MODULAIR at the Pocomoke City site in the Maryland Department of the Environment (MDE) Ambient Air Monitoring Network. The duration of co-location spanned 14 to 29 days, and we explored agreement for the following pollutants: black carbon (BC), $PM_{2.5}$, PM_{10}, and carbon monoxide (CO). Using methods described in Aubourg et al. (2023), we conducted linear regressions to assess agreement between regulatory monitors and the low-cost sensors.[1] Further details about the co-location, including regression results, monitors used, and pollutants measured can be found in the Appendix.

Employing Statistical Methods for Source Apportionment in South Baltimore: Non-negative Matrix Factorization (NMF)

Methods

To explore sources of air pollution in Curtis Bay, we used non-negative matrix factorization (NMF), a statistical source attribution technique. This technique is a form of unsupervised classification, which strictly uses mathematical techniques which minimize error explores our entire dataset for patterns and combines pollutants based on those patterns into *factors*. This technique was applied to data from the four locations that have co-located QuantAQ MODULAIRs and DSTech ObservAirs: locations 1, 2, 5, and 8. For the NMF analysis, we input data for 8 pollutants: PM_1, $PM_{2.5}$, PM_{10}, total suspended particles (TSP ~ PM_{40}), CO, NO, NO_2, and black carbon (BC). We can use NMF to determine the presence of a "putative coal dust" (PCD) factor, consisting of higher contributions to the factor by PM_{10}, TSP, and black carbon, relative to other factors. Before producing NMF compositions for each location, we removed any negative values among the 8 pollutants, as these observations are incompatible with non-negative matrix factorization. Next, we removed any records for which there were no complete cases (i.e., when any pollutant values were missing for a given time record). Finally, we normalize pollutant-specific data from 0 to 1. We then produced NMF compositions (contributions of each pollutant to each factor) for the four locations. We produced the NMF composition plots for each location settling on 4 factors as a satisfactory solution after exploring 3-6 factor solutions. Bootstrapping with 100 NMF runs (allowing a maximum of 1000 iterations for each individual run for Locations 1, 2, and 8; 2000 iterations for Location 5 to allow for full convergence) and sampling 25% of the dataset (Python 3.10.5) was also performed. This bootstrapping approach illustrates the stability in each pollutant's contributions to the factor by adding error bars. We then attempt to label each factor based on our knowledge of the environment in Curtis Bay. Next, to explore the frequency, intensity, and duration of putative coal dust events, we plotted time series of all putative coal dust factors and quantified when those PCD factors exceeded various thresholds: the mean, mean + 1 standard deviation (SD), mean + 2 SD, and mean + 3 SD. Additionally, we quantify the average and maximum length of events for each threshold for the dust factors at each location.

To compare terminal activity patterns to observed pollutants and putative coal dust factors, we produced time lapses from 1-minute resolution camera footage and then manually coded activities, such as train, bulldozer, and ship activities near the terminal (0 = absence of the activity, 1 = being the presence of the activity). We used coded camera data from the southernmost camera for these analyses. We applied student's t-tests to log-10 transformed pollutant data comparing when activities occurred versus when these activities were not occurring. Statistical analyses were performed in R Version 4.2.3.

Results

NMF Compositions

We generated NMF compositions for each location using 4 NMF factors (Figure 5). Using knowledge of the industrial environment in Curtis Bay and a combination of each pollutant's contribution to each factor, diurnal variability, and wind influences, each factor was identified as "putative coal dust" (PCD), "diurnal combustion, "local combustion", "regional", "cars," "dust," or a combination of these labels.

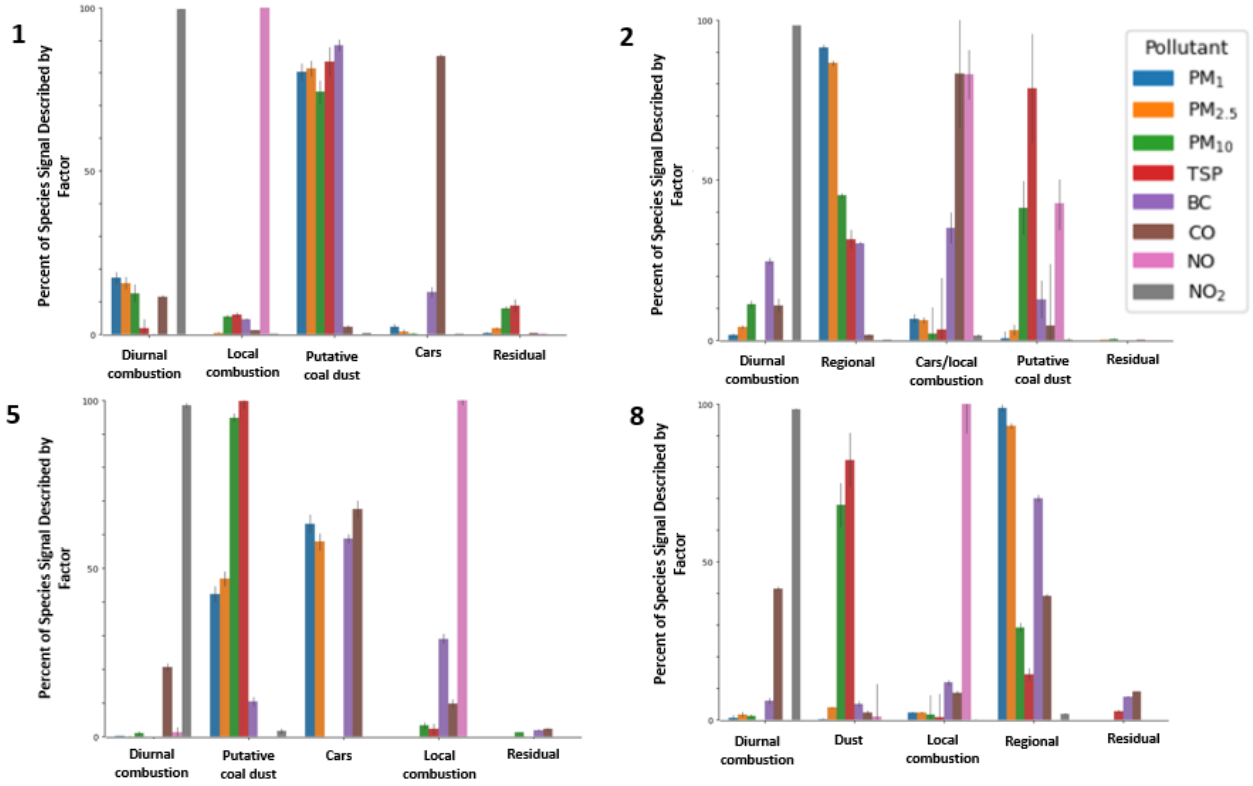

Figure 5. Non-negative matrix factorization (NMF) factor compositions at Locations 1, 2, 5, and 8 in the South Baltimore Air Monitoring Network. ***Note.*** Sample sizes (minutes) by location: Location 1: n = 130,088; 2: n = 109,931; 5: n = 103,385; 8: n = 127,995.

For "putative coal dust" (PCD), we sought factors comprised of a combination of major contributions from PM_{10}, total suspended particles (TSP), and black carbon (BC). We identified a "diurnal combustion" factor that had high contributions from nitrogen dioxide (NO_2) and followed a diurnal pattern. We labeled a factor as "local combustion" if there were relatively high contribution from nitric oxide (NO), a pollutant species directly emitted from tailpipes but quickly oxidizing to NO_2, in addition to contributions from BC and fine particles. Similarly, we labeled factors as "cars" if there was a presence of fine particles and a dominant contribution from carbon monoxide (CO). We assigned a label of "regional" to a factor if it was comprised of relatively high contributions from fine particulate matter such as PM_1, $PM_{2.5}$, and BC. Finally, we labeled the factors with high contributions from PM_{10} and TSP as "dust" instead of "putative coal dust" if there were low BC contributions to the factor.

At Location 1, we observed the presence of a strong PCD factor, consisting of PM_1, $PM_{2.5}$, PM_{10}, TSP, and black carbon contributing nearly 70% each to the total factor. Other factors at Location 1 include diurnal combustion, local combustion, and cars. At Location 2, the putative coal dust factor appears to be diluted by a ~40% contribution from NO, suggesting nearby diesel emissions. Other factors at Location 2 include diurnal combustion, a regional factor with strong (over 90%) contributions from PM_1 and $PM_{2.5}$, with the final factor as local combustion. At Location 5, the traditional putative coal dust factor emerges as well, with significantly less of a contribution by black carbon compared to Location 1. Other factors at Location 5 include diurnal combustion, cars, and local combustion. Finally, at Location 8, the presence of a PCD factor is less clear due to significantly smaller contributions from black carbon in a factor with higher contributions from PM_{10} and TSP. Additionally, because Location 8 was furthest from the terminal, it is less likely putative coal dust would consist of PM_{10} and TSP sized particles because their larger size would favor settling prior to arriving to Location 8. In that case, what looks like a typical "regional" factor at other locations may be a putative coal dust factor at Location 8. We labeled other factors as diurnal combustion, dust (very low contribution from black carbon), and local combustion.

What is the frequency, intensity, and duration of putative coal dust events?

Across all locations, the putative coal dust factor exceeded the highest threshold (mean + 3 standard deviations) once nearly every hour and a half, including the dust and regional factors at Location 8.

At Location 1, the peak putative coal dust (PCD) factor peaked on November 23, 2022; December 20-31, 2022; and February 23, 2023 (industrial fire south of the terminal) (Figure 6). Of the 130,088 minutes captured during the complete-case analysis, the PCD factor exceeded the mean threshold during 37.2% of the time, which is equivalent to approximately 30 days (726 hours) of deployment time (Table 1). The PCD factor exceeded the highest threshold, the mean + 3SD, 1% of those minutes. The average duration of events (consecutive minutes exceeding a given threshold) was 14.3 minutes for the mean threshold and 6.3 minutes for the highest threshold, mean + 3 SD. The maximum length of event for that highest threshold was 137 minutes (over two hours).

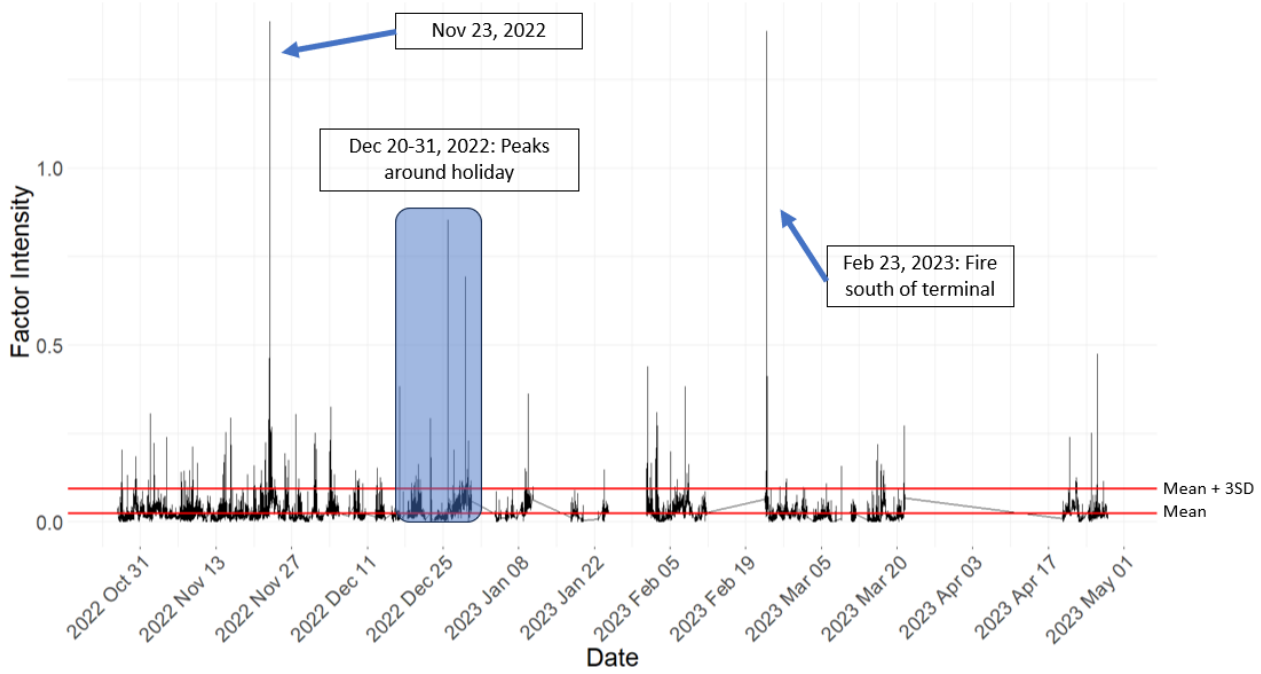

Figure 6. Time series of putative coal dust (PCD) factor and threshold exceedances at Location 1, South Baltimore Air Monitoring Network, Baltimore, MD, October 26, 2022-April 27, 2023 (n=130,088 minutes). ***Note***. Mean, mean + 3 standard deviation thresholds are denoted with red horizontal lines. Dates of observed PCD peaks are annotated. December 20-31, 2022 shaded to highlight full time range.

Table 1. Putative coal dust (PCD) factor threshold exceedances and durations at Location 1, South Baltimore Air Monitoring Network, Baltimore, MD, October 26, 2022-April 27, 2023.

Threshold	Exceedances, n (%)	Exceedances / Hr	Mean duration (SD) (min)	Max. duration (min)
Mean	48,405 (37.2)	22.32	14.3 (54.5)	1209
Mean+1SD	12,600 (9.7)	5.82	10.1 (34.7)	527
Mean+2SD	3,443 (2.6)	1.56	7.2 (19.4)	346
Mean+3SD	1,354 (1.0)	0.6	6.3 (12.0)	137
Note. Total observations = 130,088 minutes. SD = standard deviation. Hr = hour. Max = maximum.				

At Location 2, of the 109,931 minutes captured during the complete-case analysis, and we observed major peaks in the PCD factor at Location 2 on February 10, March 28, and April 20, 2023 (Figure 7). The PCD factor exceeded the mean threshold 31.2% of the time while the factor exceeded the mean + 3SD threshold 1.3% of the time (Table 2). The mean PCD value was exceeded approximately 24 days (572 hours) of deployment time. The average duration of events (consecutive minutes exceeding a given threshold) was 5.1 minutes for the mean threshold and 4.0 minutes for the highest threshold, mean + 3 SD. The maximum length of event for that highest threshold was 36 minutes.

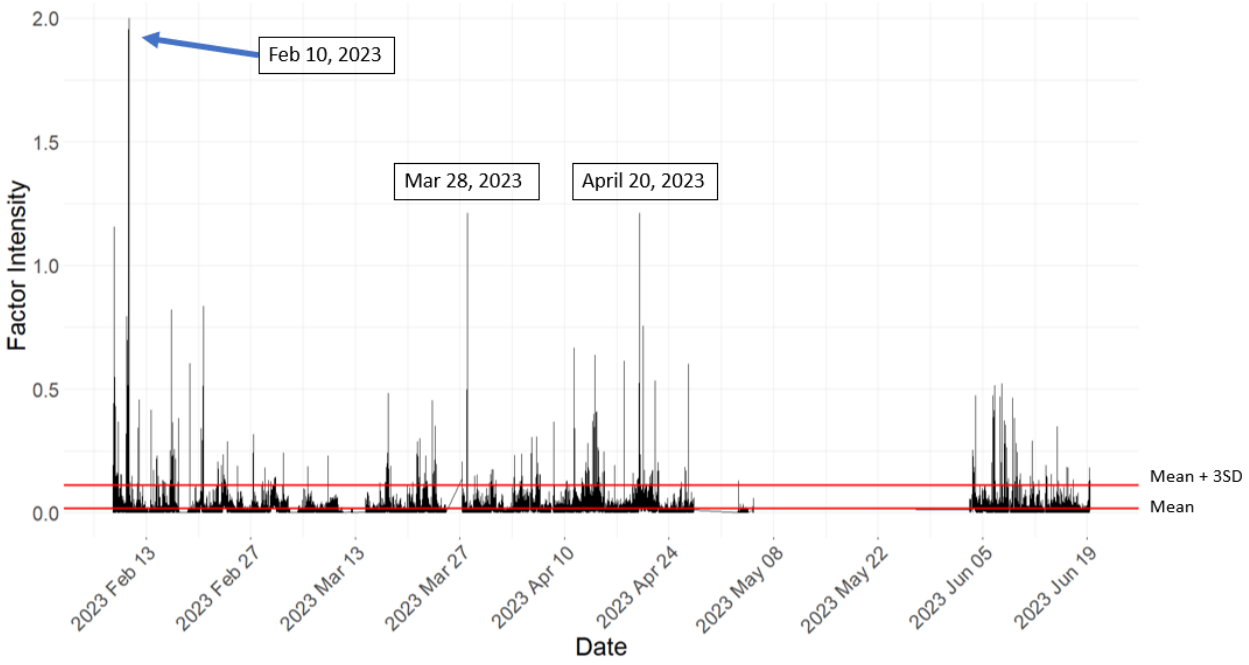

Figure 7. Time series of putative coal dust (PCD) factor and threshold exceedances at Location 2, South Baltimore Air Monitoring Network, Baltimore, Maryland, February 8, 2023-June 19, 2023 (n = 109,931 minutes). ***Note.*** Mean, mean + 3 standard deviation thresholds are denoted with red horizontal lines. Dates of observed PCD peaks are annotated.

Table 2. Putative coal dust (PCD) factor threshold exceedances and durations at Location 2, South Baltimore Air Monitoring Network, Baltimore, MD, February 8, 2023-June 19, 2023.

Threshold	Exceedances, n (%)	Exceedances / Hr	Mean duration (SD) (min)	Max. duration (min)
Mean	34,334 (31.2)	18.72	5.1 (12.9)	450
Mean+1SD	8,471 (7.7)	4.62	4.6 (6.4)	100
Mean+2SD	3,160 (2.9)	1.74	4.2 (4.8)	55
Mean+3SD	1,493 (1.3)	0.78	4.0 (4.3)	36
Note. Total observations = 109,931 minutes. SD = standard deviation. Hr = hour. Max = maximum.				

At Location 5, we have data that spans two distinct time periods (roughly July-September 2022 and May 2023) (Figure 8). Between September 2022 and May 2023, we did not have an ObservAir black carbon monitor deployed at Location 5, and as a result, we were not able to calculate any NMF factors during that period. PCD peaks at Location 5 were observed on September 4, 2022; September 16, 2022; and May 6, 2023. The PCD factor exceeded the mean threshold 37.2% of the time, and the factor exceeded the mean + 3SD threshold 1% of the time (Table 3). The mean PCD value exceeded approximately 28 days (669 hours) of deployment time at Location 5. Further, we note that the mean duration of dust events for the mean threshold is 6 minutes, while the mean duration for the highest threshold, mean + 3SD, is 3.9 minutes. The maximum length of event for the highest threshold was 105 minutes.

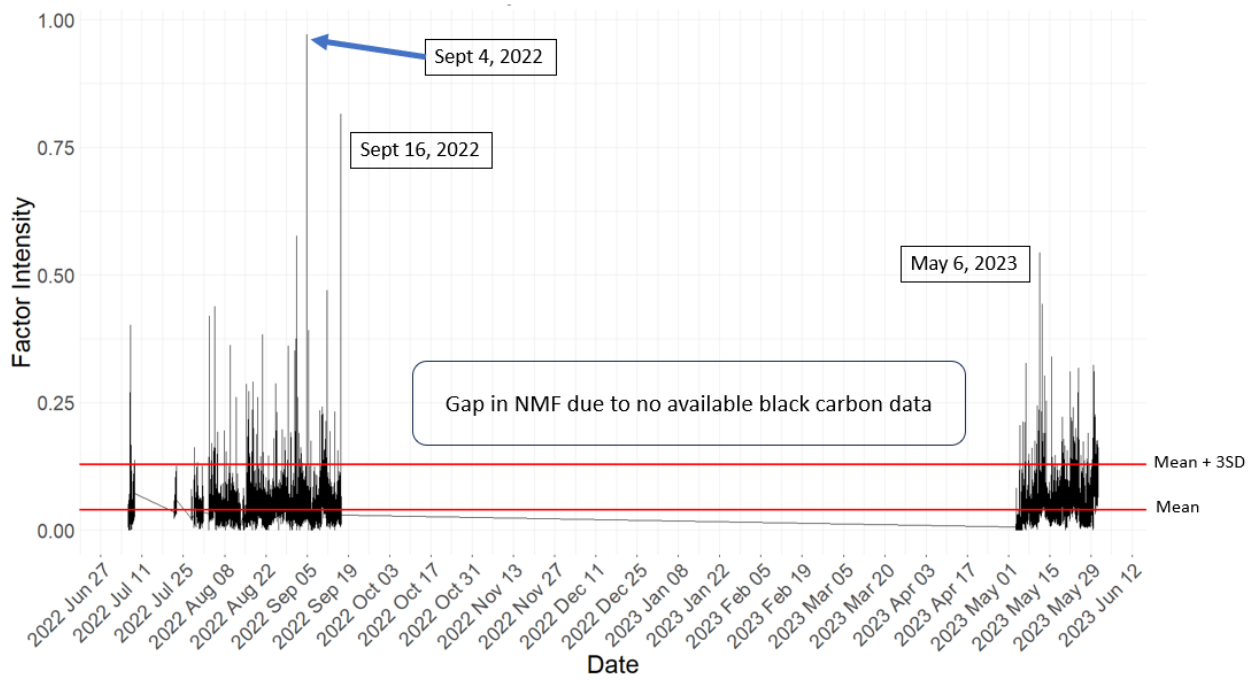

Figure 8. Time series of dust factor and threshold exceedances at Location 5, South Baltimore Air Monitoring Network, July 6, 2022-September 16, 2022; May 3, 2023-May 31, 2023 (n = 103,385 minutes). ***Note.*** Mean, mean + 3 standard deviation thresholds are denoted with red horizontal lines. Dates of observed PCD peaks are annotated.

Table 3. Putative coal dust (PCD) factor threshold exceedances and durations at Location 5, South Baltimore Air Monitoring Network, July 6, 2022-September 16, 2022; May 3, 2023-May 31, 2023.

Threshold	Exceedances, n (%)	Exceedances / Hr	Mean duration (SD) (min)	Max. duration (min)
Mean	40,119 (38.8)	23.3	6.0 (21.4)	749
Mean+1SD	12,105 (11.7)	7.0	5.0 (11.9)	260
Mean+2SD	4,236 (4.1)	2.5	4.2 (6.7)	146
Mean+3SD	1.575 (1.5)	0.9	3.9 (7.1)	105
Note. Total observations = 103,385 minutes. SD = standard deviation. Hr = hour. Max = maximum.				

At Location 8, we explored frequency, intensity, and duration of events for two factors: dust (Figure 9) and regional (Figure 10). Location 8 covered 127,995 minutes, with observed peaks for the dust factor on December 31, 2022 and February 7, 2023 and observed peaks for the regional factor on December 30, 2022 and March 18, 2023. These differing peak times allude to the different pollutant compositions for each factor. For both factors, the highest threshold was exceeded 1-2% of the sampling time.

Clear differences emerge when exploring the average and maximum durations of events for the dust and regional factors at Location 8 (Table 4: dust; Table 5: regional). The regional factor has considerably higher mean and maximum durations for all thresholds. This may be due to the prevalence of regional influences. For example, the mean duration of events for the dust factor is 4.1 minutes, while the same statistic is double that (8.2 minutes) for the regional factor.

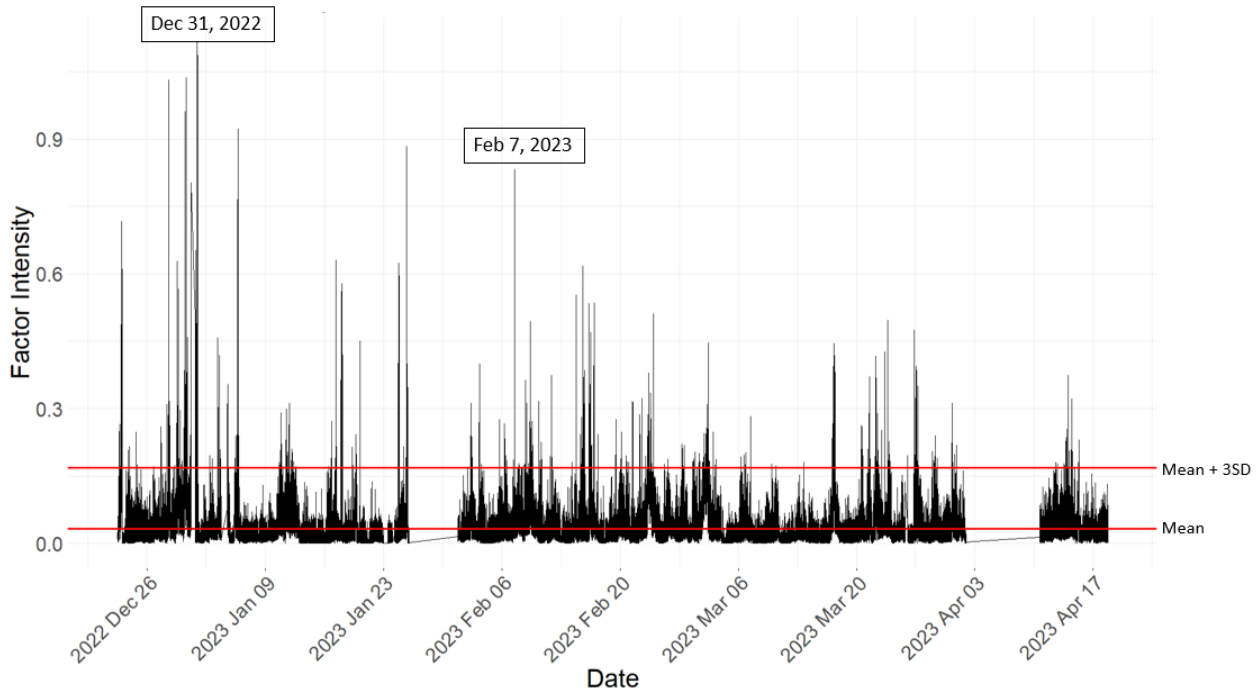

Figure 9. Time series of dust factor and threshold exceedances at Location 8, South Baltimore Air Monitoring Network, December 22, 2022-April 18, 2023 (n = 127,995 minutes). ***Note.*** Mean, mean + 3 standard deviation thresholds are denoted with red horizontal lines. Dates of observed dust peaks annotated.

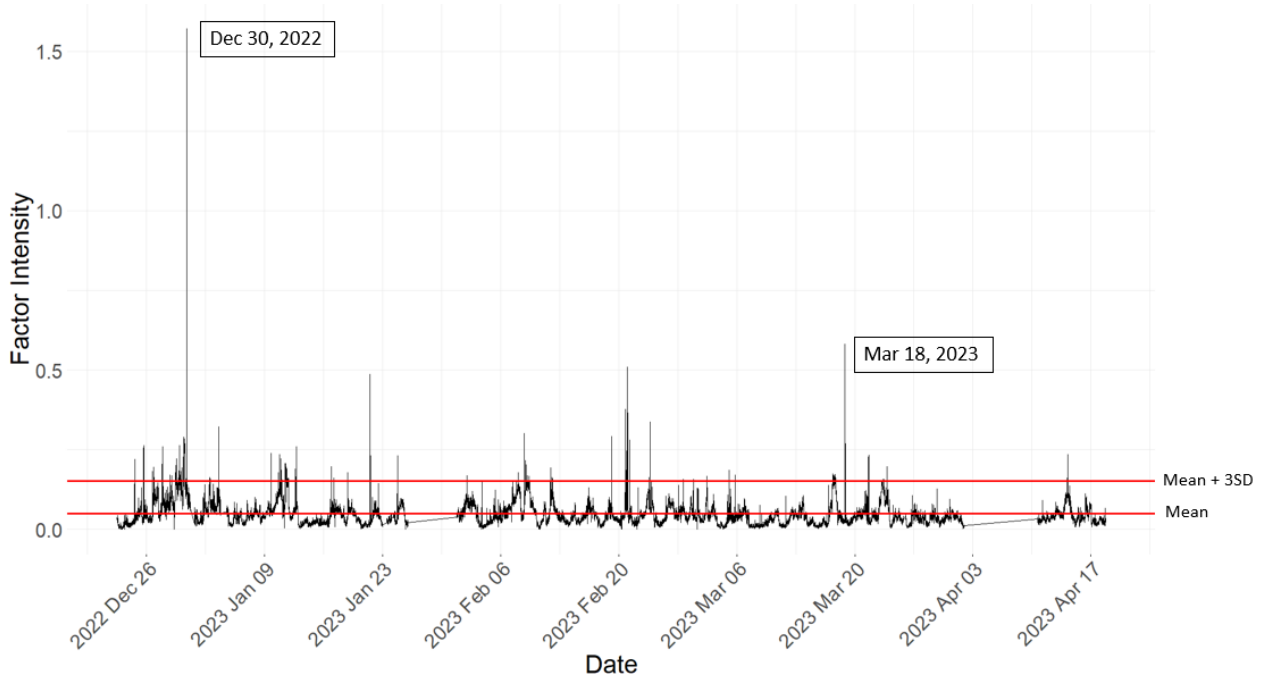

Figure 10. Time series of regional factor and threshold exceedances at Location 8, South Baltimore Air Monitoring Network, December 22, 2022-April 18, 2023 (n = 127,995 minutes). ***Note.*** Mean, mean + 3 standard deviation thresholds are denoted with red horizontal lines. Dates of observed regional peaks annotated.

Table 4. Dust factor threshold exceedances and durations at Location 8, South Baltimore Air Monitoring Network, December 22, 2022-April 18, 2023.

Threshold	Exceedances, n (%)	Exceedances / Hr	Mean duration (SD) (min)	Max. duration (min)
Mean	41,072 (32.0)	19.2	4.8 (10.6)	473
Mean+1SD	12,600 (9.8)	5.88	4.2 (6.9)	124
Mean+2SD	4,915 (3.8)	2.28	4.2 (5.5)	60
Mean+3SD	2,260 (1.8)	1.08	4.1 (4.3)	43
Note. Total observations = 127,995 minutes. SD = standard deviation. Hr = hour. Max = maximum.				

Table 5. Regional factor threshold exceedances and durations at Location 8, South Baltimore Air Monitoring Network, December 22, 2022-April 18, 2023.

Threshold	Exceedances, n (%)	Exceedances / Hr	Mean duration (SD) (min)	Max. duration (min)
Mean	49,402 (38.6)	23.2	19.7 (67.7)	1136
Mean+1SD	16,559 (12.9)	7.7	19.8 (57.2)	679
Mean+2SD	6,518 (5.0)	3.0	16.7 (50.0)	673
Mean+3SD	1,826 (1.4)	0.8	8.2 (22.0)	267
Note. Total observations = 127,995 minutes. SD = standard deviation. Hr = hour. Max = maximum.				

While the regional factor appears to behave differently when compared to the putative coal dust factors at Locations 1, 2, 5, in addition to the dust factor at Location 8, there appears to be a clear trend. For the dust factors, as we move from the terminal to further out (from Location 1 to 8), there is a decrease in the mean duration of the event. We would expect this, considering proximity to the coal terminal.

How do the PCD factor and air pollutants vary during known events reported in real-time to the collaborative team? And can the PCD factor identify additional unknown events?

Over the sampling period, our collaborative team identified potential putative coal dust events in real time, through camera observations, knowledge of weather conditions, and monitoring cloud data from our deployed low-cost monitors. On February 3, 2023, a bulldozer became stuck on the southern pile of the terminal around 11:30am. As a result, the sprayer system had to be turned off. This may have resulted in fugitive coal dust from the facility. Between 12pm and 3pm, we observed 4 distinct peaks in the putative coal dust (PCD) factor: at approximately 12:00, 1:00, 1:15, and 2pm (Figure 11). Further, during all four of these PCD spikes, there are co-incident increases in the near combustion factor. If we explore on a pollutant-specific level, we note that the PCD peak at 12pm co-occurs with increases in $PM_{2.5}$, black carbon, and carbon monoxide, but without any increases in coarse particles (Figure 12). This may suggest putative coal dust co-incident with combustion from equipment on the pile. The latter three peaks in the PCD factor, however, co-occur with increases in $PM_{2.5}$, PM_{10}, TSP, and slight increases in black carbon, suggesting fugitive putative coal dust. Normal operations are reported to have re-started at the terminal at 2:45pm.

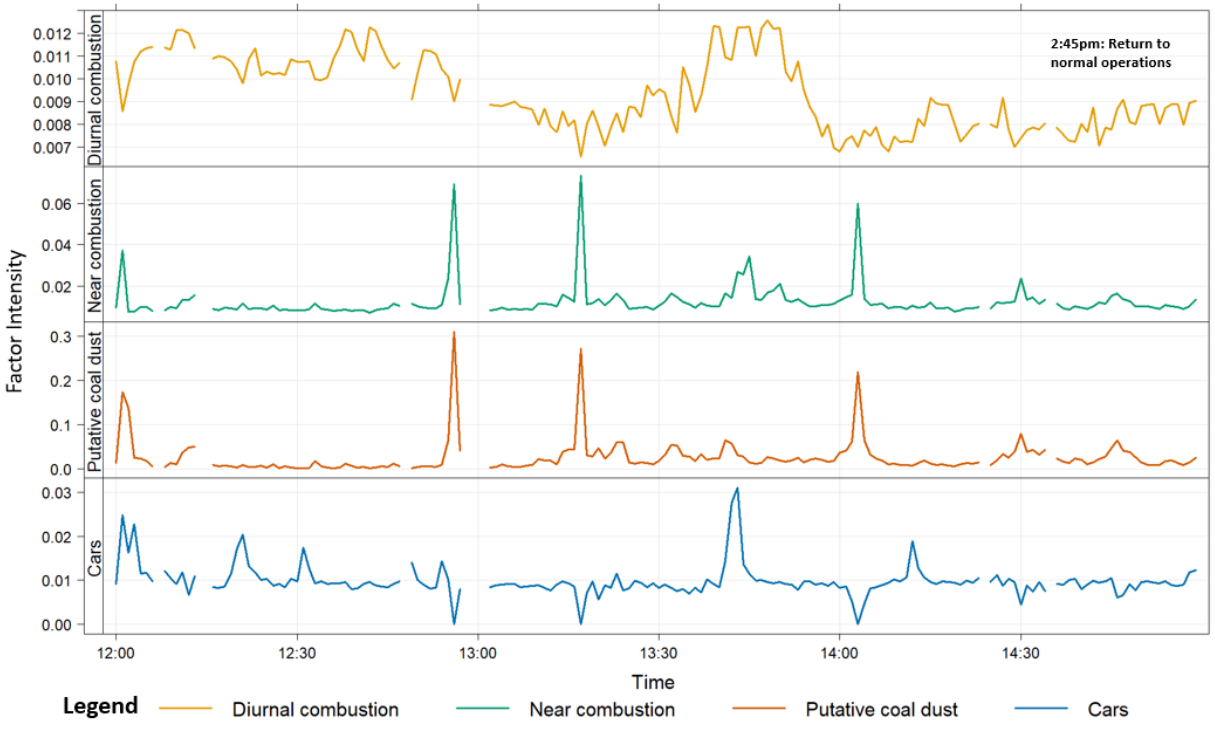

Figure 11. Time series of all non-negative matrix factorization (NMF) factors (diurnal combustion, near combustion, putative coal dust, and cars) at Location 1, February 3, 2023 terminal bulldozer event (12pm-3pm). Note. Gap in putative coal dust factor caused by missing black carbon data.

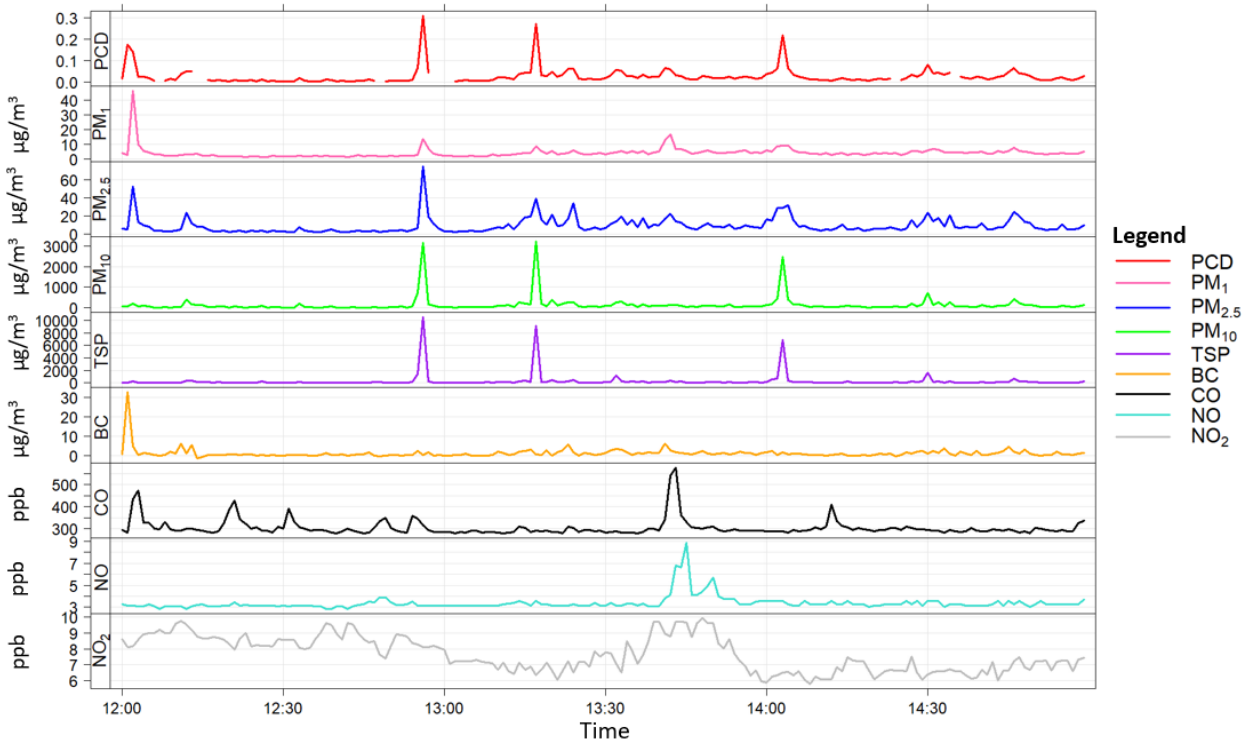

Figure 12. Time series of putative coal dust (PCD) factor, PM_1, $PM_{2.5}$, PM_{10}, total suspended particles (TSP), black carbon (BC), carbon monoxide (CO), nitric oxide (NO), and nitrogen dioxide (NO_2) at Location 1, February 3, 2023 terminal bulldozer event (12pm-3pm).

Knowing that the putative coal dust factor increases during major dust events identified by the collaborative team, we also explored unidentified events by determining times in which the PCD factor exceeded the mean + 3 standard deviation (SD) threshold. For example, when we explore exceedances of the mean + 3SD threshold of the PCD factor at Location 1, we note an increase in the PCD factor at late 2022 around the December holiday (Figure 13). This occurred while the other three factors remained relatively stable. As shown in Figure 14, between 3:30 and 3:45am, there were simultaneous peaks in the putative coal dust factor, PM_{10}, $PM_{2.5}$, TSP, black carbon. There is also a nitric oxide (NO) peak; however, this does not co-occur with putative coal dust-relevant factors and pollutants.

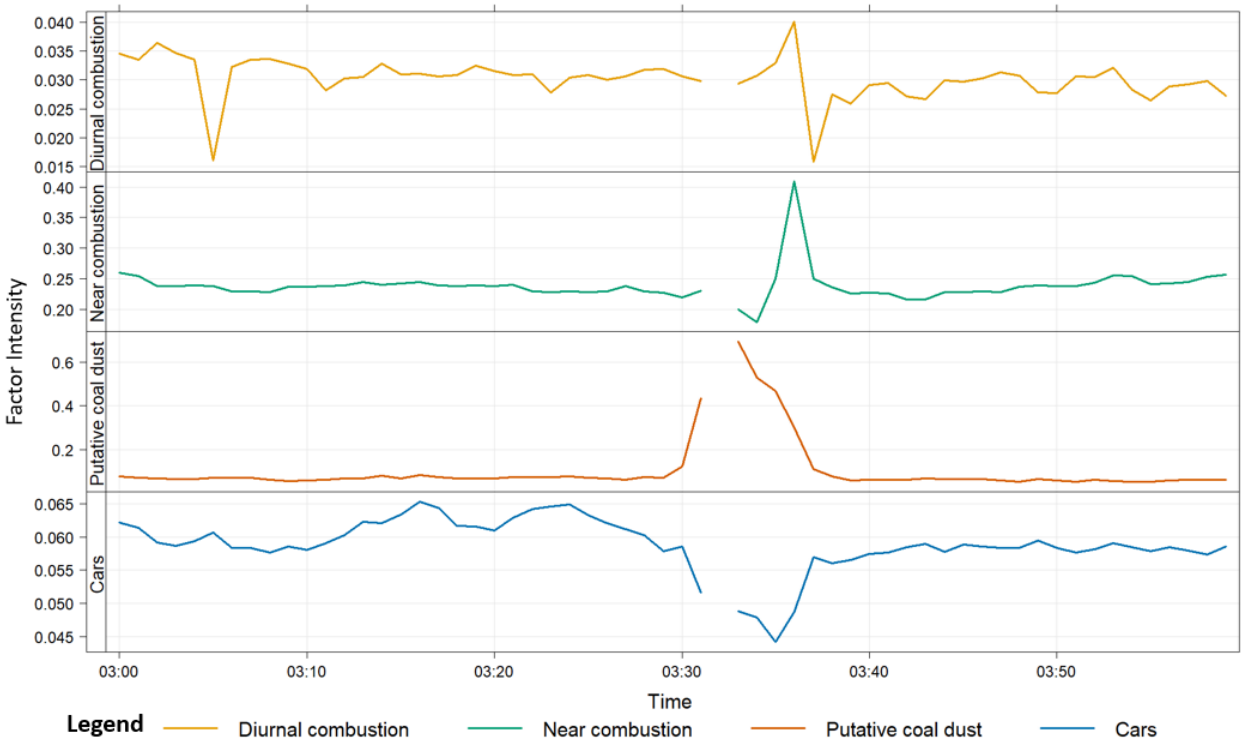

Figure 13. Time series of all non-negative matrix factorization (NMF) factors (diurnal combustion, near combustion, putative coal dust, and cars) at Location 1, December 30, 2022 (3am-4am). ***Note.*** Gap in putative coal dust factor caused by missing black carbon data.

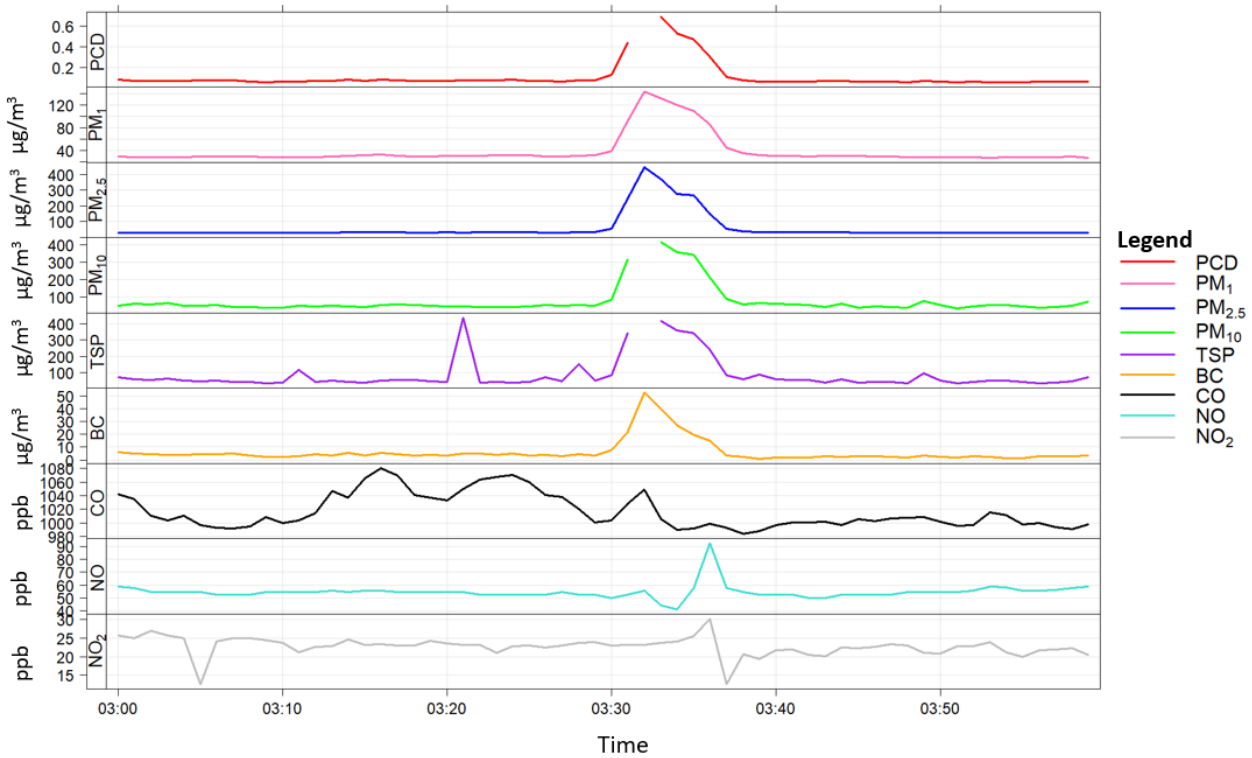

Figure 14. Time series of putative coal dust (PCD) factor, PM_1, $PM_{2.5}$, PM_{10}, total suspended particles (TSP), black carbon (BC), carbon monoxide (CO), nitric oxide (NO), and nitrogen dioxide (NO_2) at Location 1, December 30, 2022 (3am-4am).

What are hourly and daily patterns of selected coal terminal activities?

We identify three major terminal activities: bulldozer activity, ship activity, and train activity (both leaving and entering the terminal) and display their hourly variation in Figure 15.

First, ship activity remains relatively stable through the day, while train activity tends to peak between 12am and 6am, followed by a dramatic decrease until 6am, with a gradual increase until the following midnight. Bulldozer activity also tends to peak in the early morning hours, with oscillations between more and less activity throughout the day. Further, train and ship activity tend to peak on Fridays, while bulldozer activity tends to peak on Thursdays.

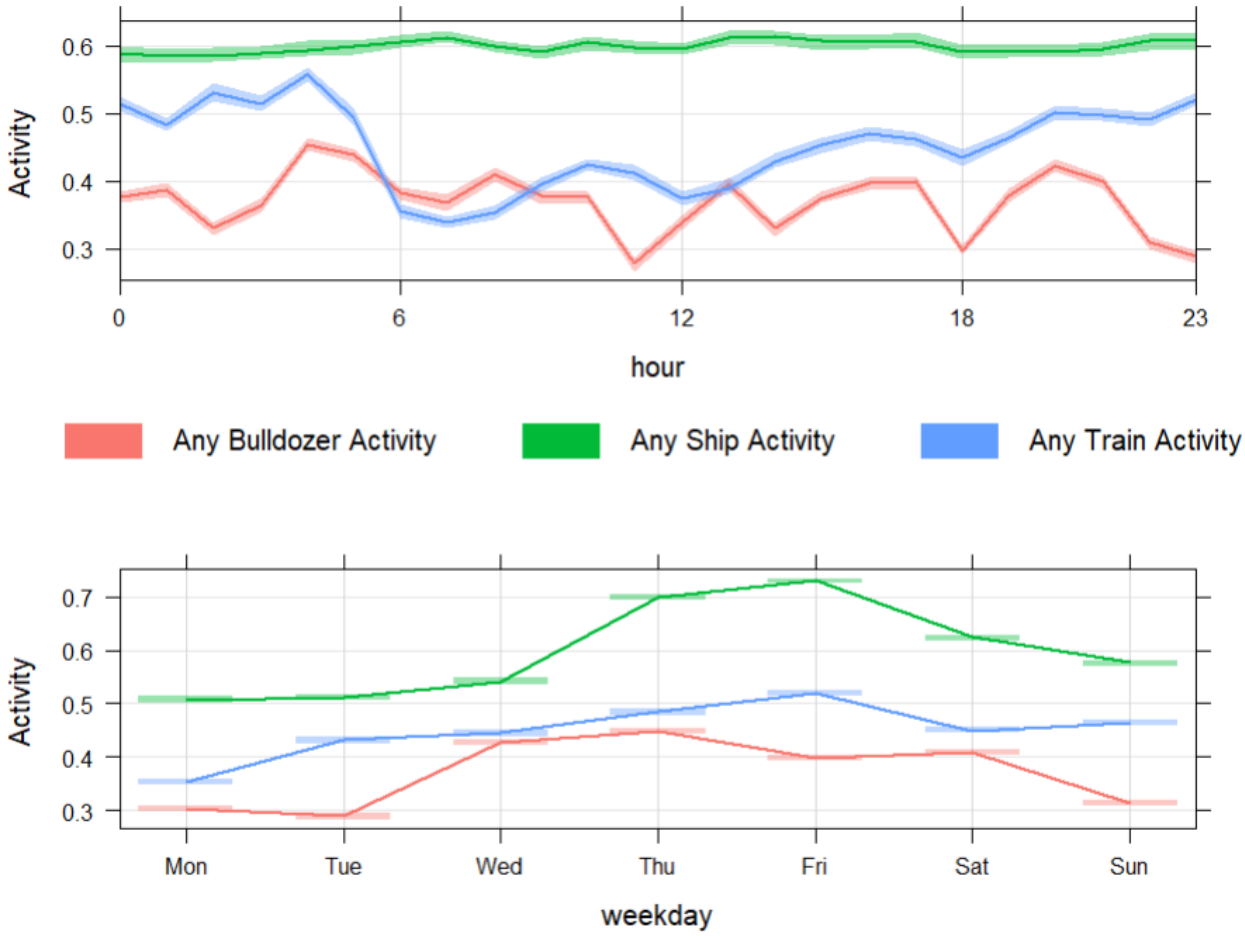

Figure 15. Hourly and daily frequency of bulldozer, ship, and train activities at the Curtis Bay coal terminal, Baltimore, Maryland, September 16, 2022-March 8, 2023. ***Note.*** Mean and 95% confidence interval in mean.

How does the continuous value of the putative coal dust factor vary according to wind direction and visually observed coal terminal activity patterns?

At Location 1, the geometric mean of log-10 transformed values of all pollutants and putative coal dust factor are higher when the activity is occurring vs. when the activity is not occurring for most cases. These differences are also statistically significant at the p=0.05 level. There is an exception: When there is any train activity at the terminal, the geometric mean of the log10-transformed black carbon concentration is not higher than the geometric mean when the activity is not occurring; however, this difference is not statistically significant.

At Location 2, the geometric mean of log-10 transformed values of all pollutants and putative coal dust factor is higher when the wind is blowing downwind of the terminal towards the monitor (these cases are also statistically significant at the p=0.05 level). For bulldozer activity, the only statistically significant case is for black carbon. This is consistent with the fact that the bulldozers are diesel-fueled, and diesel combustion emits black carbon and smaller size fraction particles. During times of ship activity, the geometric mean of the log_{10}-transformed $PM_{2.5}$ concentrations was higher than when there was no ship activity; however, this result was not statistically significant. For PM_{10}, TSP, black carbon, and the putative coal dust factor, the opposite was true – the geometric means were lower when a ship was present at the terminal. This may be explained by coal dust being loaded from the terminal to the ship, resulting in less coal at the terminal, and fewer opportunities for coal to move from the terminal towards Location 2. Finally, regarding train activity, the geometric means for PM_{10}, TSP, black carbon, and the putative coal dust factor were elevated during times of train activity. Unlike ships, the trains move around the full perimeter of the terminal and *add* coal to the terminal. More coal on the terminal means more material that could potentially leave the facility and infiltrate the community. The full tables depicting the t-test results for Locations 1 and 2 are included in the Appendix.

Further, we also compared arithmetic means of dust factor (putative coal dust at Locations 1, 2, and 5 and dust at Location 8) across locations, with a focus on downwind (from the terminal) wind direction, bulldozer activity, ship activity and train activity. As seen in Figure 16, when wind is blowing from the terminal towards each of the four respective monitors, the means of the dust factor are higher at Locations 1, 2, and 8 than when the wind is not blowing from the terminal. These differences are statistically significant ($p < 0.05$).

For the terminal-specific boxplots, we can only explore these comparisons for Locations 1, 2, and 8, due to there being no NMF factor for Location 5 that coincides with coded camera data (September 16, 2022 – March 8, 2023). Recall that there was not a black carbon monitor at Location 5 during this period.

For bulldozer activity, the mean dust factor is higher during times of bulldozer activity than when there is no bulldozer activity at Locations 1, 2, and 8 (Figure 17). However, these differences are only statistically significant for Locations 1 and 8. For ship activity, the mean dust factor is higher during ship activity (vs. times of no ship activity) only for Location 1 (statistically significant), while the mean dust factor is lower during ship activity for Locations 2 and 8 (statistically significant) (Figure 18). Location 1's closer proximity to ships compared to Locations 2 and 8, may explain these differences. Finally, for train activity, the mean dust factor during times of train activity (compared to times of no

train activity) at all three locations (all statistically significant. This, again, may be explained by the train covering the perimeter of the terminal.

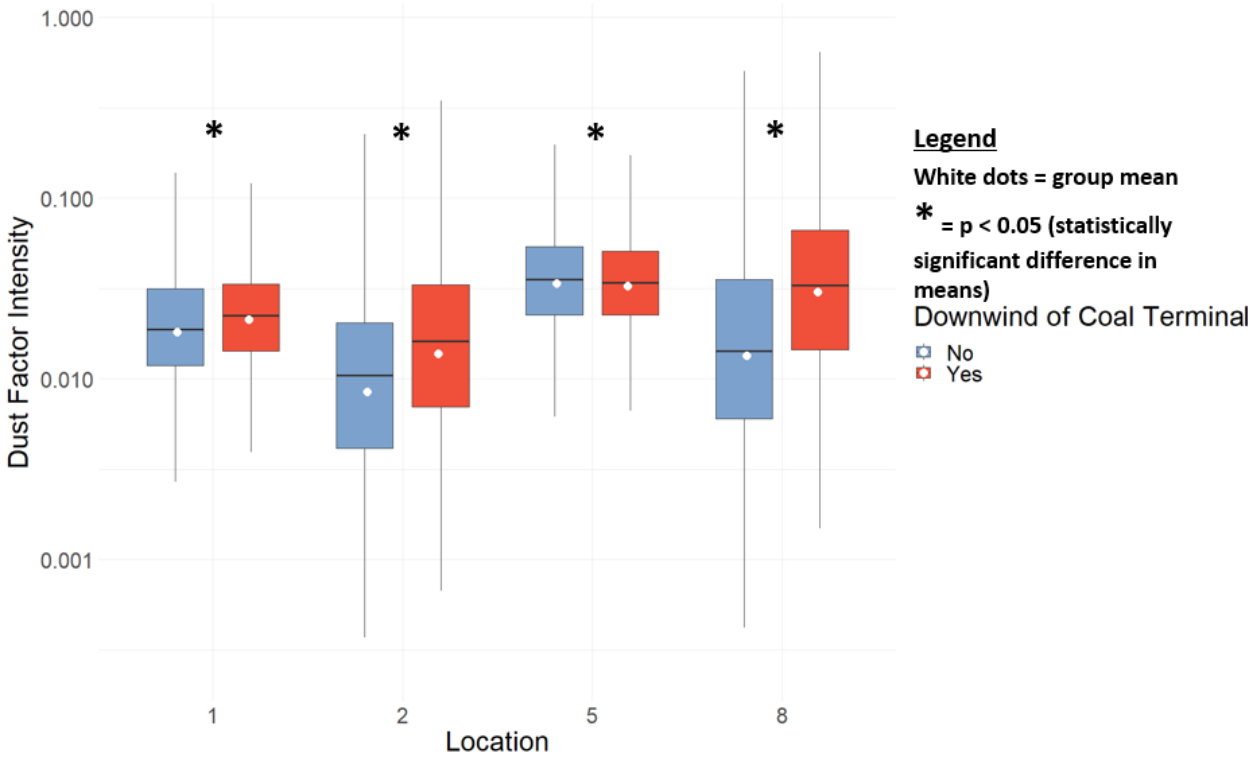

Figure 16. Dust factor boxplots stratified by downwind from the terminal vs. not downwind from the terminal at all locations, May 25, 2022 – July 17, 2023. ***Note.*** "Dust" at Locations 1, 2, and 5 is putative coal dust (PCD), whereas it is dust at Location 8. Asterisks denote statistical significance ($p < 0.05$) from Welch t-test for difference of means.

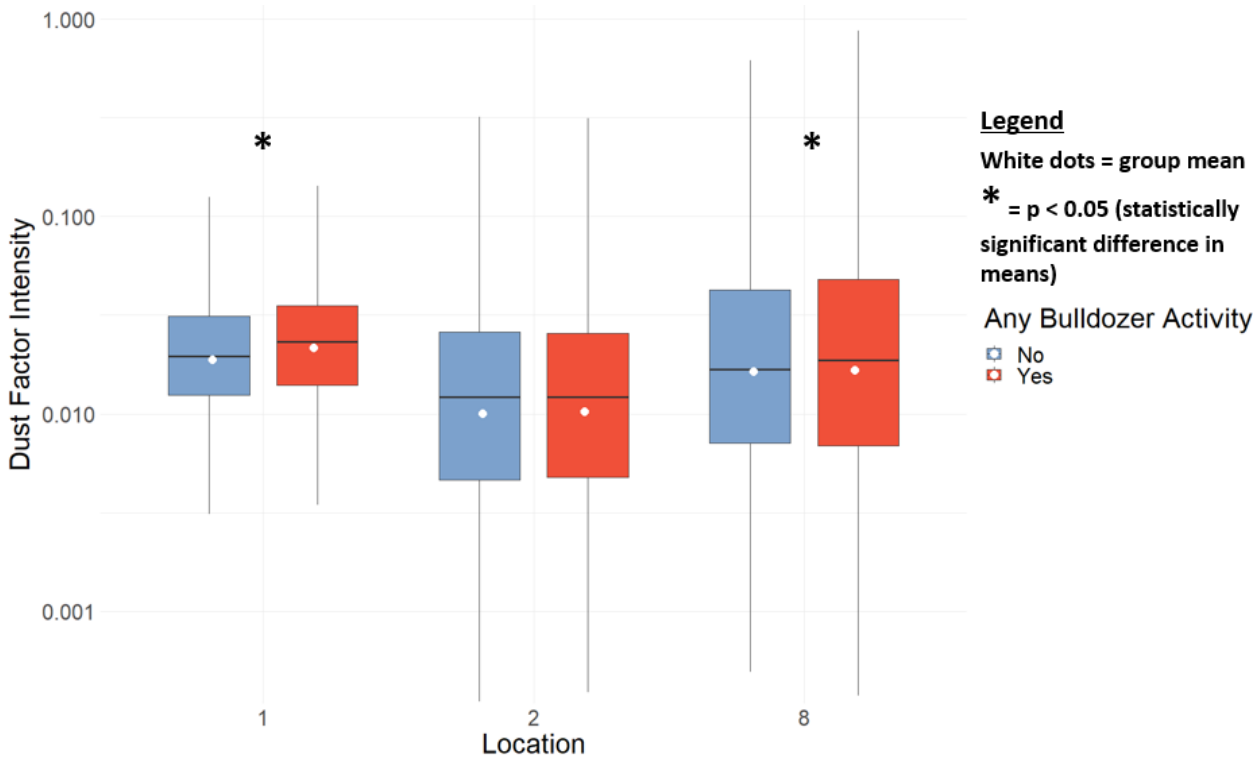

Figure 17. Dust factor boxplots stratified by terminal bulldozer activity at all Locations 1, 2, and 8, September 16, 2022 – March 8, 2023. ***Note.*** "Dust" at Locations 1 and 2 is putative coal dust (PCD), whereas it is dust at Location 8. There is no data for Location 5 because there was no calculable PCD factor due to lack of black carbon data. Asterisks denote statistical significance ($p < 0.05$) from Welch t-test for difference of means.

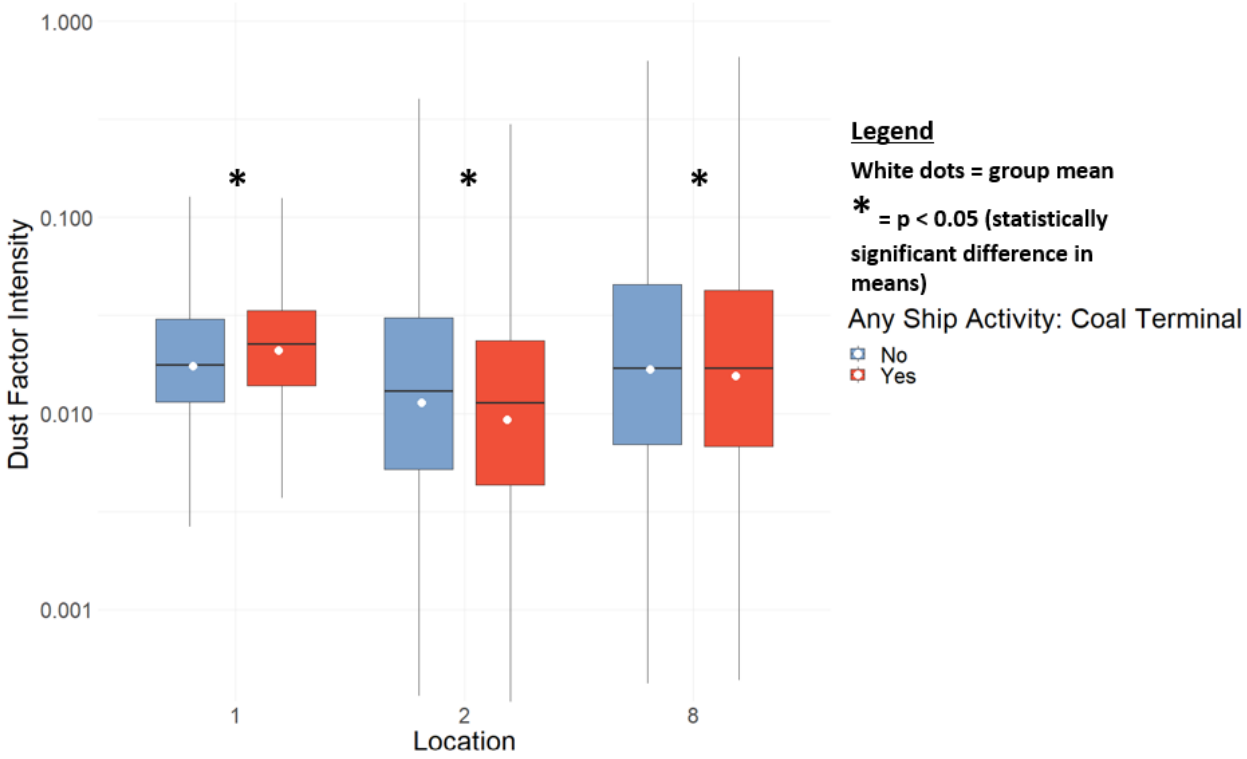

Figure 18. Boxplots of means of the dust factor stratified by terminal ship activity at Locations 1, 2, and 8, September 16, 2022 – March 8, 2023. ***Note.*** "Dust" at Locations 1 and 2 is putative coal dust (PCD), whereas it is dust at Location 8. There is no data for Location 5 because there was no calculable PCD factor due to lack of black carbon data. Asterisks denote statistical significance ($p < 0.05$) from Welch t-test for difference of means.

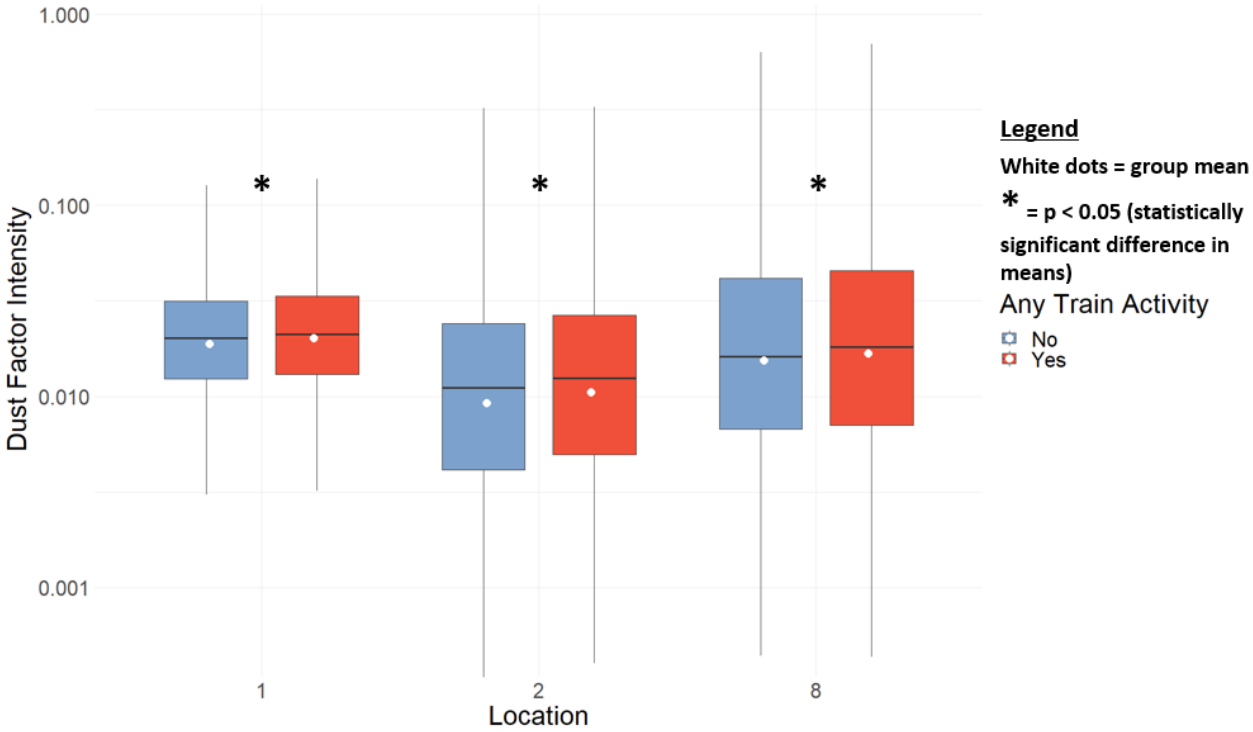

Figure 19. Boxplots of means of the dust factor stratified by terminal train activity at Locations 1, 2, and 8, September 16, 2022 – March 8, 2023. ***Note.*** "Dust" at Locations 1 and 2 are putative coal dust (PCD), whereas it is dust at Location 8. There is no data for Location 5 because there was no calculable PCD factor due to lack of black carbon data. Asterisks denote statistical significance ($p < 0.05$) from Welch t-test for difference of means.

Conclusions

Non-negative matrix factorization (NMF) appears to be a helpful tool in terms of source apportionment (i.e., linking combinations of pollutants back to sources). We applied NMF to data from four locations in the South Baltimore Air Monitoring Network, and clear putative coal dust (PCD) factors emerged at locations closest to the terminal. Further, closer to the terminal, we noted that the mean duration of dust (PCD) events was higher relative to locations farther from the terminal. These factors corresponded with both collaborative team-identified coal dust events, in addition to helping to identify additional events around the network. Further statistical tests suggest that pollutant concentrations and the putative coal dust factor are elevated both during bulldozer and train activity at the coal terminal and when the wind blows downwind from the terminal towards network sensor locations near the fenceline of the terminal. While there is not a clear putative coal dust factor at Location 8, this does not indicate an absence of coal dust at the location. As noted in previous sections, there appeared to be coal dust at this location via physical settled dust characterization methods.

References

1. Aubourg MA, Sawtell G, Deanes L, et al. Community-driven research and capacity building to address environmental justice concerns with industrial air pollution in Curtis Bay, South Baltimore. *Frontiers in Epidemiology*. 2023;3. Accessed December 13, 2023. https://www.frontiersin.org/articles/10.3389/fepid.2023.1198321

Appendix

Table A.1. Date Ranges Covered by QuantAQ MODULAIR and DSTech ObservAir in the South Baltimore Air Monitoring Network, Baltimore, MD (mm/dd/yy).

Location	QuantAQ MODULAIR	DSTech ObservAir
1	07/13/22 - 07/17/23	10/19/22 - 05/03/23
2	11/11/22 - 07/08/23	02/08/23 - 06/26/23
3	10/06/22 - 04/19/23	N/A
4	09/07/22 - 07/17/23	N/A
5	05/25/22 - 07/17/23	07/05/22 - 09/16/22; 05/03/23 - 05/31/23
6	11/07/22 - 07/17/23	N/A
7	11/23/22 - 04/30/23	N/A
8	07/05/22 - 06/07/23	12/22/22 - 04/19/23
9	02/14/23 - 07/17/23	N/A
10	07/05/22 - 07/17/23	N/A

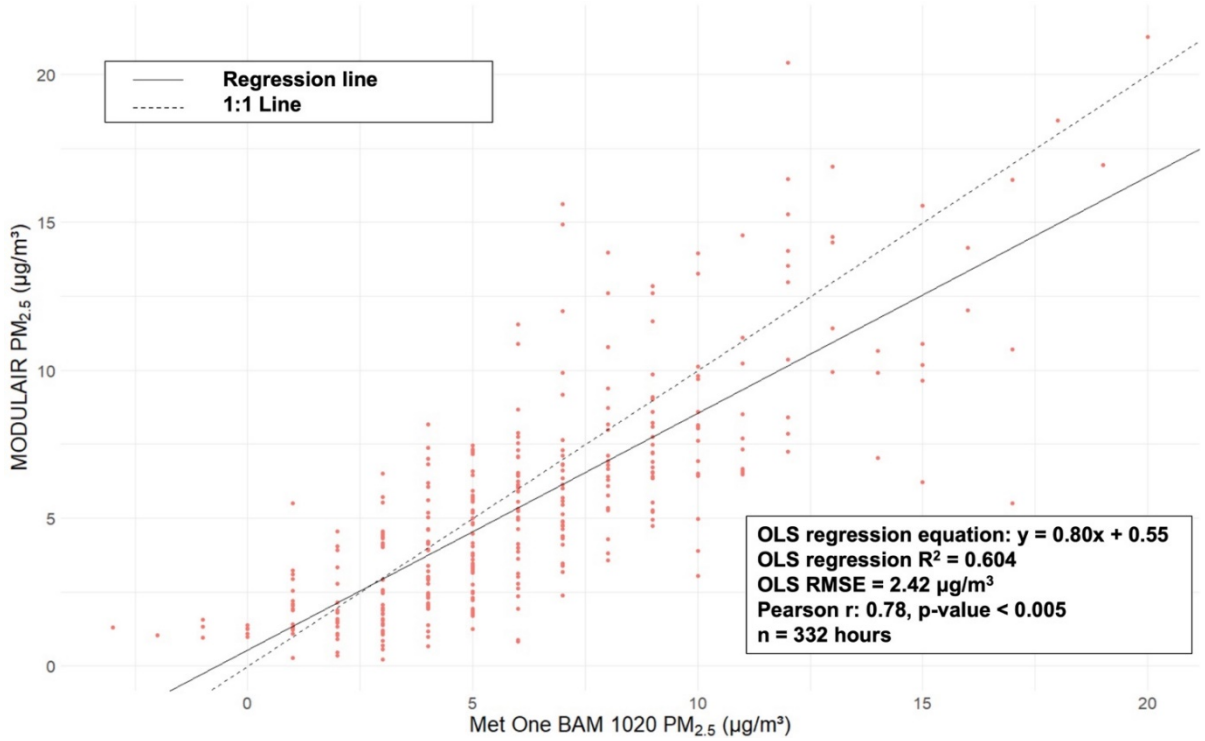

Figure A.1. Comparison between co-located, hourly-averaged QuantAQ MODULAIR (low-cost sensor) and Met One Instruments Continuous Particulate Monitor BAM 1020 (regulatory monitor) $PM_{2.5}$ measurements ($\mu g/m^3$) at the Howard County Near Road site in the Maryland Department of the Environment Ambient Air Monitoring Network (14-day co-location). ***Note***. OLS = Ordinary least squares; in the OLS regression model, MODULAIR $PM_{2.5}$ is the dependent variable, y, and Met One BAM 1020 $PM_{2.5}$ is the independent variable, x. RMSE = root-mean-square error. n = sample size.

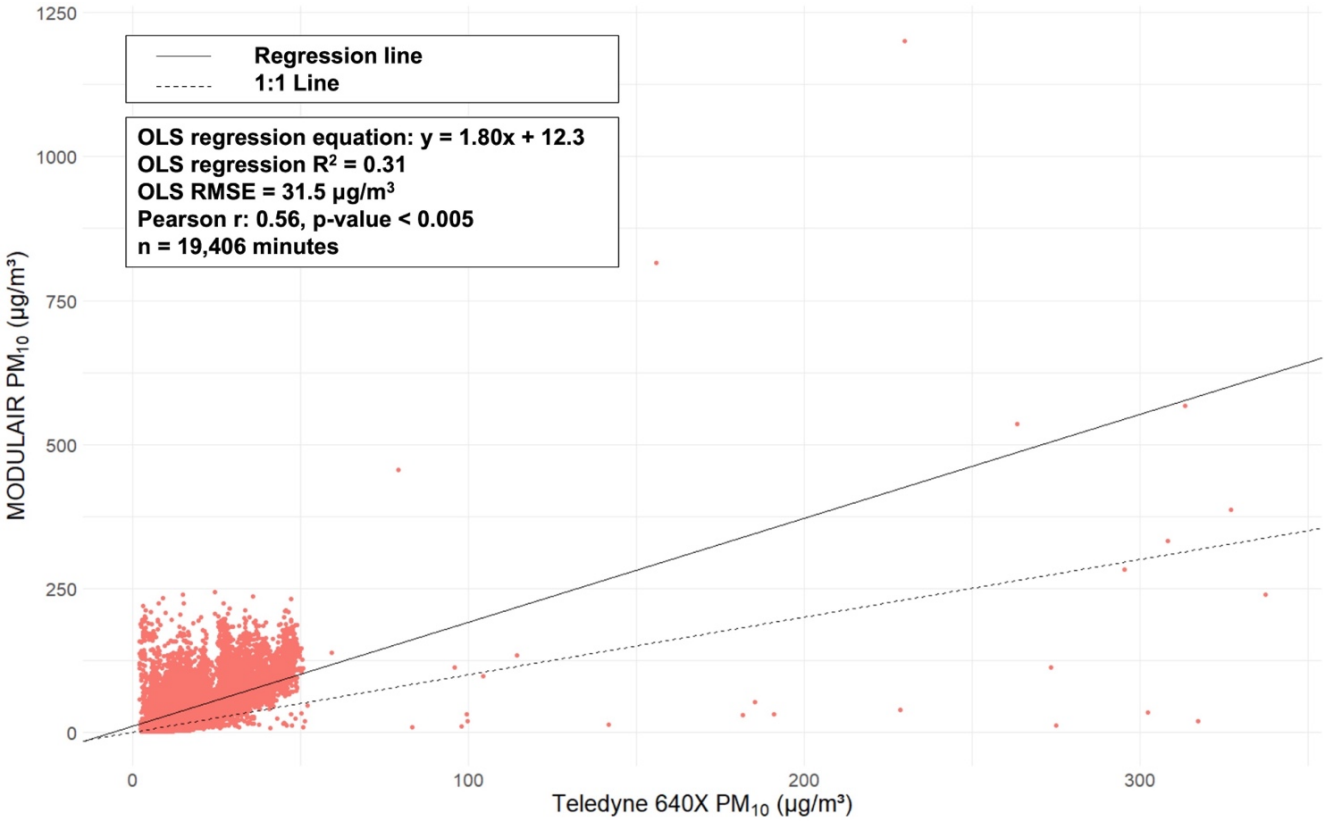

Figure A.2. Comparison between co-located, minute-averaged QuantAQ MODULAIR (low-cost sensor) and Teledyne API 640X (regulatory-grade monitor) $PM_{2.5}$ measurements (µg/m^3) at the Pocomoke City site in the Lower Eastern Shore Ambient Air Quality Monitoring Project (14-day co-location). ***Note.*** OLS = Ordinary least squares; in the OLS regression model, MODULAIR $PM_{2.5}$ is the dependent variable, y, and Teledyne API 640X $PM_{2.5}$ is the independent variable, x. RMSE = root-mean-square error. n = sample size.

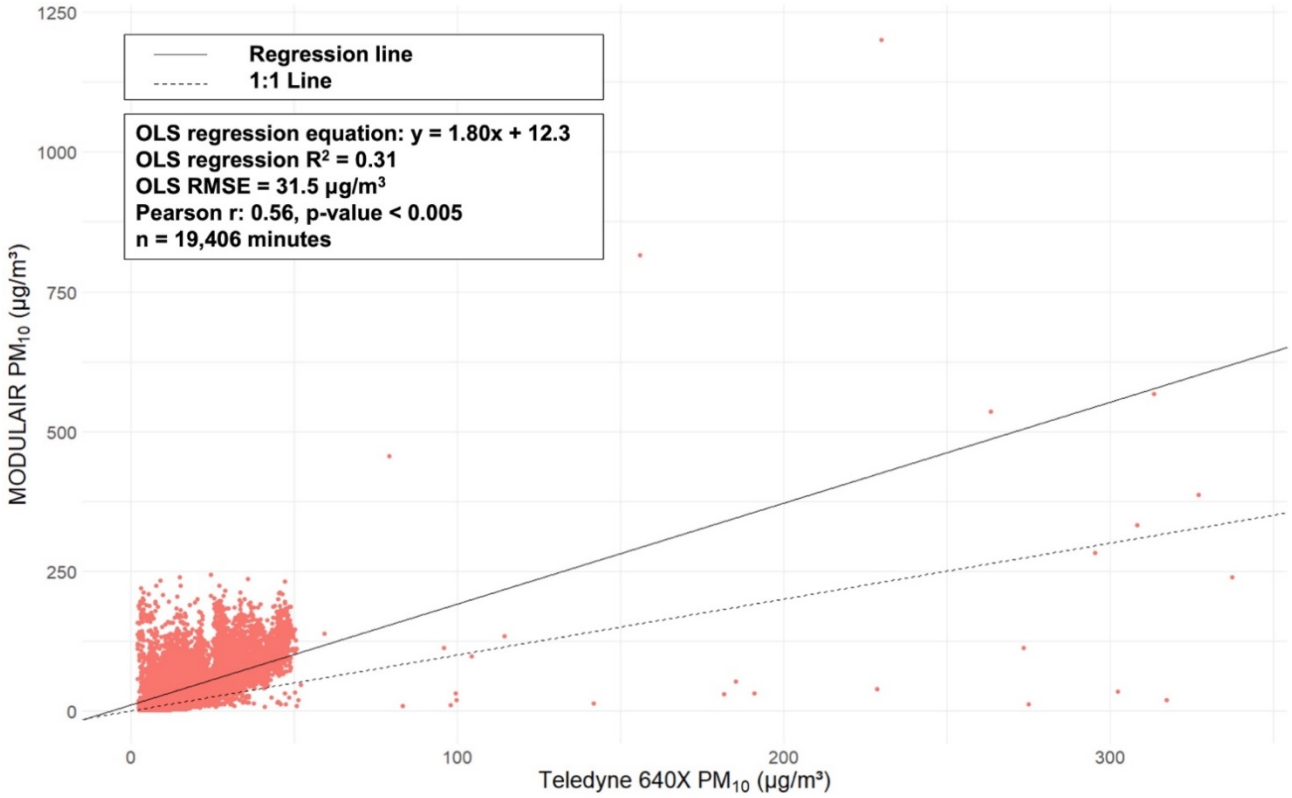

Figure A.3. Comparison between minute-averaged QuantAQ MODULAIR (low-cost sensor) and Teledyne 640X (regulatory-grade monitor) PM_{10} measurements (µg/m^3) at the Pocomoke City site in the Lower Eastern Shore Ambient Air Quality Monitoring Project (14-day co-location). ***Note.*** OLS = Ordinary least squares; in the OLS regression model, MODULAIR PM_{10} is the dependent variable, y, and Teledyne API 640X PM_{10} is the independent variable, x. RMSE = root-mean-square error. n = sample size.

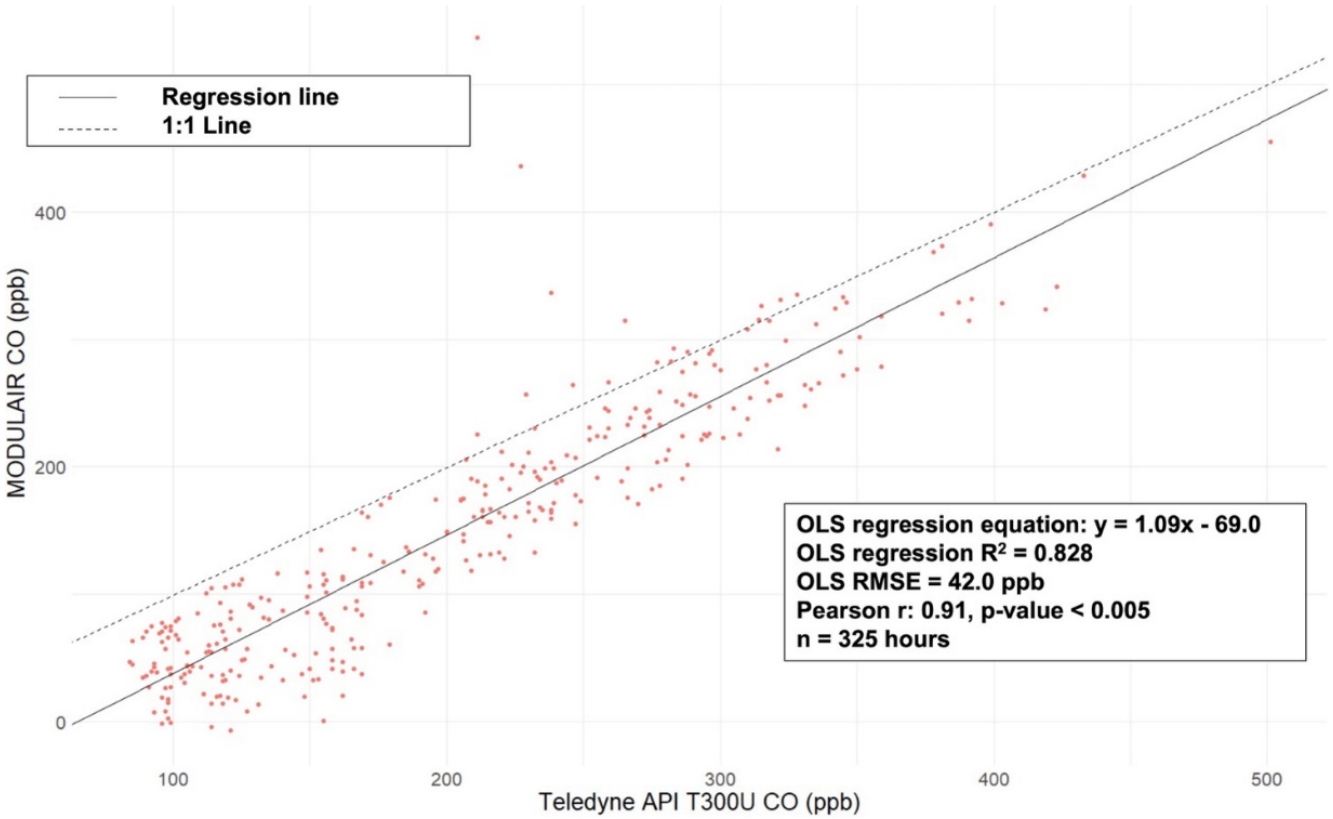

Figure A.4. Comparison between hourly-averaged QuantAQ MODULAIR (low-cost sensor) and Teledyne API T300U (regulatory monitor) carbon monoxide (CO) measurements (ppb) at the Howard County Near Road site in the Maryland Department of the Environment Ambient Air Monitoring Network (14-day co-location).
Note. OLS = Ordinary least squares; in the OLS regression model, MODULAIR CO is the dependent variable, y, and Teledyne API T300U CO is the independent variable, x. RMSE = root-mean-square error. n = sample size.

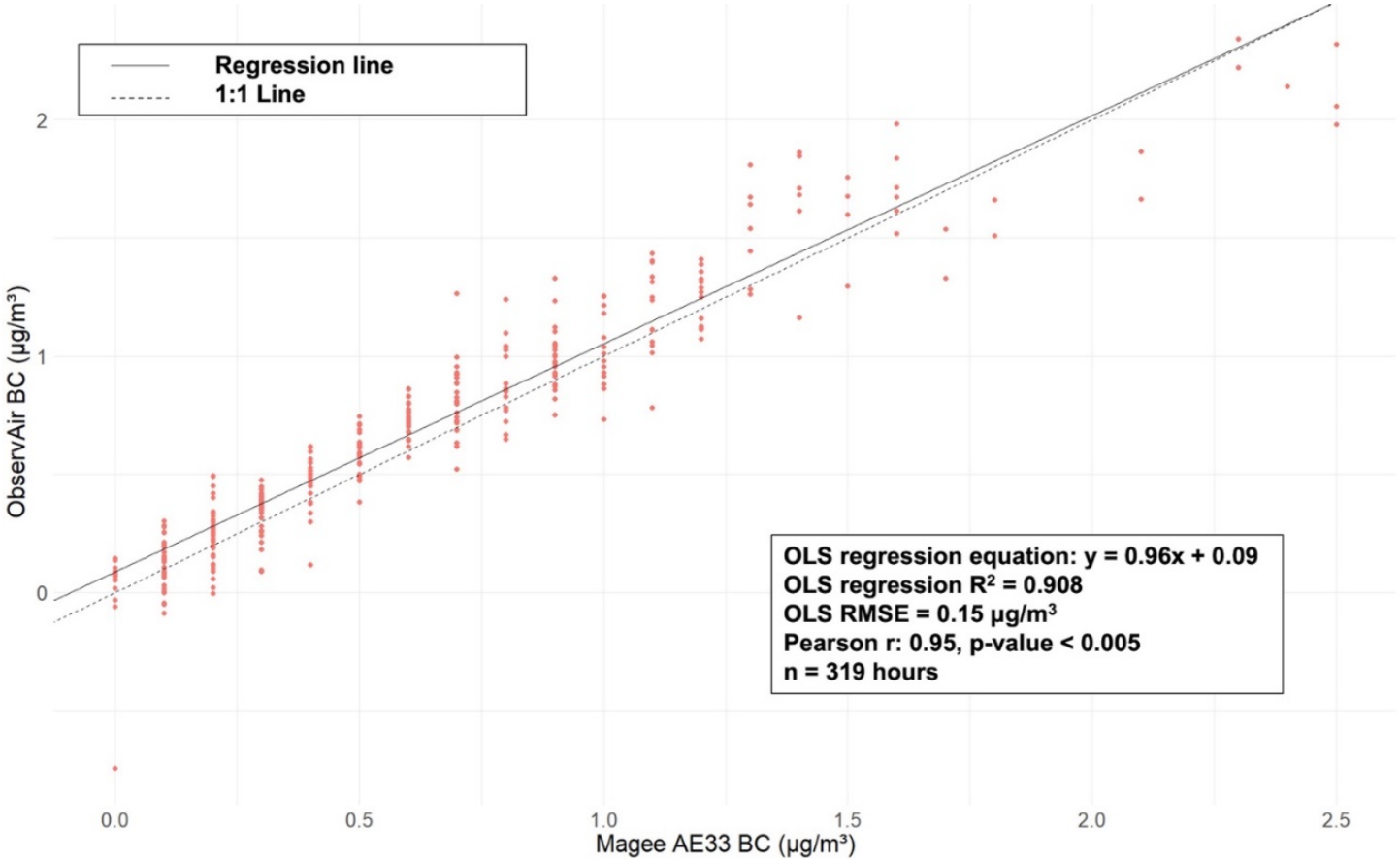

Figure A.5. Comparison between co-located, hourly-averaged Distributed Sensing Technologies ObservAir (low-cost sensor) and Magee Scientific Aethalometer AE33 (regulatory agency monitor) black carbon (BC) measurements (µg/m^3) at the Howard County Near Road site in the Maryland Department of the Environment Ambient Air Monitoring Network (14-day co-location). ***Note.*** OLS = Ordinary least squares; in the OLS regression model, ObservAir BC is the dependent variable, y, and Magee AE33 BC is the independent variable, x. RMSE = root-mean-square error. n = sample size.

Table A.2. Association of wind direction and community-observed coal terminal activity patterns with offsite 1-min time-weighted average air pollutants measured at location 1, Curtis Bay, South Baltimore, MD (October 26, 2022 - April 27, 2023).

T1

	$PM_{2.5}$ (µg/m³)						PM_{10} (µg/m³)						Total suspended particles (µg/m³)						Black carbon (µg/m³)						Putative coal dust factor					
				95% CI						95% CI						95% CI						95% CI						95% CI		
	n	%	Geo. mean	Lower	Upper	*p*-value[a]	n	%	Geo. mean	Lower	Upper	*p*-value[a]	n	%	Geo. mean	Lower	Upper	*p*-value[a]	n	%	Geo. mean	Lower	Upper	*p*-value[a]	n	%	Geo. mean	Lower	Upper	*p*-value[a]
Location 1 at southern fenceline of coal terminal																														
Downwind of coal terminal																														
No	88,553	68	**7.89**	**8.60**	**8.68**		88,553	68	**19.1**	**19.0**	**19.2**		88,553	68	**22.2**	**22.1**	**22.4**		88,555	68	**0.713**	**0.708**	**0.719**		88,184	68	**0.018**	**0.018**	**0.018**	
Yes	40,790	32	**8.15**	**9.50**	**9.61**	**<0.005**	40,790	32	**24.3**	**24.1**	**24.5**	**<0.005**	40,790	32	**28.5**	**28.2**	**28.7**	**<0.005**	40,807	32	**0.871**	**0.862**	**0.880**	**<0.005**	40,761	32	**0.021**	**0.021**	**0.021**	**<0.005**
Any ship activity																														
No	36,385	39	**8.04**	**7.98**	**8.10**		36,385	39	**16.2**	**16.1**	**16.4**		36,385	39	**18.5**	**18.3**	**18.7**		36,386	39	**0.684**	**0.676**	**0.692**		36,322	39	**0.017**	**0.017**	**0.018**	
Yes	57,662	61	**9.76**	**9.71**	**9.81**	**<0.005**	57,662	61	**23.1**	**22.9**	**23.3**	**<0.005**	57,662	61	**26.9**	**26.7**	**27.1**	**<0.005**	57,674	61	**0.820**	**0.813**	**0.827**	**<0.005**	57,447	61	**0.021**	**0.021**	**0.021**	**<0.005**
Any bulldozer activity																														
No	58,739	59	**8.68**	**8.63**	**8.72**		58,739	59	**19.1**	**19.0**	**19.3**		58,730	59	**22.1**	**21.9**	**22.3**		58,741	59	**0.771**	**0.764**	**0.777**		58,550	59	**0.019**	**0.019**	**0.019**	
Yes	41,456	41	**10.01**	**9.95**	**10.08**	**<0.005**	41,456	41	**22.4**	**22.2**	**22.6**	**<0.005**	41,456	41	**25.9**	**25.6**	**26.1**	**<0.005**	41,467	41	**0.830**	**0.821**	**0.839**	**<0.005**	41,359	41	**0.022**	**0.021**	**0.022**	**<0.005**
Any train activity																														
No	50,534	54	**8.71**	**8.66**	**8.76**		50,534	54	**19.9**	**19.7**	**20.1**		50,534	54	**23.1**	**22.8**	**23.3**		50,547	54	0.766	0.759	0.774		50,354	54	**0.019**	**0.019**	**0.019**	
Yes	43,846	46	**9.42**	**9.36**	**9.48**	**<0.005**	43,846	46	**20.5**	**20.3**	**20.6**	**<0.005**	43,846	46	**23.6**	**23.3**	**23.8**	**<0.005**	43,846	46	0.765	0.757	0.773	0.8441	43,748	46	**0.020**	**0.020**	**0.020**	**<0.005**

Note. CI = confidence interval.

[a]*p*-values estimated from t-tests using $\log_{10}$ transformed variables.

[b]All pollutants, downwind designation, and putative coal dust factor are limited to NMF complete-case analysis with ranges from October 26, 2022 - April 27, 2023.

[c]Camera data collected from September 16, 2022 - March 8, 2023, but NMF complete-case analysis limits to inclusion of camera activities to October 26, 2022 - March 8, 2023.

Table A.3. Association of wind direction and community-observed coal terminal activity patterns with offsite 1-min time-weighted average air pollutants measured at location 2, Curtis Bay, South Baltimore, MD (February 8, 2023 – June 19, 2023).

	$PM_{2.5}$ (µg/m³)						PM_{10} (µg/m³)						Total suspended particles (µg/m³)						Black carbon (µg/m³)						Putative coal dust factor					
				95% CI						95% CI						95% CI						95% CI						95% CI		
	n	%	Geo. mean	Lower	Upper	*p*-value[a]	n	%	Geo. mean	Lower	Upper	*p*-value[a]	n	%	Geo. mean	Lower	Upper	*p*-value[a]	n	%	Geo. mean	Lower	Upper	*p*-value[a]	n	%	Geo. mean	Lower	Upper	*p*-value[a]
Location 2 at northern fenceline of coal terminal																														
Downwind of coal terminal																														
No	67,088	62	**7.71**	**7.66**	**7.76**		67,088	62	**14.9**	**14.8**	**15.0**		67,088	62	**17.4**	**17.3**	**17.5**		67,088	62	**0.46**	**0.46**	**0.47**		53,782	59	**0.0085**	**0.0084**	**0.0086**	
Yes	41,573	38	**10.24**	**10.17**	**10.30**	**<0.005**	41,573	38	**22.2**	**22.1**	**22.4**	**<0.005**	41,573	38	**25.9**	**25.7**	**26.1**	**<0.005**	41,573	38	**0.67**	**0.66**	**0.67**	**<0.005**	36,894	41	**0.0138**	**0.0137**	**0.0140**	**<0.005**
Any ship activity																														
No	10,439	33	7.74	7.66	7.82		10,439	33	**16.8**	**16.6**	**17.1**		10,439	33	**19.4**	**19.0**	**19.7**		10,439	33	0.42	0.41	0.43		8,689	34	**0.0113**	**0.0110**	**0.0117**	
Yes	21,472	67	7.84	7.77	7.91	0.894	21,472	67	**15.7**	**15.6**	**15.9**	**<0.005**	21,472	67	**18.3**	**18.1**	**18.6**	**<0.005**	21,472	67	0.41	0.41	0.42	0.088	17,093	66	**0.0093**	**0.0091**	**0.0095**	**<0.005**
Any bulldozer activity																														
No	15,826	48	7.90	7.83	7.98		15,826	48	16.5	16.3	16.7		15,826	48	19.1	18.8	19.4		15,826	48	**0.40**	**0.40**	**0.41**		13,055	49	0.0100	0.0098	0.0103	
Yes	17,154	52	7.95	7.87	8.02	0.444	17,154	52	16.2	16.0	16.4	0.009	17,154	52	18.9	18.6	19.1	0.265	17,154	52	**0.45**	**0.45**	**0.46**	**<0.005**	13,770	51	0.0103	0.0100	0.0105	0.171
Any train activity																														
No	13,530	42	7.74	7.66	7.82		13,530	42	**15.5**	**15.3**	**15.7**		13,530	42	**17.8**	**17.6**	**18.1**		13,530	42	**0.37**	**0.36**	**0.38**		10,867	42	**0.0093**	**0.0090**	**0.0095**	
Yes	18,368	58	7.85	7.77	7.92	0.054	18,368	58	**16.5**	**16.3**	**16.7**	**<0.005**	18,368	58	**19.3**	**19.1**	**19.6**	**<0.005**	18,368	58	**0.45**	**0.45**	**0.46**	**<0.005**	14,902	58	**0.0105**	**0.0102**	**0.0107**	**<0.005**

Note. CI = confidence interval.

[a]*p*-values estimated from t-tests using $\log_{10}$ transformed variables.

[b]All pollutants, downwind designation, and putative coal dust factor are limited to NMF complete-case analysis with ranges from February 8, 2023 - June 19, 2023.

[c]Camera data collected from September 16, 2022 - March 8, 2023, but NMF complete-case analysis limits to inclusion of camera activities to February 8, 2023 - March 8, 2023.

4. Community-wide Air Pollution Burden in Curtis Bay, South Baltimore, Maryland

Research questions addressed

From cumulative and source-specific perspectives, what is the air pollution burden in the Curtis Bay community and what are the implications for public health and environmental justice?

South Baltimore Air Monitoring Network

Background

Community members have expressed concerns about several air pollutants in Curtis Bay, including criteria pollutants $PM_{2.5}$ and PM_{10}. Data provided to the community and the Maryland Department of the Environment (MDE) by the Department of Environmental Health and Engineering, Johns Hopkins Bloomberg School of Public Health (BSPH) ("V5_combined_Nov11_2023_ET" for daily concentration calculations and associated statistics, verified against "V6_combined_Nov29_2023_ET", which was used for minute data and directional analysis) were used to characterize the burden of these two pollutants in Curtis Bay. 1-minute resolution summary statistics can be found in the Appendix.

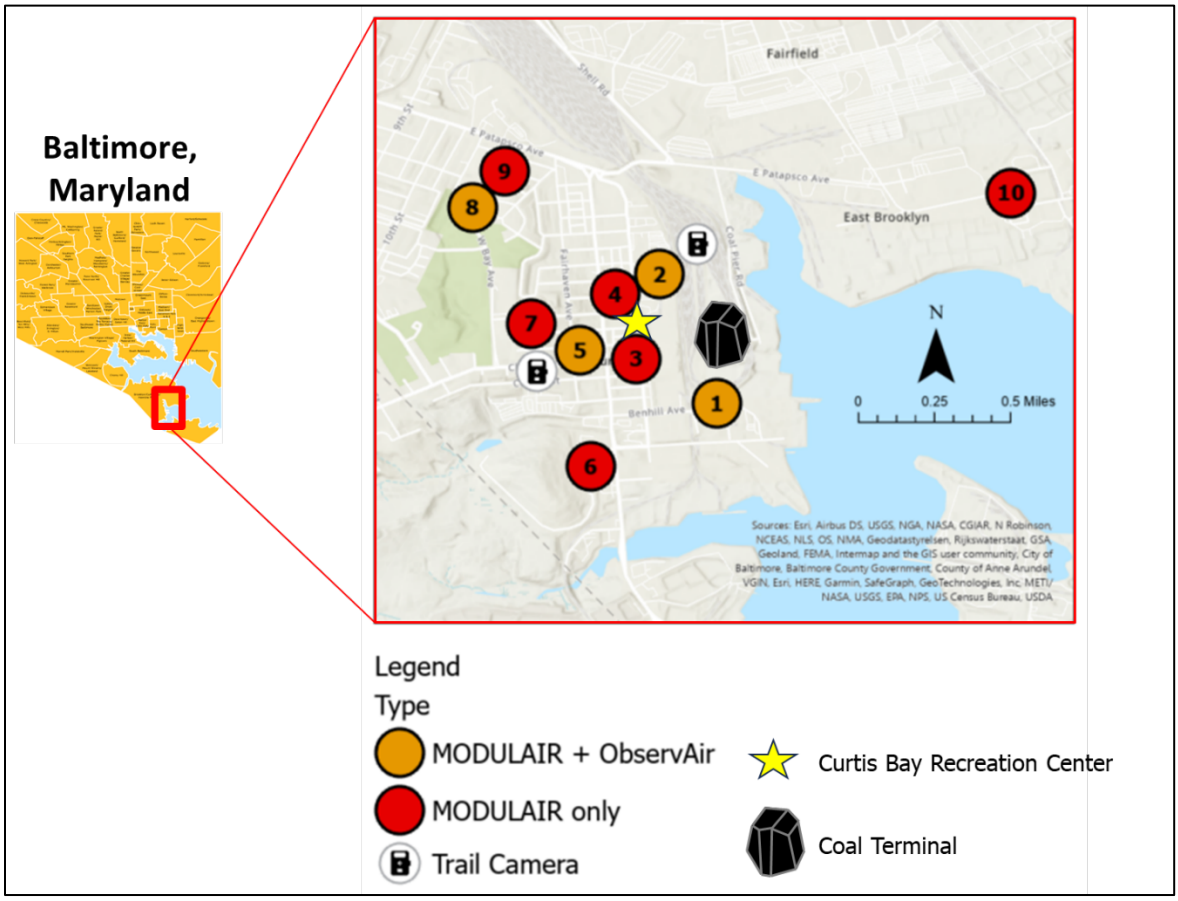

Figure 1. South Baltimore Air Monitoring Network, Baltimore, Maryland. Established Spring 2022 in Curtis Bay, South Baltimore, Maryland. Note. Locations are approximate to ensure monitor host anonymity.

Smoke-impacted Data

During late spring and summer of 2023, Maryland experienced an unprecedented number of days with air quality impacted by wildfire smoke. Wildfires across North America, and particularly Canada, increased in intensity, duration, and total area burned, due to an abnormally warm and dry winter and early spring this year. Fires were essentially continuous in various parts of Canada from early May through September 2023, sending waves of smoke across the continental United States throughout the summer, as meteorological conditions dictated. Frequent episodes of smoke across Maryland this spring and summer created periods of heightened fine particulate matter at values not seen in several years. MDE is currently in the process of demonstrating to the Environmental Protection Agency (EPA) the exceptional nature of these events and their impact on air quality across the state. Once concurred by the EPA, all dates demonstrated to have been impacted by the wildfire events will be excluded from regulatory consideration. This analysis will examine the data both inclusive and exclusive of those dates currently under review as exceptional events due to wildfire smoke. The following dates have been excluded due to smoke, when indicated: April 13, April 21, May 12, June 1-3, June 7 and 8, June 11, June 15, June 19, June 28-30, and July 11-13 – all dates are for 2023.

Time series of daily average concentrations for both $PM_{2.5}$ and PM_{10} are included for comparison with the National Ambient Air Quality Standards (NAAQS). Tables with the arithmetic mean, median, 98th percentile, standard deviation, deployment maximum, maximum date, and number of days included in analysis for each sensor are provided for $PM_{2.5}$, while tables for PM_{10} include the arithmetic mean, the number of days in excess of the NAAQS, maximum daily PM_{10}, and the maximum date are provided for reference. Box plots of concentrations at each site for when the sensor was and was not down wind of the coal export terminal are included for comparison as well.

$PM_{2.5}$

QuantAQ's MODULAIR sensors provide minute observations for all pollutants and meteorological parameters. Using the CHARMED dataset and the 'openair' R package, the minute $PM_{2.5}$ concentration data were averaged to hourly values, observing a 75% data capture threshold, so that hours with fewer than 45 minutes were excluded from analysis. Resultant hourly values were used to calculate daily (24-hour) concentrations for comparison with the NAAQS. Daily mean concentrations were computed for each day of deployment in Excel, from the hourly $PM_{2.5}$ concentration data processed and exported from R. To create a more robust dataset in line with Federal data quality requirements (40 CFR Appendix-N-to-Part-50 3.0(c)), daily average concentrations were considered valid "if at least 75% of the hourly averages (i.e., 18 hourly values) for the 24-hour period are available." All daily concentration values with less than 24 hours, but at least 18, were kept "using the number of available hours within the 24-hour period as the divisor." Days with fewer than 18 hours were "considered valid if, after substituting zero for all missing hourly concentrations, the resulting 24-hour average daily value is greater than…or equal to 35.5 $\mu g/m^3$", in exceedance of current standards. After averaging minute data to hourly values and further to daily values in R and Excel, there were 407 days across the study area, when at least one site produced a valid daily concentration. When excluding smoke-impacted data, there were 390 days. All values are truncated at one decimal place.

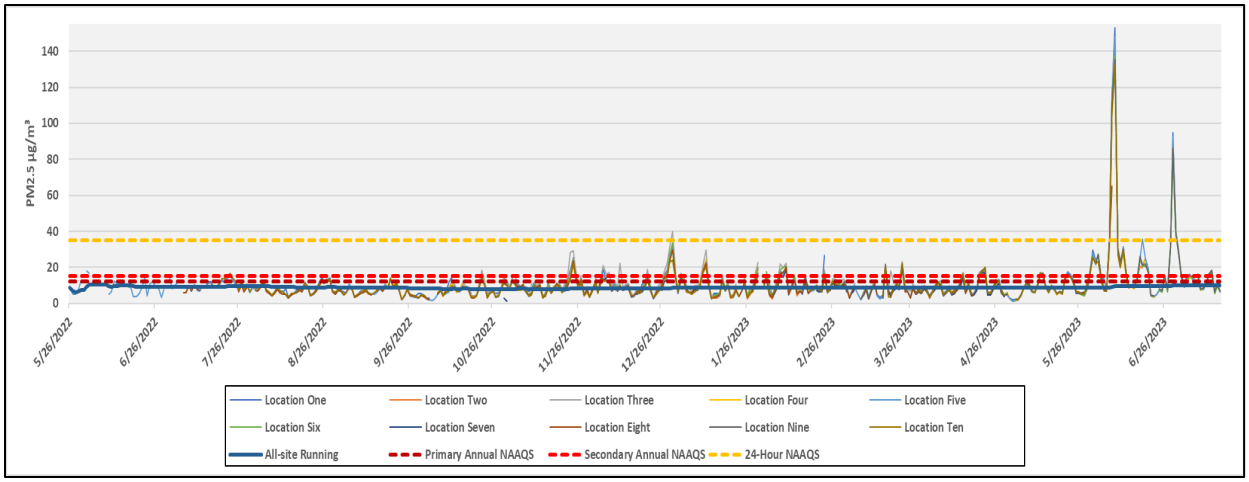

Figure 2. Time series of the 24-hour average $PM_{2.5}$ concentrations across the network and at each individual location, with smoke-impacted data included NAAQS are in red(annual) & orange(24-hour) for reference.

Using the complete data (5/26/22-7/16/23) set to create daily averages across all locations, the mean $PM_{2.5}$ concentration in Curtis Bay is 10.1 µg/m³, which is below current primary and secondary annual NAAQS. When using the entire raw minute dataset for the full period of deployment (5/26/22-7/16/23), averaging the $PM_{2.5}$ concentrations for each minute from all sensors in the Curtis Bay network, the mean is 10.4 µg/m³.

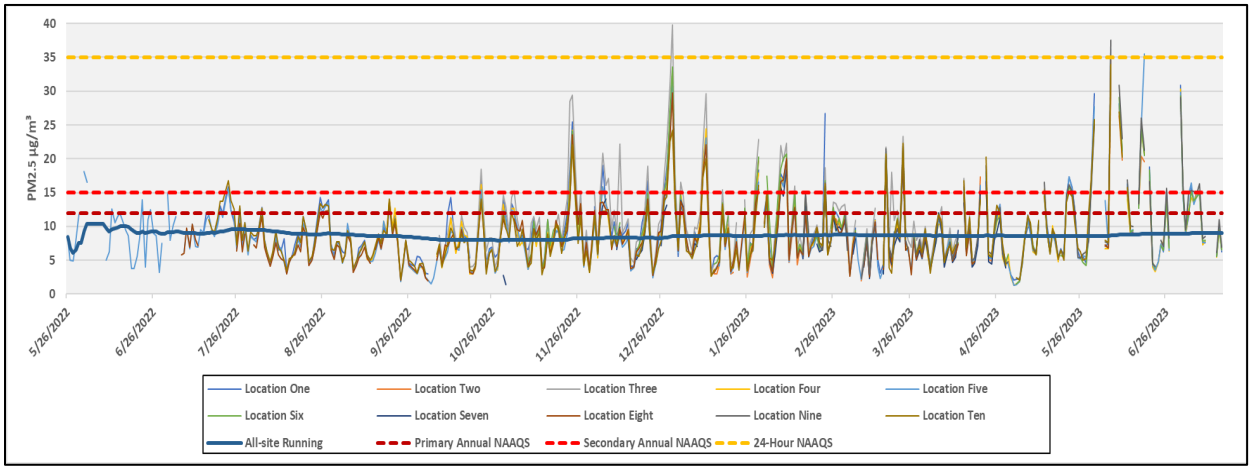

Figure 3. Time series of the 24-hour average $PM_{2.5}$ concentrations across the network and at each individual location, with smoke-impacted data excluded; NAAQS are in red(annual) & orange(24-hour) for reference.

Excluding smoke-impacted data (5/26/22-7/16/23), as seen in Figure 2. Above, yields an annual mean $PM_{2.5}$ concentration of 9.0 µg/m³.

Attainment of the NAAQS is determined using Design Value (DV) statistics, which are calculated with three years of valid data that are not available currently for the network in Curtis Bay. Annual values have been estimated for the next two years using the complete, averaged network data and quarters based on the dates of the deployment, for comparison with the primary and secondary annual NAAQS. Averaging by quarter to account for some seasonal variability, the three-year design value for the area is estimated to be 9.4 µg/m³. The fourth quarter of the first year and the first quarter of the second year

include data that were smoke-impacted by wildfires across Canada; if the concentrations are removed for those dates (4/13,4/21,5/12,6/1-3, 6/7-8, 6/11, 6/15, 6/19, 6/28-6/30, & 7/11-13/23), the design value would be 9 µg/m³. Both values are in attainment of the current annual NAAQS for $PM_{2.5}$.

Tables 1. & 2. $PM_{2.5}$ estimates for 2022-2025, by quarter. Table 3. (left) includes all valid sensor data; Table 4. (right) has smoke-impacted data related to wildfires excluded.

Quarter	22-23	23-24	24-25
Q1 5/26-8/24/22	8.791405	15.39102	12.09121
Q2 8/25-11/23/22	7.431479	7.431479	7.431479
Q3 11/24/22-2/22/23	9.878504	9.878504	9.878504
Q4 2/23-5/25/23	8.386291	8.386291	8.386291
Mean	8.62192	10.27182	9.446872

Quarter	22-23	23-24	24-25
Q1 5/26-8/24/22	8.791404509	10.70460929	12.09121364
Q2 8/25-11/23/22	7.431479497	7.431479497	7.431479497
Q3 11/24/22-2/22/23	9.878504278	9.878504278	9.878504278
Q4 2/23-5/25/23	8.171634459	8.171634459	8.171634459
Smoke-Excl. Mean	8.568255686	9.046556881	9.393207969

The 98th percentile of the distribution of 24-hour concentration values across all sampling sites was approximated using the procedure from 40 CFR Appendix-N-to-Part-50 4.04.5(a) as a guide. There were 211 days when at least one sensor returned a valid 24-hour concentration in 2022, which produces a 98th percentile of 16.9 µg/m³. For 2023, the number of days when at least one sensor returned a valid 24-hour concentration that's included in the available dataset was 196, with a 98th percentile of 39.0 µg/m³. The average for the two years is 27.9 µg/m³, which is below the primary and secondary 24-hour NAAQS of 35 µg/m³. Using the same procedure, the dataset with smoke-impacted data removed had 179 days of daily $PM_{2.5}$ concentrations, and thus the 98th percentile for this 2023 dataset is 26.8 µg/m³. The average for the two years with smoke-impacted data removed is 21.8 µg/m³, also below the current primary and secondary 24-hour NAAQS of 35 µg/m³. The 98th percentile of the complete data set (5/26/22-7/16/23) is 28.5 µg/m³, which would also be in attainment of current NAAQS.

There is some variation in the $PM_{2.5}$ concentration values seen across the individual sensor locations in Curtis Bay, some of which is displayed below in Tables 3. and 4., which were created using daily average data. After exclusion of smoke impacted data, no site is currently above the NAAQS levels for $PM_{2.5}$.

Table 3. Descriptive $PM_{2.5}$ statistics for individual monitoring locations in Curtis Bay and a nearby MDE regulatory monitor at Lake Montebello. MDE site data from AQS.

Site	Arithmetic Mean PM2.5	Median 24-Hour PM2.5	98th Percentile 24-Hour PM2.5	Standard Deviation	Maximum 24-Hour PM2.5	Maximum Date	#Days Captured
Location One	11.0	8.6	30.2	12.1	159.1	6/8/2023	334
Location Two	11.6	8.1	34.7	16.9	148.6	6/8/2023	107
Location Three	10.5	9.2	24.9	5.7	40.9	12/30/2022	227
Location Four	10.5	8.0	31.1	12.6	152.9	6/8/2023	288
Location Five	9.9	7.8	29.4	11	153.9	6/8/2023	406
Location Six	12.2	8.9	37.6	13.5	143.5	6/8/2023	213
Location Seven	8.5	7.5	18.6	4.2	22.8	1/11/2023	103
Location Eight	8.5	7.2	21.5	7.1	103.7	6/7/2023	271
Location Nine	13.3	9.1	56.5	16.3	140.3	6/8/2023	139
Location Ten	9.7	7.9	25.5	10.2	137.7	6/8/2023	296
Lake Montebello	8.2	6.7	21.1	9.1	114.3	6/8/2023	398

Table 4. Descriptive PM2.5 statistics for individual monitoring locations in Curtis Bay and nearby a MDE regulatory monitor at Lake Montebello, with smoke-impacted data removed. MDE site data from AQS.

Site	Arithmetic Mean PM2.5	Median 24-Hour PM2.5	98th Percentile 24-Hour PM2.5	Standard Deviation	Maximum 24-Hour PM2.5	Maximum Date	#Days Captured
Location One	9.6	8.3	24.6	5.2	37.6	6/9/2023	317
Location Two	9.3	7.5	20.5	5.6	35.6	6/9/2023	101
Location Three	10.5	9.2	24.9	5.6	40.9	12/30/2022	224
Location Four	8.9	7.8	24.3	5.3	37.4	6/9/2023	273
Location Five	8.7	7.6	23.1	5	37.6	6/9/2023	389
Location Six	10.2	8.7	25.4	5.8	38.6	6/9/2023	196
Location Seven	8.4	7.4	18.6	4.2	22.8	1/11/2023	101
Location Eight	8.1	7.2	20.3	4.2	31.7	12/30/2022	268
Location Nine	10.1	8.6	26.7	6.1	39.7	6/9/2023	122
Location Ten	8.7	7.7	21.2	4.5	35.1	6/9/2023	287
Lake Montebello	7.3	6.5	17.7	4.1	33.9	7/1/2023	384

The values seen in Curtis Bay are higher than those at nearby MDE monitoring sites by ~1-3 µg/m³. $PM_{2.5}$ is largely regarded as a regional pollutant, though Curtis Bay sensors may have some local contribution as well; when the wind direction was downwind versus not downwind of the coal terminal, $PM_{2.5}$ mean concentrations were statistically significantly higher at all sites, except location 10 (see Fig. 3, next page).

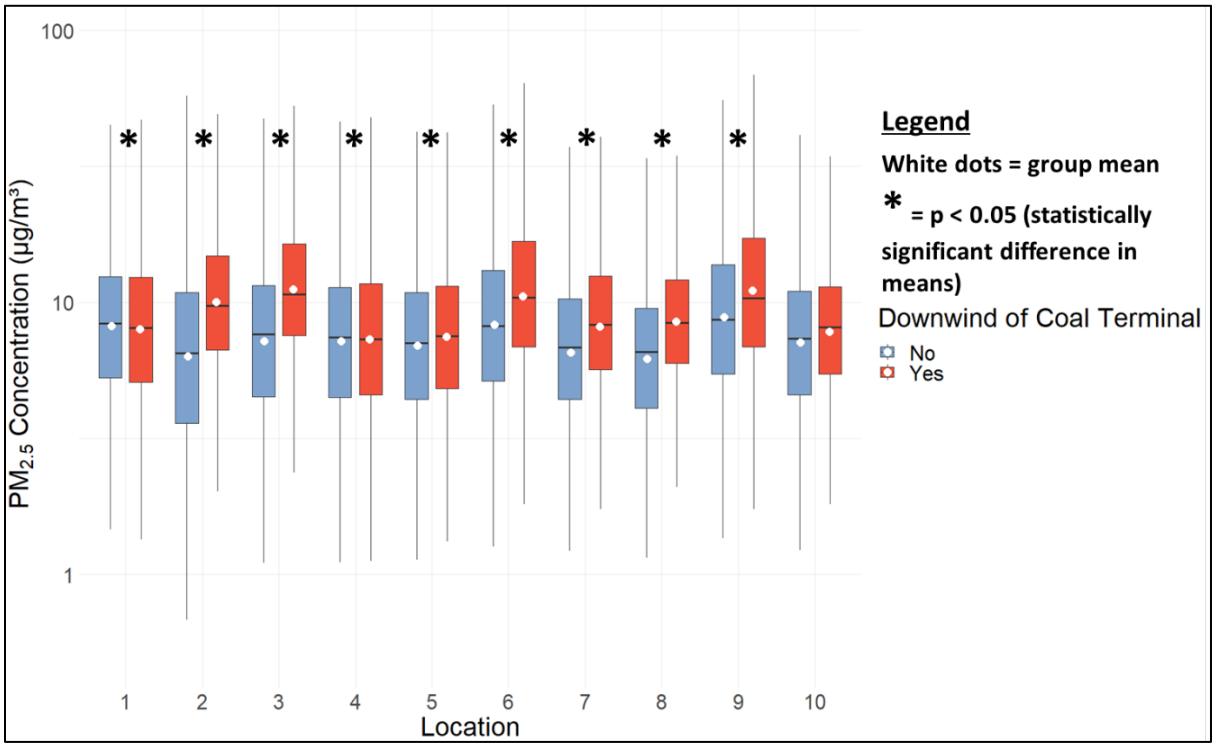

Figure 4. Comparison of MODULAIR $PM_{2.5}$ (µg/m³) across the South Baltimore Air Monitoring Network. Note. Sample sizes differ between locations due to rolling deployment. All "Downwind-Yes" means are statistically significantly greater than "Downwind-No" means at the p <0.05 level using Welch t-tests except for Location Ten, where the mean is higher, but the difference is not statistically significant. Provided by BSPH.

Location Three

Focusing on the data with smoke-impacted data excluded, the highest mean $PM_{2.5}$ values were observed at Location Three, located on an urban residential block, on the northwest corner of the

intersection of Church Street and Curtis Avenue, both major streets in the area, approximately 300' west of a warehouse construction site and 500' west of the coal export facility.

Directional analysis with polar plots and raw minute data created in 'openair' suggests $PM_{2.5}$ concentrations at Location Three are influenced by a source in the immediate vicinity of the sensor, possibly vehicular traffic/engine idling, and/or tobacco smoke; the highest $PM_{2.5}$ and CO concentrations are associated with all directions (360˚) in light winds (~1 m/s^{-1}), indicating a source in close proximity. Creating a pairwise polar plot of the correlation of $PM_{2.5}$ to CO, the strongest correlation between the two pollutants is seen in the direction of Church Street.

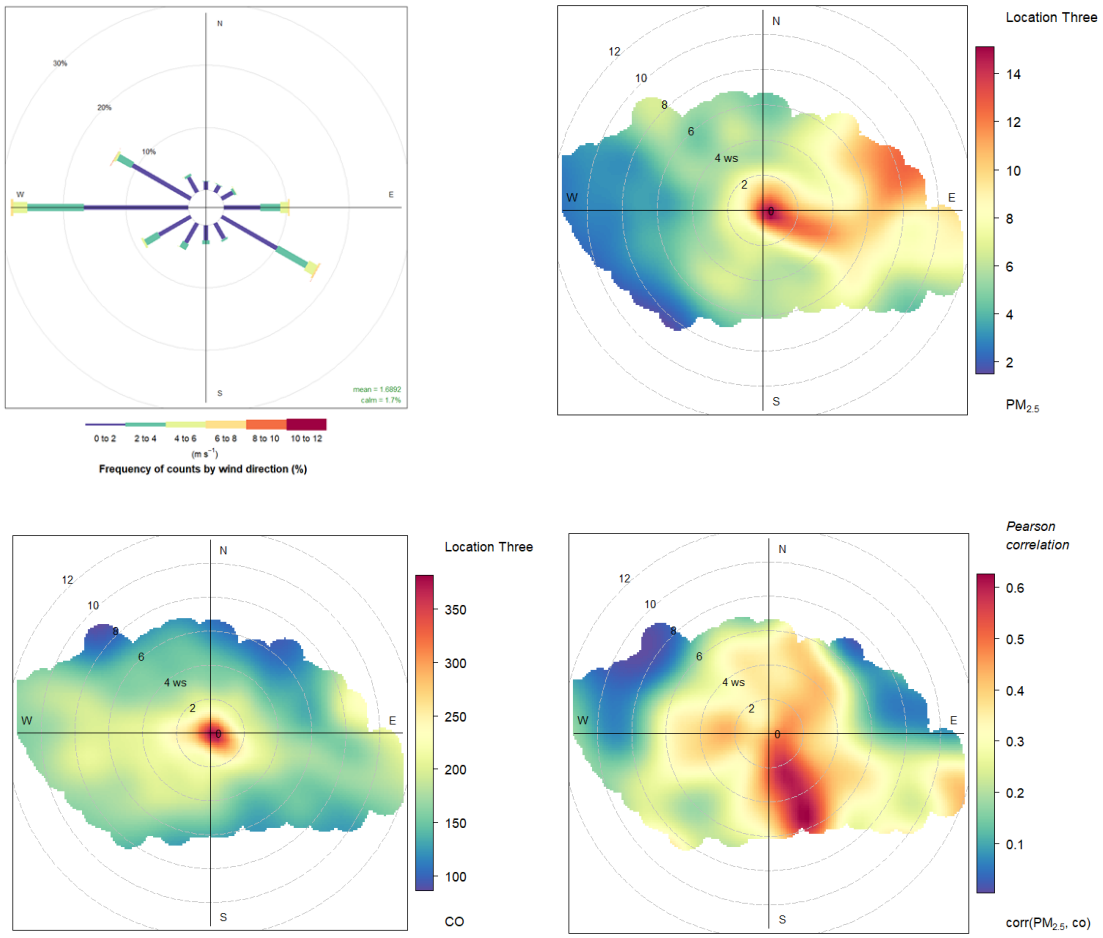

Figures 5-8. 5**.** (Top left) Wind rose for Location Three 6**.** (Top right) Polar plot of $PM_{2.5}$ concentrations, binned by wind speed & direction 7**.** (Bottom left) Polar plot of observed CO in ppb 8**.** (Bottom right) Pearson correlation of $PM_{2.5}$ and CO, by wind direction & speed.

Location Six

The second highest mean $PM_{2.5}$ across the deployment period was observed at Location Six; this location had the highest observed PM_{10} values as well, which is looked at in more detail in that section.

Location Six is closest to Aspen Street, near the northern edge of the parking lot of a night club, among some vegetation, ~100' west of Pennington Avenue, and ~100' to the southeast of a construction equipment rental company.

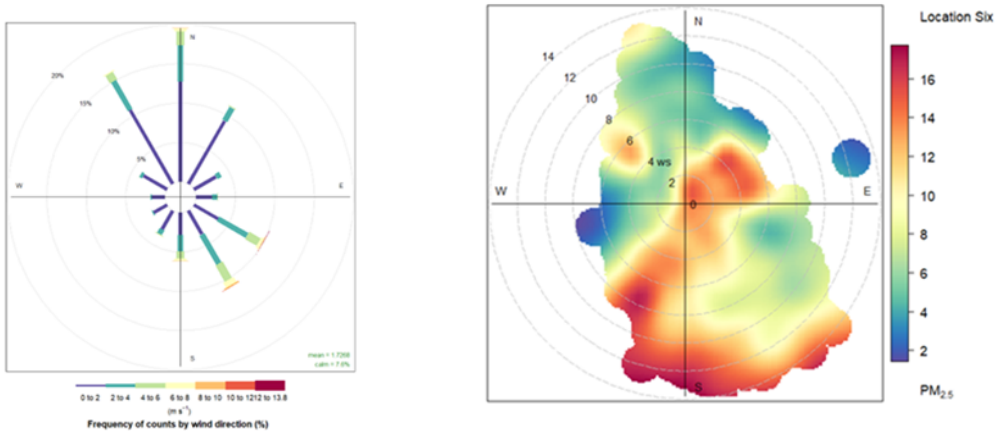

Figures 9-10. 9**.** (Left) Wind rose for Location Six 10**.** (Right) Polar plot of $PM_{2.5}$ concentrations, binned by wind speed & direction.

Directional analysis of the $PM_{2.5}$ concentrations at Location Six indicates that the highest average mean $PM_{2.5}$ values are associated with high winds (~20-30 mph) from the south, with other significant concentrations seen from the east and northwest.

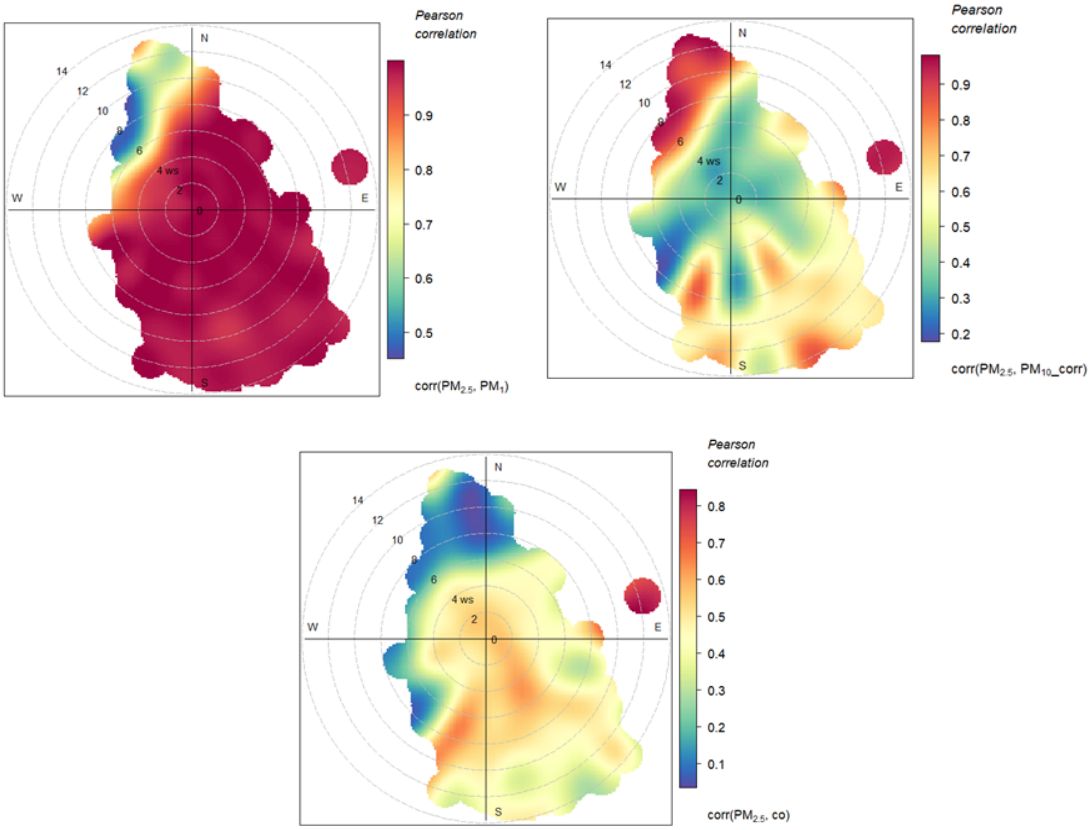

Figures 11-13. 11. (Top left) Pearson correlation polar plot of $PM_{2.5}$ and PM_1 for Location Three 12. (Top right) Pearson correlation polar plot of $PM_{2.5}$ and PM_{10} concentrations 13. (Bottom) Pearson correlation polar plot of $PM_{2.5}$ and CO.

Values from the south, and most other directions, are highly correlated to PM_1 and possibly indicate a regional contribution. Correlations with other pollutants highlight other possible contributions to the highest $PM_{2.5}$ concentrations at Location Six; PM_{10} to the northwest that may be related to construction equipment operation, and CO to the east, indicating traffic as another possible source of $PM_{2.5}$ pollution.

WHO Guidelines for PM2.5

For comparison with the World Health Organization's (WHO's) annual $PM_{2.5}$ Air Quality Guidelines, daily data was averaged from across the network to account for $PM_{2.5}$ variations across the neighborhood of Curtis Bay. Focusing on the first complete year of the entire dataset (5/26/22-5/25/23) of 24-hour average $PM_{2.5}$, including and excluding data from the smoke effect period, the annual mean $PM_{2.5}$ across all sensors is 8.6 µg/m³. Comparing this to current World Health Organization Air Quality Guidelines (AQG) from 2022[1], seen in Table 5 below, this is 3.6 µg/m³ above the current annual AQG of 5 µg/m³, but in achievement of Interim 4.

Table 5. The World Health Organization's recommended Air Quality Guidelines and interim targets for annual mean $PM_{2.5}$.

Recommendation	$PM_{2.5}$ (µg/m³)
Interim target 1	35
Interim target 2	25
Interim target 3	15
Interim target 4	10
AQG level	**5**

The 24-hour AQG is compared with the 99th percentile of the annual distribution of 24-hour average concentrations, which is equivalent to approximately three days in exceedance of the guideline. Using the complete distribution of 24-hour average concentrations, the 99th percentile is 22.0 µg/m³; excluding smoke-influenced data, the 99th percentile is 22.1 µg/m³. Both values are below Interim 4 WHO recommendation of 25 µg/m³.

Table 6. The World Health Organization's recommended Air Quality Guidelines and interim targets for 24-hour mean $PM_{2.5}$.

Recommendation	$PM_{2.5}$ (µg/m³)
Interim target 1	75
Interim target 2	50
Interim target 3	37.5
Interim target 4	25
AQG level	**15**

The greatest reductions in mortality and morbidity, according to the latest WHO Global Air Quality Guidelines document, are achieved by attaining the AQG levels, though in higher pollution environments, progress is measured by reductions according to the interim targets. All interim targets for the $PM_{2.5}$ AQGs have been achieved, from which "one could expect significant reductions in risks for acute and chronic human health effects from air pollution. Progress towards the guideline values [AQG levels] should, however, be the ultimate objective of air quality management and health risk reduction in all areas." (WHO Regional Office for Europe, 2006)

PM_{10}

PM_{10} data were processed in the same manner detailed above for $PM_{2.5}$ data; minute concentrations from the CHARMED dataset were averaged to hourly values with a 75% data capture threshold, so that hours with fewer than 45 minutes were excluded. Hourly values were used to calculate 24-hour concentrations for comparison with the NAAQS.

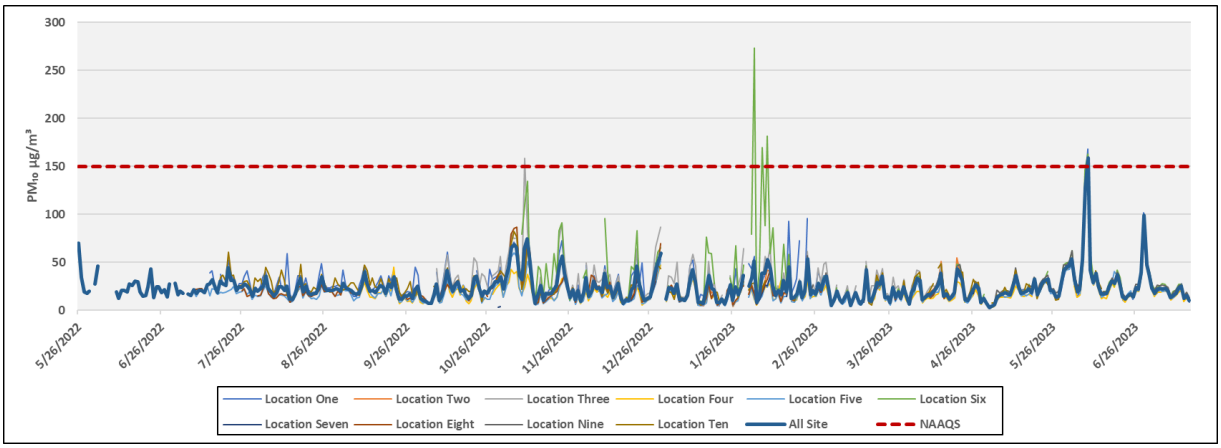

Figure 14. Time series of the 24-hour average PM_{10} concentrations across the Curtis Bay network, with smoke-impacted data included; NAAQS are in red for reference.

The average 24-hour PM_{10} concentration across the Curtis Bay network is 23.7 µg/m³. The average of raw minute concentrations across the deployment was slightly higher at 24.2 µg/m³. Average daily PM_{10} concentrations for the year in Curtis Bay are higher than nearby MDE regulatory monitors but have largely been under the NAAQS level.

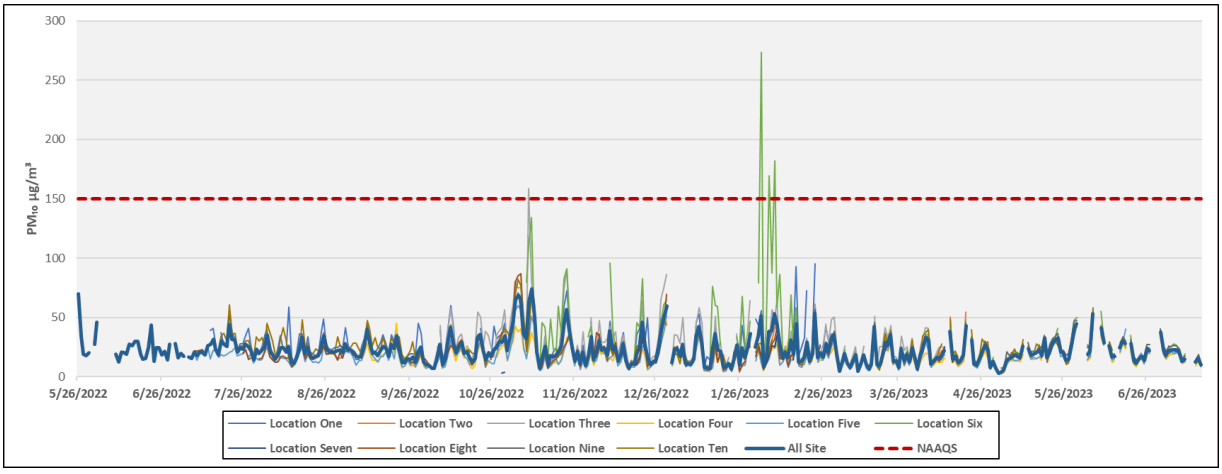

Figure 15. Time series of the 24-hour average PM_{10} concentrations across the Curtis Bay network, with smoke-impacted data excluded; NAAQS are in red for reference.

Using the complete data set without exclusions, averaged as whole for each day, the EPA 24-hour standard for PM_{10} of 150 µg/m³ was exceeded on one day. Taken individually, Locations One through Five and Nine each exceeded the NAAQS threshold once. The only site to exceed more than once during the length of the deployment is Location Six, which did so four times. Excluding smoke affected data and again using the complete data set averaged daily, there were no days that the 24-hour PM_{10} concentration exceeded the 150 µg/m³ threshold. Individually, there was one exceedance at Location Three and three at Location Six.

Table 7. Descriptive PM_{10} statistics for individual monitoring locations in Curtis Bay, including smoke-impacted data, and nearby MDE regulatory monitor. MDE site data from AQS (5/26/02 - 6/30/23) and preliminary data from MDE (7/1 - 7/16/23).

Site	Arthimetic Mean PM_{10}	#Days >150µg/m³	Max 24-hour PM_{10}	Max Date	#Days Captured
Location One	27.3	1	167.7	6/8/2023	328
Location Two	23.7	1	162.0	6/8/2023	103
Location Three	30.7	1	158.5	11/9/2022	183
Location Four	17.8	1	157.2	6/8/2023	283
Location Five	19.1	1	159.4	6/8/2023	405
Location Six	34.5	4	273.2	2/3/2023	200
Location Seven	18.6	0	45.4	2/23/2023	97
Location Eight	20.8	0	86.7	11/6/2022	264
Location Nine	26.3	1	153.9	6/8/2023	138
Location Ten	26.0	0	146.2	6/8/2023	290
MDE Monitor					
Glen Burnie	11.3	0	89.5	6/29/2023	70

Considering locations that have exceeded the 150 µg/m³ 24-hour threshold only once during the deployment, with or without smoke-impacted data, if the data are expected to be similar for the next one and a half to two years, these locations wouldn't average more than the allotted once per year and would thus be in attainment of the NAAQS for PM_{10}. Any two exceedances of the 150 µg/m³ standard over the next two years would cause Location Six to be in excess of the 24-hour PM_{10} standard.

Table 8. Descriptive PM_{10} statistics for individual monitoring locations in Curtis Bay, excluding smoke-impacted data, and nearby MDE regulatory monitor. MDE site data from AQS (5/26/02 - 6/30/23) and preliminary data from MDE (7/1 - 7/16/23).

Site	Arthimetic Mean PM_{10}	#Days >150µg/m³	Max 24-hour PM_{10}	Max Date	#Days Captured
Location One	26.0	0	95.4	2/23/2023	311
Location Two	20.7	0	54.8	4/20/2023	96
Location Three	30.7	1	158.5	11/9/2022	182
Location Four	16.3	0	46.9	12/30/2022	268
Location Five	17.9	0	69.6	5/26/2022	388
Location Six	32.6	3	273.2	2/3/2023	183
Location Seven	18.2	0	45.4	2/23/2023	95
Location Eight	20.8	0	86.7	11/6/2022	262
Location Nine	22.4	0	56.9	2/23/2023	121
Location Ten	24.8	0	82.2	11/5/2022	281
MDE Monitor					
Glen Burnie	9.7	0	20.5	5/30/2023	66

Location Six stands out with the highest yearly average and maximum 24-hour average, in addition to the three (or four exceedances) of the 150 µg/m³ standard. All four exceedance days occurred on weekdays in early February - 2/3, 2/6, and 2/8/23 - with the additional smoke-impacted exceedance on June 8, 2023. When the wind direction was downwind versus not downwind of the coal terminal, PM_{10} mean concentrations were statistically significantly higher at all sites (see Fig. 16, below).

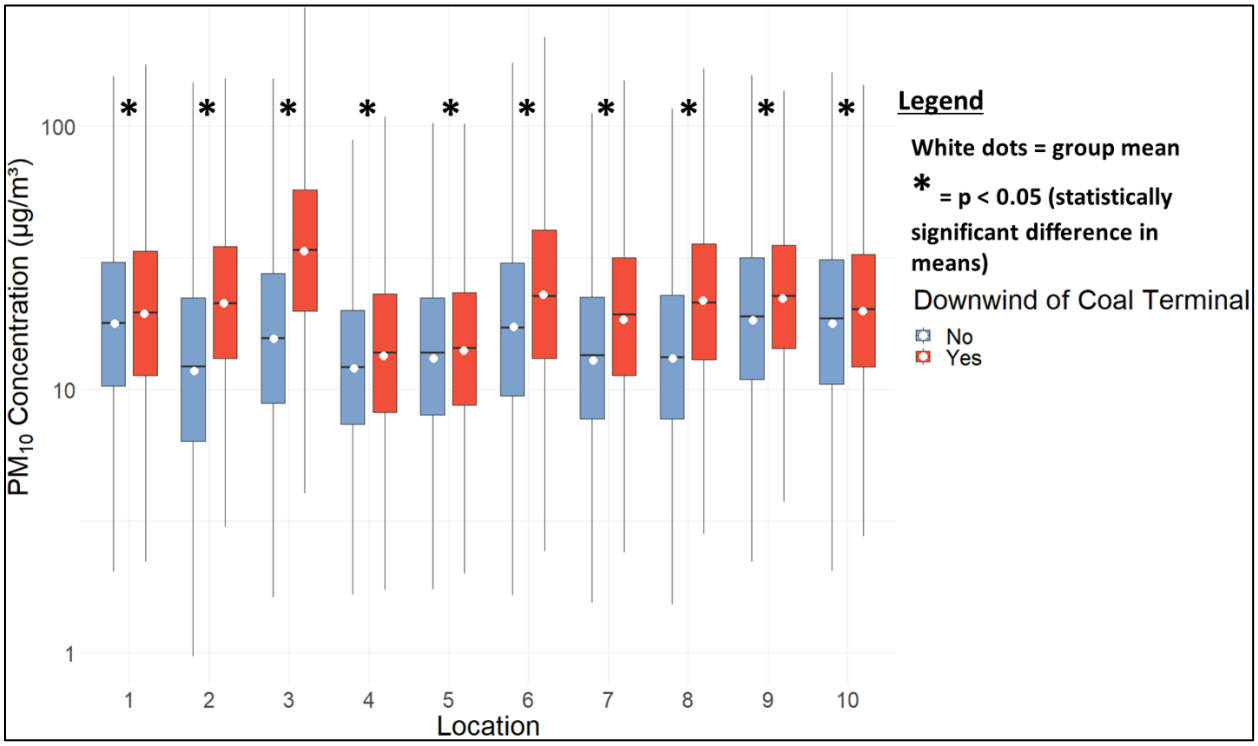

Figure 16. Comparison of MODULAIR PM_{10} (µg/m³) across the South Baltimore Air Monitoring Network. Note. Sample sizes differ between locations due to rolling deployment. All "Downwind-Yes" means are statistically significantly greater than "Downwind-No" means at the p <0.05 level using Welch t-tests. Provided by BSPH.

Location Six

Examining the diurnal pattern of PM_{10} at Location Six using minute data, a clear workday pattern can be seen.

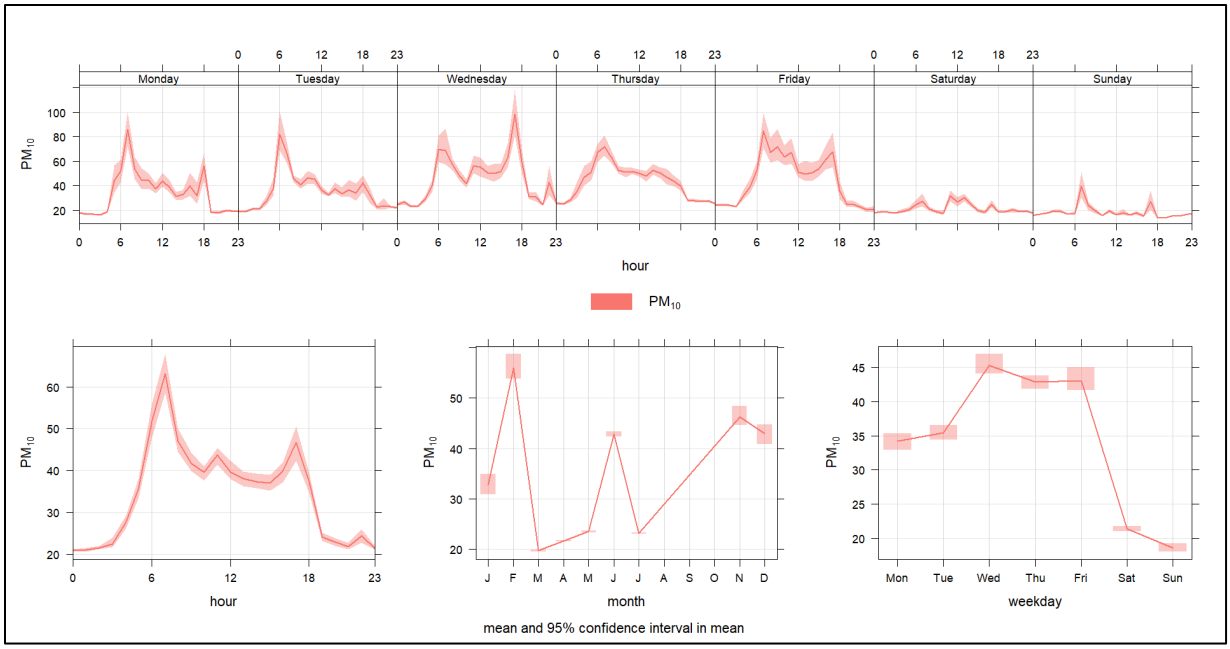

Figure 17. Time variation of PM_{10} minute concentrations at Location Six, created in 'openair' with minute data.

Directional analysis using minute data at Location Six, shows winds predominate from the north and northwest at this location (~40%). Moderate wind speeds in the range of 4-8 ms^{-1} from the northwest are associated with the highest minute concentrations of PM_{10}.

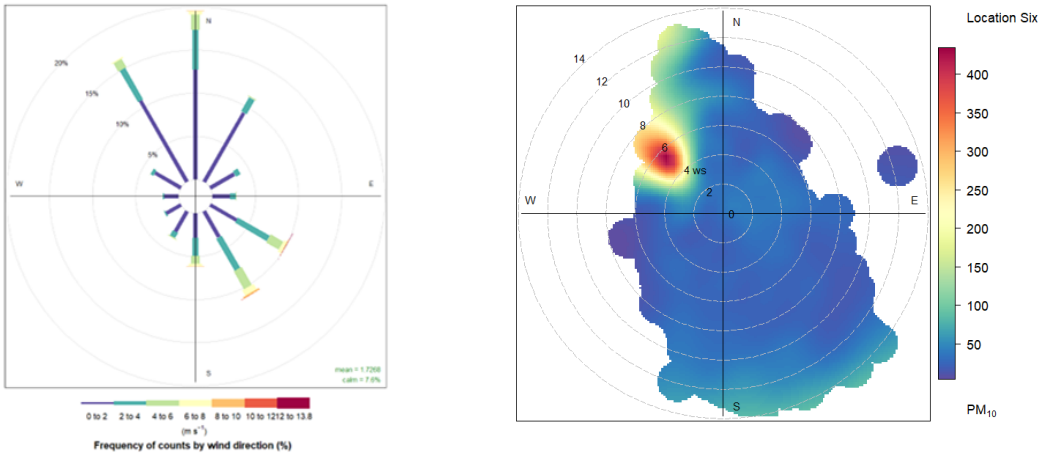

Figures 18-19. 18. (Left) Wind rose for Location Six 19. (Right) Polar plot of PM_{10} concentrations, binned by wind speed & direction.

Location Six is ~100' to the southeast of a construction equipment rental company; it's likely that the high PM_{10} concentrations from that direction are related, though another source of PM_{10} can be seen to the south in the polar plot, associated with higher winds(~14ms^{-1}). A frequency plot (n=1000) and a conditional probability function (CPF) at the 90th percentile for Location Six illustrate two more potential PM_{10} sources to the east and southeast.

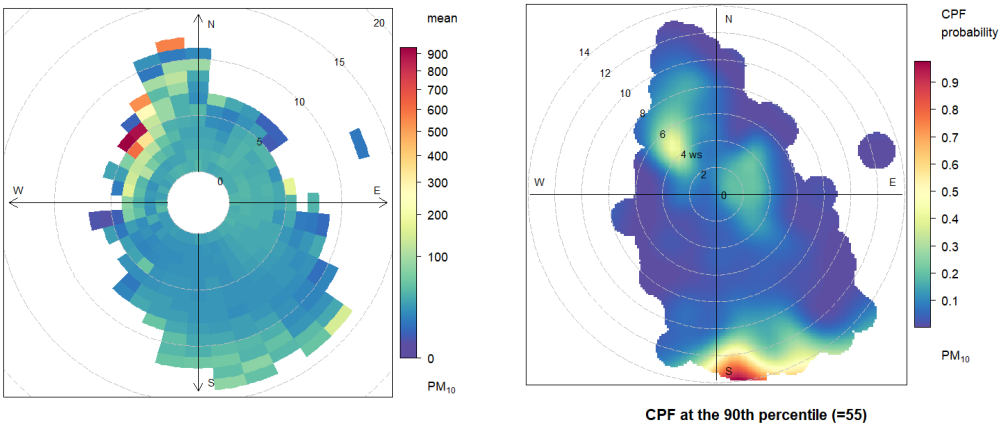

Figures 20-21. 20. (Left) Polar frequency plot for all wind speed and direction combinations where n ≥1000. 21. (Right) Conditional probability function for PM_{10} concentrations at Location Six, ≥ 55µg/m³.

The higher values seen on the frequency plot and the CPF to the south and east of the sensor are possibly related to traffic on Pennington Avenue, which runs north south and lies to the east of Location Six; there are strong correlations between PM_{10} and CO, and PM_{10} and NO seen on the plots below.

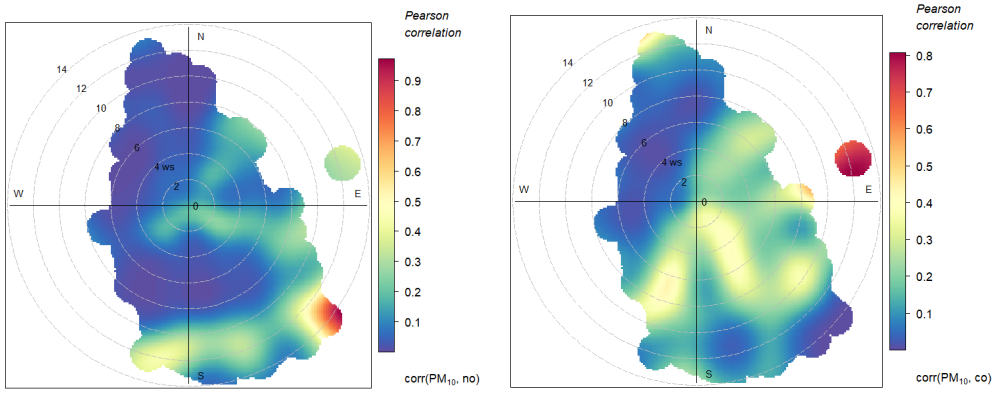

Figures 22-23. 22. (Left) Pearson correlation polar plot for PM_{10} and NO and 23. (Right) for PM_{10} and CO at Location Six.

Location Three

The second highest PM_{10} concentrations (~30-55 µg/m³) of the deployment were observed at Location Three. Directional analysis shows the highest PM_{10} minute concentrations are associated with east of the sensor in light to moderate winds (0-25 mph).

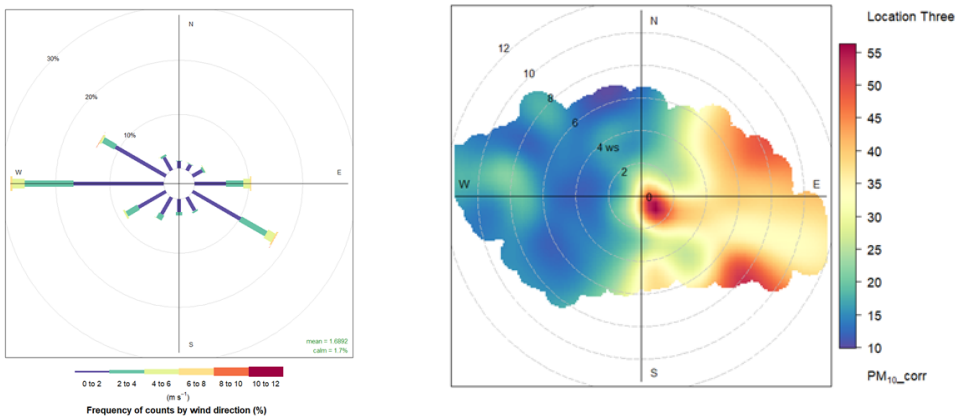

Figures 24-25. 24. (Left) Windrose for Location Three and 25. (Right) Polar plot for PM_{10} at Location Three.

The diurnal variation seen in Figure 25 below highlights a workday pattern with increased values occurring Monday through Friday, peaking each day after 6 AM, and decreased concentrations on Saturdays and Sundays.

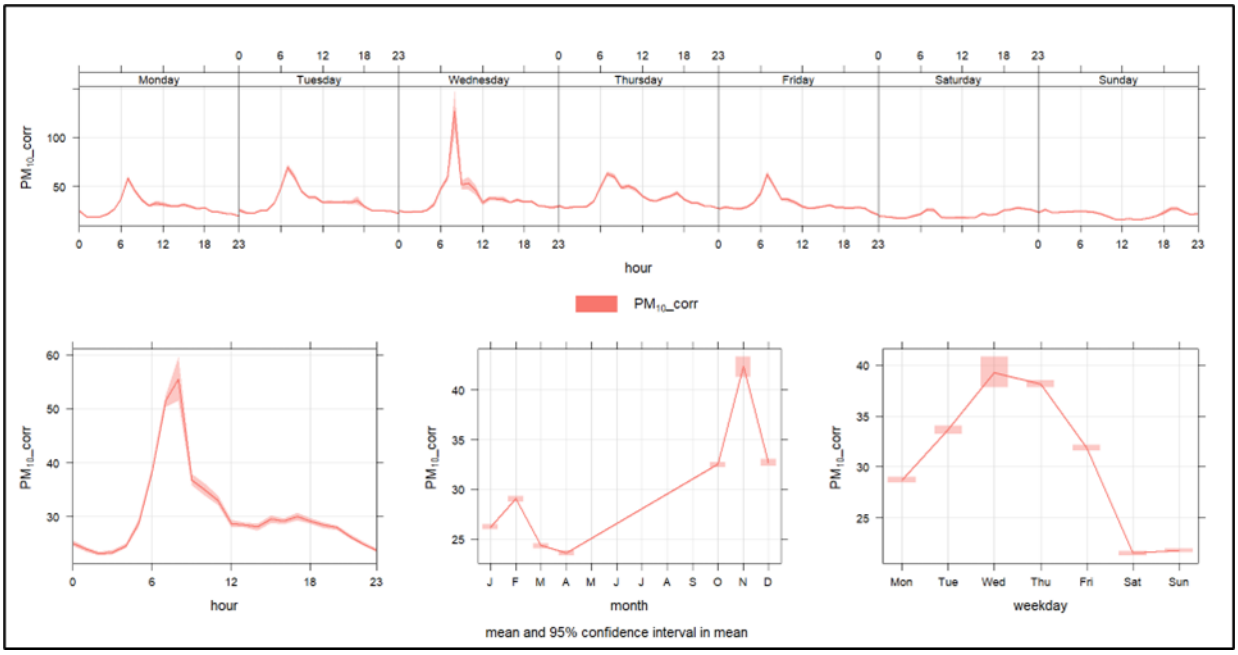

Figure 26. Time variation for PM_{10} at Location Three.

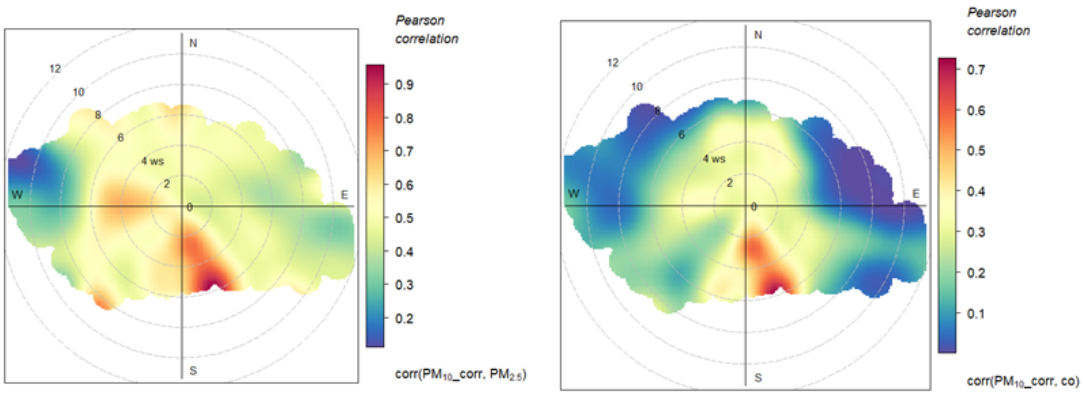

Figures 27-28. 27. (Left) Pearson correlation polar plot for PM_{10} and $PM_{2.5}$ and 28. (Right) for PM_{10} and CO at Location Three.

PM_{10} is strongly correlated with $PM_{2.5}$ and CO to the south, southeast of Location Three, suggesting a contribution from vehicle traffic.

WHO Guidelines for PM10

For comparison with the annual PM_{10} Air Quality Guideline, daily data was averaged from across the network to account for variation across the neighborhood. Looking at the first complete year of the data (5/26/22-5/25/23) of 24-hour average PM_{10}, including data from the smoke effect period, the annual mean PM_{10} across all sensors is 22.6 µg/m³; excluding data from the smoke effect period, the annual mean PM_{10} is 22.5 µg/m. Comparing this to current World Health Organization Air Quality Guidelines (AQG) released in 2022 (see table below), these are 7.6 and 7.5 µg/m³ above the current annual AQG of 15 µg/m³. This would be in achievement of Interim 3 of the annual mean Air Quality Guideline.

Table 9. The World Health Organization's recommended Air Quality Guidelines and interim targets for annual mean PM_{10}.

Recommendation	PM_{10} (µg/m³)
Interim target 1	70
Interim target 2	50
Interim target 3	30
Interim target 4	20
AQG level	**15**

The 24-hour AQG is compared with the 99th percentile of the annual distribution of 24-hour average PM_{10} concentrations, which is equivalent to approximately three days in exceedance of the guideline. Using the first year of complete data, the 99th percentile of the distribution of 24-hour average concentrations is 65.3 µg/m³, both including and excluding smoke-influenced data. PM_{10} concentrations in Curtis Bay are below the WHO's Interim 3 guideline of 75 µg/m³ (see Table 7. below).

Table 10. The World Health Organization's recommended Air Quality Guidelines and interim targets for 24-hour mean PM_{10}.

Recommendation	PM_{10} (µg/m³)
Interim target 1	150
Interim target 2	100
Interim target 3	75
Interim target 4	50
AQG level	**45**

Considerations

While the highest average concentrations at any one site may be influenced by the nearest facilities as potential sources of pollutants, other industrial activities in the area are likely contributing to concentrations at all sites throughout the South Baltimore Monitoring Network. This reflects the cumulative impact of human, industrial, and natural activities in the area both currently and across several decades.

The World Health Organization's Air Quality Guidelines were designed to be forward and aspirational and are described by the WHO[2] as "neither standards nor legally binding criteria" but are "designed to offer guidance in reducing the health impacts of air pollution". The guidelines contain "not only the AQG levels which are the ultimate objective" but include interim levels to guide reduction efforts in areas that experience higher air pollution levels, in a timely and incremental manner. While the AQGs were developed in consultation with public health, scientific, medical, and environmental organizations, and experts from around the world, the EPA has cautioned against comparing them directly with the NAAQS, which remain the legal standard for ambient air quality in the United States.

The NAAQS for $PM_{2.5}$ and PM_{10} are based on three years of data as opposed to the yearly statistics of the AQGs, while PM_{10} is based on a different metric altogether – the number of values above a fixed level, rather than averages and percentiles. Additionally, regulatory decisions regarding the NAAQS are based on data collected by approved monitors – either Federal Reference Method or Federal Equivalency Method.

While sensors can be excellent indicators of current and general air quality, they are often not as well sited nor maintained by trained personnel as is the case with regulatory monitoring equipment run by state air quality agencies. Independent evaluations by California's South Coast Air Quality Monitoring District (AQ-SPEC) have found the specific sensor type used in Curtis Bay measure $PM_{2.5}$ with a high bias compared to reference grade monitors by 1-3 µg/m³.[3]

Complete summary statistics, including sample sizes, and box plots for black carbon (addressed in a different section, but included below for reference by BSPH) are listed in Appendix 4A.

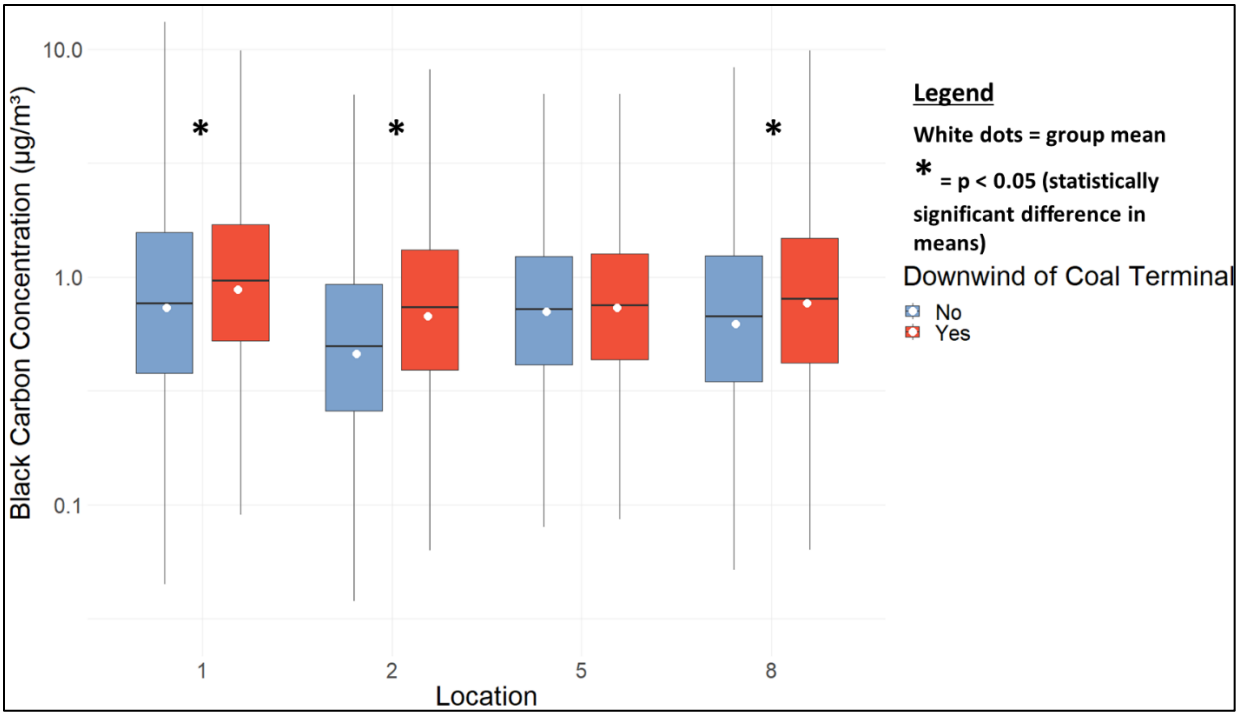

Figure 29. Comparison of mean ObservAir Black Carbon (BC) (µg/m³) concentration across the South Baltimore Air Monitoring Network. Note. Sample sizes differ between locations due to rolling deployment. All "Downwind-Yes" means are statistically significantly greater than "Downwind-No" means at the p <0.05 level using Welch t-tests, except Location 5, where the downwind mean is lower, but the difference is not statistically significant. Provided by CHARMED.

Mobile monitoring of black carbon and methane with NOAA's ARC

Introduction and Methods

A mobile pollutant measurement platform developed jointly by the University of Maryland (UMD) and National Oceanic and Atmospheric Administration's (NOAA's) Air Resources Laboratory (ARL) to track meteorology and to quantify concentrations of short-lived pollutants and greenhouse gases. The Air Resources Car, or "NOAA's ARC," was designed for on and off-road measurement of trace gases and aerosol parameters (Figure 30). The ARC carries an extensive set of research-grade instruments to measure meteorological variables and air pollutants (Table 11). Time resolution for most instruments is quick, <5 s and data are collected every 1 s to investigate pollutants at the neighborhood scale and pinpoint sources.

For this work we focus on black carbon (BC) and methane (CH_4). BC, also known as soot or graphitic carbon, because it has major adverse impacts on human health and contributes to global and local climate change. Major sources are coal dust, fires, and diesel exhaust. Methane is a powerful greenhouse gas and indicator of other sorts of pollution. Major urban sources include leakage from the natural gas delivery system, coal operations, and biogenic processes in wastewater treatment plants and landfills. This mobile laboratory has been driven down nearly every street in Baltimore and has found hot spots for poor air quality as indicated in the results section.

Figure 30. NOAA's ARC or Air Resources Car with roof rack supporting a sonic anemometer and inlets for trace gases and aerosols (forward) and other meteorological sensors (aft).

Table 11. Measurement capabilities of UMD/NOAA mobile laboratory, NOAA's ARC.

Variable	**Method, Manufacturer**	**Uncertainty (95% C.I.)**
Position (Lat./Long.)	Differential GPS, Garmin G600	10^{-4} degrees Lat (~10 m)
Wind Speed and Direction	3-D Sonic Anemometer + Differential GPS	0.1 m s^{-1}
Temperature, Relative Humidity, Pressure, Altitude	Vaisala Model PTU300	0.2 °C, 2% RH, 0.1 hPa, 1 m
O_3	UV Absorption, TECO Model 49	2 ppb
$CH_4/CO_2/CO/H_2O$	Cavity Ring Down, Picarro G2401-m	4.2 ppb CO, 50 ppb CO_2, 1.0 ppb CH_4
CH_4/Ethane	Mid-IR Absorption, Aeris Ultra LDS	2 ppb CH_4, 0.5 ppb C_2H_6
^{13}C CH_4/CO_2 isotopes	Cavity Ring-Down, Picarro G2201-i	0.16‰ $\delta^{13}C$-CO_2 1.15‰ $\delta^{13}C$-CH_4
NO_2	Cavity Attenuated Phase Shift, Teledyne T500U	0.5 ppb
$NO/NO_2/NOx$	Cavity Attenuated Phase Shift, Teledyne N500	0.5 ppb
SO_2	Pulsed Fluorescence TECO Model 43	0.5 ppb
Black Carbon (BC)	Light Attenuation, 7- l Aethalometer (370-950 nm), Magee AE43	30 % (precision ~10%)
Aerosol Scattering (b_{sp})	3-l Nephelometer (450, 550, 700 nm)	$2x10^{-6}$ m^{-1}
Volatile Organic Compounds	Whole Air Samples for GC	Species dependent

Results

Black Carbon

NOAA's ARC was deployed in the Baltimore, MD and Washington, DC area on 64 days between 21 March and 29 June 2023. Data shown here were all collected on weekdays, generally between 10 am and 5 pm local time. The routes traveled and species measured were guided by community environmental groups who provide intimate knowledge and experience with local air quality problems.

Observations of BC (Figure 31) revealed several hot spots where concentrations reached the level of potential health threat, i.e., frequently exceeded 1.63 mg m^{-3}, the 90th percentile. In Baltimore, these are generally along major highways (I-95, I-895, and I-695), in the downtown area, and near the community of Curtis Bay.

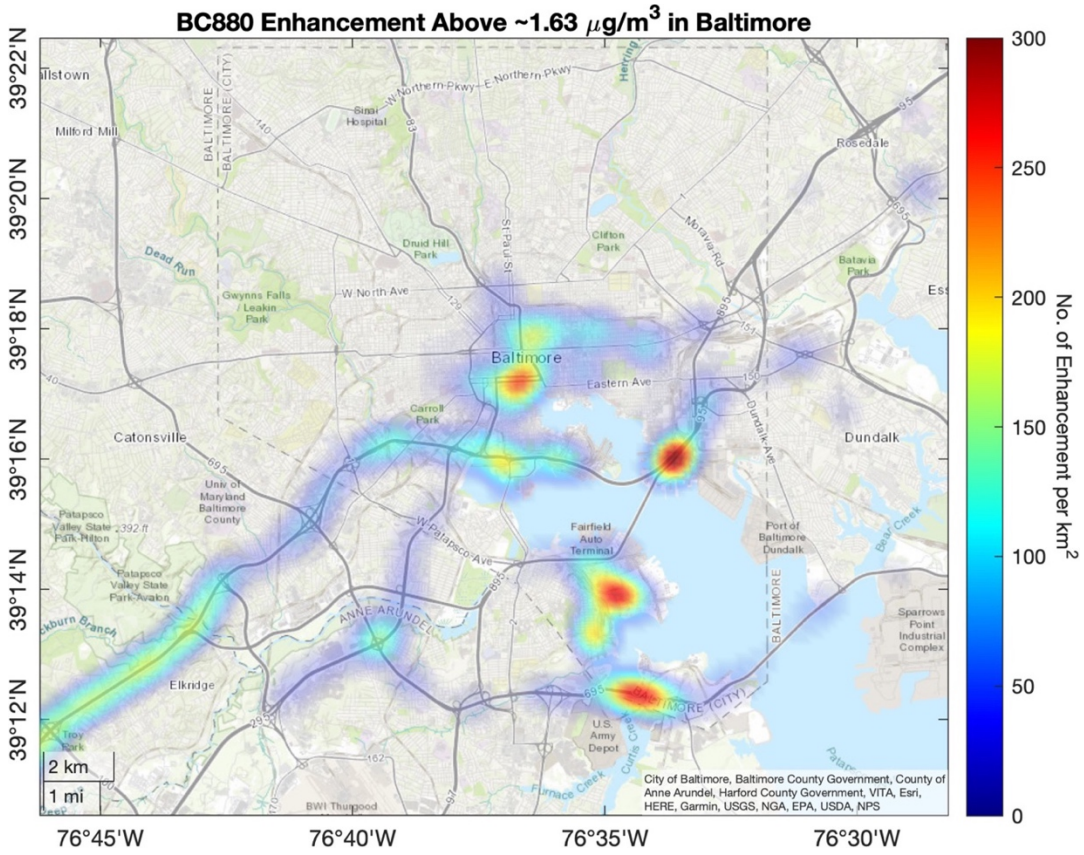

Figure 31. Intensity plot of the number of times BC was observed in the range of health threats, above 1.63 mg m^{-3} in a box 1 km on a side during 29 cruises of NOAA's ARC between March and May 2022, generally near midday of weekdays. Note maxima along major highways, downtown, and around Curtis Bay.

To take a closer look at Curtis Bay, we drove (on 27 April 2023) eight laps down Pennington Ave. heading generally south (176°), and up Curtis Ave. heading generally north (356°) (Figure 32). BC concentrations were higher overall – adverse health effects, including respiratory problems and inhibited cognitive development in children, have been reported for annual mean BC of ~0.6 mg m^{-3}. Multiple sources contribute to the high background including coal dust, industry, and diesel exhaust.

Concentrations were remarkably higher (by more than a factor of three) and more variable on Pennington Ave. than on Curtis Ave. (Figure 33). Both avenues were basically flat, at altitudes near sea-level. Weather was generally mild with weak winds out of the SSE. Most variables are similar but Pennington Ave., with three stoplights, shows substantially more BC aerosol loading. Based on Maryland Department of Transportation (MDOT) observations, Pennington Ave. averages about 20% more truck and bus traffic than Curtis Ave. but this cannot account for a factor of 3 difference in mean BC. There are

three stoplights on Pennington Ave. plus one where Pennington, Curtis, and Patapsco Ave. intersect on the north end. These induce stop-and-go traffic that can lead to greater BC emissions.

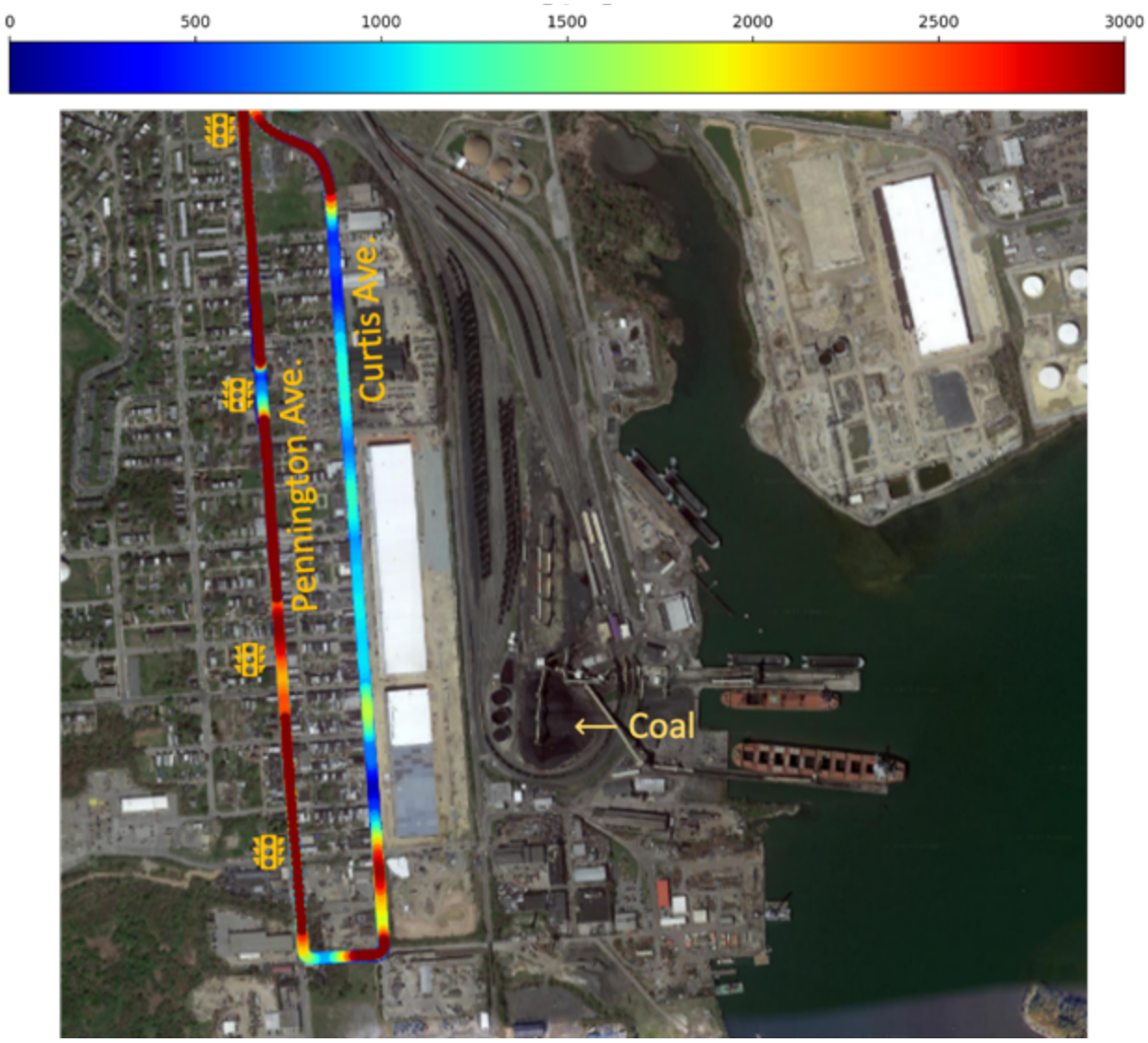

Figure 32. Satellite image of the Curtis Bay neighborhood with BC measured from NOAA's ARC on 27 April 2023 (11:24 am to 12:13 pm EDT) indicated by the colored tracks. See color-bar for concentrations (ng m^{-3}). The Bay itself lies to the east. The avenues in this neighborhood run almost north-south (356° to 176°). Icons indicate approximate locations of stoplights including one near the northern intersection of Pennington and Curtis Aves.

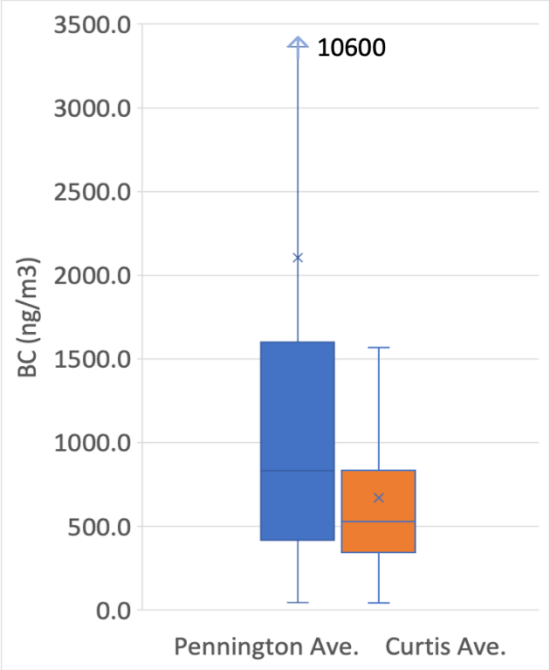

Figure 33. Boxplot showing overall high concentrations of BC but much more on Pennington Ave. due to diesel vehicles in stop-and-go traffic.

Throughout Baltimore, MD especially in the Curtis Bay community, high concentrations of BC are frequently measured; surface monitors confirm the prevalence of substantial BC throughout the year validating citizens' health concerns. Concentrations, however, vary sharply in time and space – in a case study, BC concentrations along Pennington Ave. averaged three times higher than along Curtis Ave., just ~150 m away. $PM_{2.5}$ showed less spatial variability, indicating that this Criteria Pollutant is less suitable for studies of environmental justice (EJ). High local temperatures from the UHI effect increase the BC problem but the high density of diesel trucks in stop-and-go traffic appears to be the dominant cause.

These two parallel avenues have similar meteorology, numbers of vehicles, and speeds. The stop-and-go traffic on Pennington Ave., resulting from three stoplights, causes diesel trucks to accelerate more frequently. Accelerating trucks can run rich causing a burst of soot. We must stress that traffic control is important for pedestrian safety, but these traffic lights have unintended consequences when heavy duty trucks enter residential areas. Tire and brake wear can contribute to PM loading and these are also intensified by stop-and-go traffic. The median and 95th percentile on Pennington Ave. were 0.8 and 10.9 mg BC m^{-3} on the days of investigation and the annual average is likely well above the level observed to cause damage to respiration and cognitive function in children.

This residential neighborhood is an appropriate candidate for air pollution mitigation to improve air quality and EJ. Concentrations of BC are more similar to those along an interstate highway than in a suburban neighborhood. MDE is examining steps to improve air quality and support the goals of EJ including replacement of diesel with electric vehicles, roadside monitoring to identify gross emitters, smoother traffic flow (better synchronization of traffic lights) or diverting heavy-duty trucks from residential neighborhoods. More green space would reduce the UHI effect and slow diesel emissions

while improving the climate. Even if all BC sources were removed there would still be a health risk from trace gases and other components of PM – current traffic mitigation plans are helpful but not enough. The results presented here could have a broad impact on strategy for abatement of air pollution on the neighborhood scale. The combination of diesel vehicles, traffic congestion, and the urban heat island effect conspire to produce locally high BC in overburdened residential communities. It's not just Baltimore – many such neighborhoods like Curtis Bay exist in major American cities and these would benefit from increased tree cover and decreased traffic.

Methane

High concentrations of methane, a powerful greenhouse gas, have been observed in the Curtis Bay neighborhood. The levels are below those posing a direct threat to human health or an explosion hazard, but plumes of methane can indicate an associated problem such noxious smells and other, more reactive or toxic, organic compounds. Decreasing methane emissions is central to Maryland's Climate Solutions Now Act.

The mobile lab NOAA's ARC has driven down nearly every street in Baltimore and found several methane hot spots. Figure 34 shows the frequency of detecting high methane concentrations in boxes 1 km on a side. The Inner Harbor and Curtis Bay stand out.

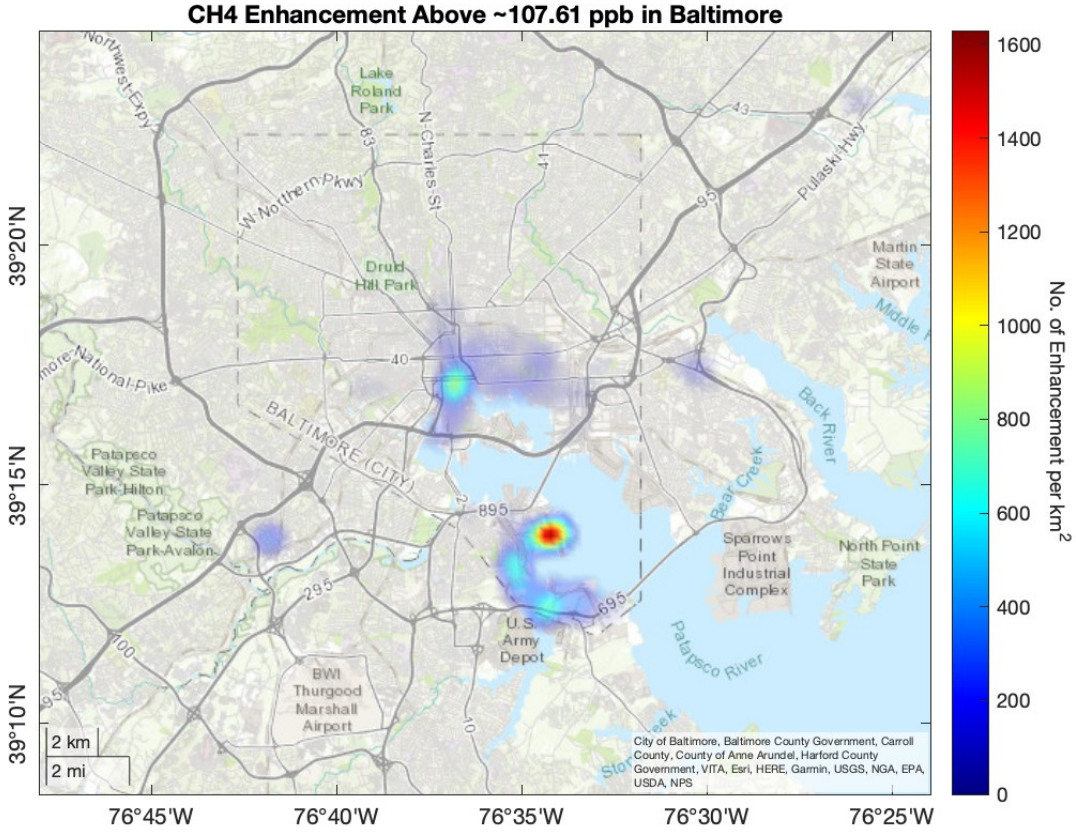

Figure 34. Intensity plot of the number of times CH4 was observed above the 90th percentile for Baltimore. Color bar indicated the number of times concentrations were more than ~100 ppb above background in squares 1 km on a side during 29 cruises of NOAA's ARC between March and May 2022, generally near midday of weekdays. Note maxima downtown, and around Curtis Bay.

Determining the origin of methane plumes in the Curtis Bay residential area is complicated by the myriad sources in the area (Figure 35):

- Waste Management Natural Gas Filling Station
- Patapsco Wastewater Treatment Plant
- CSX Coal Transfer Facility
- Quarantine Landfill
- Motor vehicles
- Leakage from the natural gas infrastructure

Fossil sources such as natural gas and coal handling tend to have other paraffins especially ethane associated with the while biogenic sources such as landfills and wastewater treatment do not. Further separation can be achieved with isotopes of carbon and hydrogen – this work is ongoing. Note the residential area Curtis Bay shows evidence of several different types of methane sources. Conclusions from these studies include several sources of methane in the Curtis Bay area could be curtailed with benefits to climate, residents' health, and EJ.

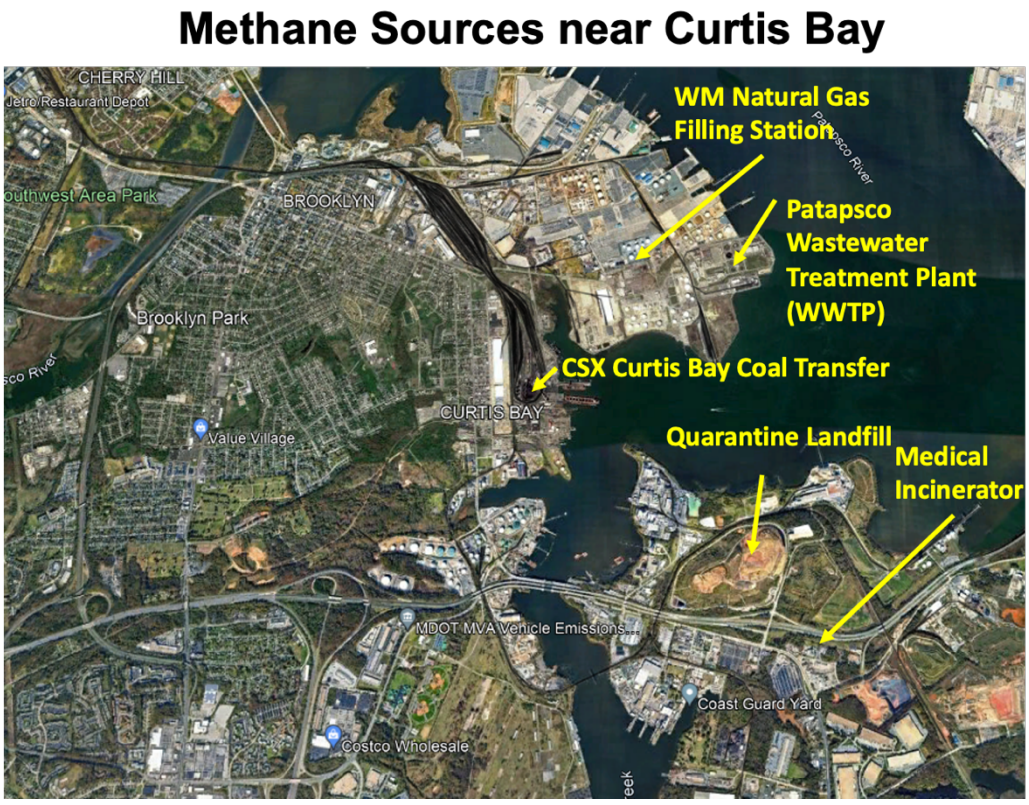

Figure 35. Satellite image of Curtis Bay with potential sources of methane and related pollutants indicated.

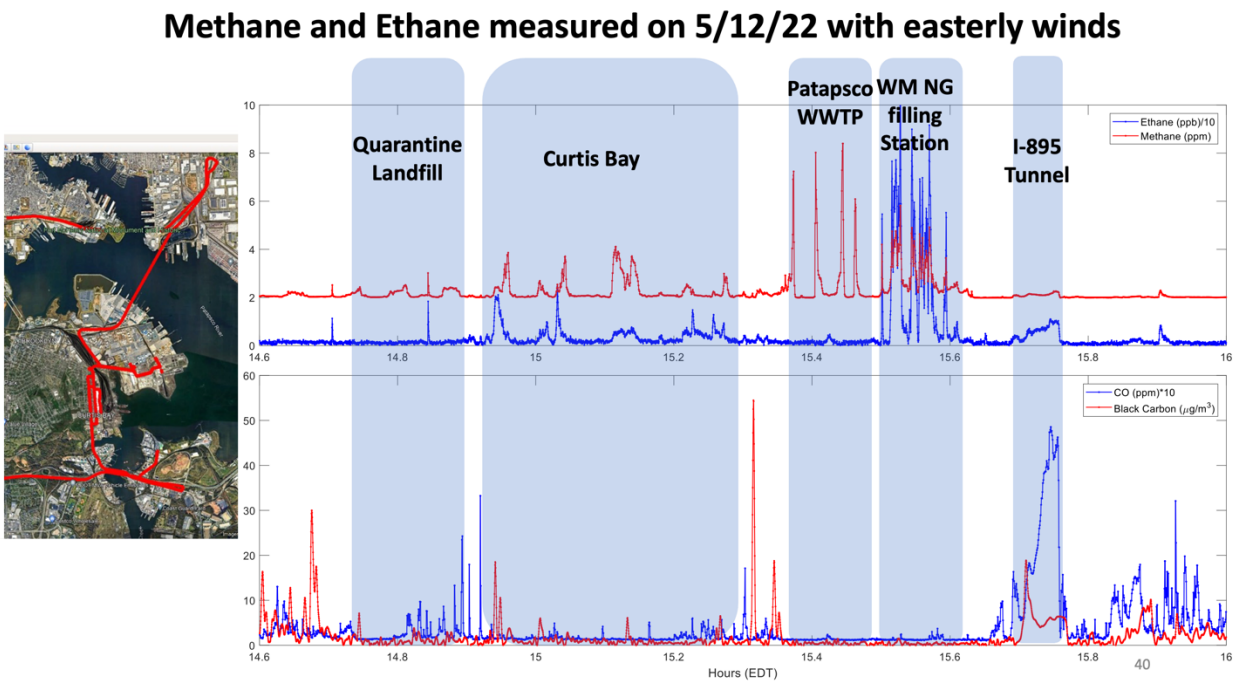

Figure 36. Methane and ethane concentrations as a function of time as observed from NOAA's ARC (top). Note biogenic sources such as the landfill and wastewater treatment plant produce high concentrations of methane with little ethane while fossil sources such as the natural gas filling station and vehicles in the tunnel produce both. Curtis Bay itself shows evidence of several methane sources. Carbon monoxide (CO) and black carbon (BC) for the same trip show when vehicular emissions dominate (bottom). Diesel engines produce most of the BC while spark-ignited engines produce most of the CO.

References

1. World Health Organization. *WHO global air quality guidelines: particulate matter (PM2.5 and PM10), ozone, nitrogen dioxide, sulfur dioxide and carbon monoxide (License: CC BY-NC-SA 3.0 IGO)*. 2021. https://iris.who.int/handle/10665/345329
2. World Health Organization. What are the WHO Air Quality Guidelines? Accessed Dec 05, 2023. https://www.who.int/news-room/feature-stories/detail/what-are-the-who-air-quality-guidelines
3. South Coast Air Quality Management District. *Field Evaluation: QuantAQ - MODULAIR-PM*. 2021. https://www.aqmd.gov/docs/default-source/aq-spec/field-evaluations/quantaq-modulair-pm---field-evaluation.pdf?sfvrsn=15

Appendix

Table A.1. Summary statistics of Distributed Sensing Technologies (DSTech) ObservAir 1-min resolution black carbon (µg/m^3) concentrations by location (cleaned at 2-second resolution, South Baltimore Air Monitoring Network, Baltimore, Maryland. Note. N = sample size.

	Location			
	1	**2**	**5**	**8**
Statistic				
N	157,670	186,114	108,599	241,018
Minimum	-4.10	-4.60	-2.40	-4.15
5%	-0.04	-0.12	0.07	-0.09
25%	0.35	0.24	0.40	0.30
Median	0.77	0.55	0.73	0.65
Mean (SD)	1.22 (1.81)	0.80 (5.58)	1.19 (2.44)	1.02 (1.46)
75%	1.55	1.06	1.25	1.24
95%	3.77	2.38	3.69	3.28
Maximum	130.19	1,894.72	333.33	81.34

Table A.2. Summary statistics of QuantAQ MODULAIR 1-minute resolution PM_{10} (µg/m^3) concentrations by location, South Baltimore Air Monitoring Network, Baltimore, Maryland. Note. N = sample size.

	Location									
	1	**2**	**3**	**4**	**5**	**6**	**7**	**8**	**9**	**10**
Statistic										
N	481,308	220,977	267,868	417,084	583,383	309,076	159,791	386,298	204,555	442,260
Minimum	0	0	0	0	0	0	0	0	0	0
25%	11	8	11	8	9	10	8	9	11	11
Median	18	15	20	13	15	18	14	15	19	19
Mean (SD)	27 (41)	22 (26)	31 (58)	18 (26)	19 (19)	34 (127)	19 (17)	21 (22)	26 (25)	26 (30)
75%	31	27	37	21	23	31	24	26	32	32
Maximum	5,151	1,365	8,889	4,664	2,571	10,199	1,349	2,289	555	6,113

Table A.3. Summary statistics of QuantAQ MODULAIR 1-minute resolution $PM_{2.5}$ ($\mu g/m^3$) concentrations by location, South Baltimore Air Monitoring Network, Baltimore, Maryland. Note. N = sample size.

	Location									
	1	**2**	**3**	**4**	**5**	**6**	**7**	**8**	**9**	**10**
Statistic										
N	482,959	221,075	269,211	417,870	584,747	310,017	160,350	387,892	204,558	443,998
Minimum	0	0	0	0	0	0	0	0	0	0
25%	5	5	5	5	5	5	5	4	6	5
Median	8	8	9	8	8	9	7	7	9	8
Mean (SD)	11 (14)	11 (16)	11 (11)	10 (14)	10 (13)	12 (15)	8 (6)	8 (8)	13 (18)	10 (11)
75%	12	13	13	12	11	14	11	10	14	11
Maximum	611	268	641	268	684	267	384	291	311	251

Table A.4. Summary statistics of QuantAQ MODULAIR 1-minute resolution PM_1 ($\mu g/m^3$) concentrations by location, South Baltimore Air Monitoring Network, Baltimore, Maryland. Note. N = sample size.

	Location									
	1	**2**	**3**	**4**	**5**	**6**	**7**	**8**	**9**	**10**
Statistic										
N	482,959	221,075	269,211	417,870	584,747	310,017	160,350	387,892	204,558	443,998
Minimum	0	0	0	0	0	0	0	0	0	0
25%	4	4	5	4	4	5	4	4	5	4
Median	7	7	8	7	7	8	6	6	8	7
Mean (SD)	10 (14)	10 (16)	10 (10)	10 (14)	9 (13)	11 (15)	8 (6)	8 (7)	12 (18)	9 (11)
75%	11	12	12	11	11	13	10	9	13	10
Maximum	449	263	515	266	460	247	379	260	298	247

Table A.5. Summary statistics of QuantAQ MODULAIR 1-minute resolution total suspended particles (TSP) (µg/m^3) concentrations by location, South Baltimore Air Monitoring Network, Baltimore, Maryland. Note. TSP is approximately PM_{40}. N = sample size.

	Location									
	1	**2**	**3**	**4**	**5**	**6**	**7**	**8**	**9**	**10**
Statistic										
N	460,013	214,844	231,738	380,918	527,451	302,668	162,923	352,327	204,555	420,671
Minimum	0	0	0	0	0	0	0	0	0	0
25%	11	9	12	8	9	11	8	9	12	12
Median	20	17	24	14	16	20	16	16	22	22
Mean (SD)	41 (162)	30 (106)	50 (212)	29 (202)	28 (127)	70 (870)	30 (152)	32 (113)	40 (207)	40 (151)
75%	40	33	51	25	29	41	30	32	41	42
Maximum	21,334	16,778	20,798	24,550	20,031	97,254	11,991	15,855	13,073	19,155

Table A.6. Summary statistics of QuantAQ MODULAIR 1-minute resolution carbon monoxide (CO) (ppb) concentrations by location, South Baltimore Air Monitoring Network, Baltimore, Maryland. Note. N = sample size.

	Location									
	1	**2**	**3**	**4**	**5**	**6**	**7**	**8**	**9**	**10**
Statistic										
N	486,119	221,915	270,922	416,450	538,099	318,851	183,961	372,127	208,165	439,161
Minimum	10	-63	21	-197	-40	-108	-45	41	-53	-73
25%	279	189	182	369	322	247	128	221	230	216
Median	329	248	226	421	355	293	184	256	280	293
Mean (SD)	389 (218)	293 (171)	291 (231)	476 (256)	379 (138)	332 (165)	200 (108)	294 (136)	325 (177)	301 (144)
75%	431	335	324	513	410	375	242	329	369	358
Maximum	11,134	2,771	10,876	11,370	11,066	10,317	5,982	10,541	10,556	2,941

Table A.7. Summary statistics of QuantAQ MODULAIR 1-minute resolution nitric oxide (NO) (ppb) concentrations by location, South Baltimore Air Monitoring Network, Baltimore, Maryland. Note. N = sample size.

	Location									
	1	**2**	**3**	**4**	**5**	**6**	**7**	**8**	**9**	**10**
Statistic										
N	486,132	222,839	271,054	413,149	538,123	318,362	181,386	379,180	206,477	439,759
Minimum	1.07	1.32	1.16	1.07	0.53	1.19	1.32	1.06	1.21	0.99
25%	1.89	1.79	2.53	1.82	2.97	1.81	1.78	1.90	1.84	1.89
Median	2.35	2.04	3.25	2.14	4.31	2.11	2.03	2.33	2.19	2.31
Mean (SD)	3.78 (9.28)	2.84 (6.53)	9.67 (21.31)	3.06 (7.94)	6.58 (10.09)	3.12 (10.20)	2.46 (4.12)	3.13 (5.41)	2.52 (5.43)	4.41 (12.12)
75%	2.86	2.34	5.08	2.48	6.36	2.44	2.33	2.87	2.49	2.81
Maximum	386.18	448.51	694.44	868.61	740.36	1,102.29	156.69	150.13	733.73	301.15

Table A.8. Summary statistics of QuantAQ MODULAIR 1-minute resolution nitrogen dioxide (NO_2) (ppb) concentrations by location, South Baltimore Air Monitoring Network, Baltimore, Maryland. Note. N = sample size.

	Location									
	1	**2**	**3**	**4**	**5**	**6**	**7**	**8**	**9**	**10**
Statistic										
N	486,268	222,899	271,125	416,708	538,128	318,884	184,035	379,204	208,167	440,541
Minimum	1	1	1	1	0	1	1	0	1	0
25%	6	10	10	8	7	10	13	5	6	6
Median	9	21	18	13	11	24	24	8	11	9
Mean (SD)	11 (7)	19 (9)	17 (8)	16 (9)	14 (8)	20 (10)	22 (9)	10 (7)	14 (9)	12 (9)
75%	14	27	24	24	21	28	28	12	22	19
Maximum	136	62	77	95	124	159	51	47	53	57